This is to certify that the
dissertation entitled

MEASUREMENT AND ANALYSIS OF HUMAN POSTERIOR BACK AND THIGH CONTOURS FOR AUTOMOTIVE SEAT DESIGN

presented by

Zhenyu Liu

has been accepted towards fulfillment
of the requirements for the

Doctoral degree in Engineering Mechanics

Major Professor's Signature

18 April 2005

Date

MEASUREMENT AND ANALYSIS OF HUMAN POSTERIOR BACK AND THIGH CONTOURS FOR AUTOMOTIVE SEAT DESIGN

By

Zhenyu Liu

A DISSERTATION

Submitted to
Michigan State University
In partial fulfillment of the requirements
for the degree of

DOCTOR OF PHILOSOPHY

Department of Mechanical Engineering

2005

ABSTRACT

MEASUREMENT AND ANALYSIS OF HUMAN POSTERIOR BACK AND THIGH CONTOURS FOR AUTOMOTIVE SEAT DESIGN

By

Zhenyu Liu

To better understand and represent the seated human posterior back, buttocks, and thigh contours, three groups of human subjects (5^{th} percentile small females, 50^{th} percentile mid-sized males, and 95^{th} percentile large males) were measured in a specially designed contour chair within typical automotive interior environment. The postures were acquired by a human motion measurement system.

The data were analyzed, and then representative seated mid-sized male posterior back, buttocks, and thigh contours were developed for both physical hardware and computer program software for automotive seating design and validation.

To explore the relations among contours of people with different anthropometric dimensions and the possibility to relate the contours of different anthropometric groups of people, a method was developed to scale the mid-sized male contours to large male or small female subjects' contours. Potentially it could be used to generate the contours for people in different groups other than small female and large male. For the first time, the scaling methodology of scaling contours of mid-sized male to small female or large male was verified by experimental data. The coefficient of correlation analysis produced very high agreements between the scaled and measured data of the contours.

Both the hardware and software from this research are being utilized in the automotive seating industries. The data collected in this research are having significant influences on the seating design and validation.

Dedication

I would like to dedicate this dissertation to my parents and my sisters, my parents-in-law, for their guidance and encouragement in everything and every way, even in my pursuing beautiful dreams.

I would like to dedicate this dissertation to my family, my wife, Lan, our wonderful children Alice Yiyang, Christine Yihuan, and Daniel Yikang, for their inspiration, support, and sacrifices.

ACKNOWLEDGEMENTS

The author would like to express his sincerest gratitude to the following people for their assistance, and encouragement in the course of preparing this dissertation.

To my advisor and mentor, Dr. Robert Hubbard, for your guiding and assisting me in every way possible. Your advice and encouragement will be with me well beyond the scope of this dissertation. Thank you.

To my graduate committee: Dr. Gary Cloud, Dr. Hongyu Tsai, and Dr. Joseph Vorro, thank you for reviewing my work.

Special thanks to Cliff Beckett, for helping me with every detail in the contour chair building, and keeping experimental equipments in excellent condition.

To Chris and Melissa Gedraitis, Bob Boughner, Richard Setyabudhy, and Akram Ali, for your effort and time put into this work.

To Automotive Seat and Package Evaluation and Comparison Tools program (ASPECT) and Human Solution, Inc., for their generous funding of my research.

TABLE OF CONTENTS

LIST OF FIGURES x

LIST OF TABLES xv

CHAPTER 1 INTRODUCTION 1

1.1 Background and Literature Review 1
1.2 Statement of The Problem 13
1.3 Objectives 13

CHAPTER 2 ANATOMICAL BASICS AND TARGETED BONY LANDMARKS .. 15

2.1 Introduction 15
2.2 Posture Descriptions 15
2.3 Positional Terminologies 19
2.4 Upper Limb 19
2.5 Spine 20
2.6 Thorax 23
2.7 Pelvis 24
2.8 The Lower Limbs 25

CHAPTER 3 MEASUREMENT OF SEATED HUMAN CONTOURS AND POSTURES 27

3.1 Introduction 27
3.2 Experimental Device and Setup 27
3.2.1 Contour Test Chair 27
3.2.1.1 Seat Pan 29
3.2.1.2 Seat Back 31
3.2.1.4 Measurement Contour Chair Accuracy 32
3.2.1.5 Seat Foam Stiffness Selection 32
3.2.2 Test Lab Space 35
3.2.3 Measurement Targets and Probe 35

3.2.5 Reference Chair 38
3.2.6 Contour Data Acquisition 40
3.2.7 Posture Data Collection 41
3.3 Testing Protocol 43
3.4 Subject Selection Criteria 45
3.5 Subject Anthropometric Data Acquisition 46

CHAPTER 4 DATA ANALYSIS APPROACHES AND RESULTS 49

4.1 Introduction 49
4.2 Initial Raw Data Treatment 49
4.2.1 Data Transformation Among Coordinate Systems 50
4.2.1.1 Translation 53
4.2.1.2 Rotation 54
4.2.2 Generating Contour Surface from Measurement Data Points 55
4.3 Seated Posture Calculations 56
4.3.1 Lower Neck Joint 57
4.3.2 Shoulder Joints 58
4.3.3 Upper Lumbar Joint 59
4.3.4 Lower Lumbar and Hip Joints 60
4.3.5 Knee Joints 62
4.3.6 Ankle Joints 63
4.3.7 Wrist Joints 63
4.3.8 Elbow Joints 64
4.4 Deformed Contours Data Analysis 65
4.4.1 Methods 65
4.4.1.1 Analyzing the Thigh and Buttocks Data Surface 66
4.4.1.2 Analyzing the Back Data Surfaces 68
4.4.2 Comparing Measured Data and J826 H-point Machine 69
4.4.2.1 The Thigh and Buttocks Data 69
4.4.2.2 The Back Contour Data 73
4.5 Defining Mid-male Contour 81
4.5.1 Defining The ASPECT Mid-male Contours 81
4.5.1.1 Thigh and Buttocks Contours 82
4.5.1.2 Back Contour 83
4.5.2 Defining The RAMSIS Mid-male Contours 93

CHAPTER 5 CONTOUR SCALING FOR LARGE MALE AND SMALL FEMALE
..... 95

5.1 Introduction 95
5.2 Development of Scaling Factors 96
5.2.1 Thoracic 97
5.2.2 Lumbar 97
5.2.3 Pelvis 98
5.2.4 Thigh 99
5.3 Scaling Procedures and Results 99
5.3.1 Small Female 100
5.3.2 Large Male 113
5.4 Correlation Comparison Between Measured and Scaled Contours . 126
5.4.1 Methods 126
5.4.2 Correlation of Large Male and Small Female Contours 127
5.4.2.1 Differences 127
5.4.2.2 Coefficients of Correlation 141
5.4.2.3 Corridors 145
5.5 Discussion of Scaling Results 154
5.5.1 Thorax 154
5.5.2 Lumbar 155
5.5.3 Pelvis 155
5.5.4 Thigh 156

CHAPTER 6 CONCLUSIONS 158

APPENDICES 162

APPENDIX A
Scaling Factors Used for Scaling Procedures 163
APPENDIX B
Scaled and Measured Small Females Results 166
APPENDIX C
Scaled and Measured Large Males Results 199

LIST OF REFERENCES 223

LIST OF FIGURES

Images in this dissertation are presented in color.

Figure 1 J826 Two-Dimensional H-point Template and Three-Dimensional H-point Machine 3

Figure 2 Two-Dimensional JOHN Model 6

Figure 3 Definition of TRA 11

Figure 4 TLC 12

Figure 5 A Typical Posture Model 17

Figure 6 Subject in Contour Measurement Chair 18

Figure 7 Targets at Lateral Epicondyle, Mid-wrist, and Acromion Probed 20

Figure 8 The Spine Column, Adapted from Chaffin [13] 22

Figure 9 Targeted at Manubrium and Xiphoid Process 23

Figure 10 Pelvis: illium, ischium, pubic symphysis 25

Figure 11 Targets on Lower Limbs 26

Figure 12 Contour Chair with Targets for Local Coordinate System 28

Figure 13 Light Box 30

Figure 14 Same Subject Measured on Stiff and Soft Foams 33

Figure 15 Measurement Target 36

Figure 16 Measurement Probe 37

Figure 17 Reference Chair 39

Figure 18 Transformed Data Points 51

Figure 19 Lofted Data Surface 52

Figure 20 From Coordinate System $Ox_1x_2x_3$ Translated to $Ox_1'x_2'x_3'$ 53

Figure 21 Cartesian Coordinate System $Ox_1x_2x_3$ Rotated to $Ox_1'x_2'x_3'$ 55

Figure 22 Calculation of Lower Neck Joint 57

Figure 23 Calculation of Shoulder Joint 58

Figure 24 Calculation of Upper Lumbar Joint 59

Figure 25 Pelvis Coordinate System 61

Figure 26 Calculation of Lower Limbs Joints 63

Figure 27 Calculation of Upper Limbs Joints 64

Figure 28 Sliced Thigh Curves (Relative to Left Femur Axis) and Back Curves .65

Figure 29 Contour Surface Analyzing Scheme 67

Figure 30 Sections of J826 H-point Machine and Subjects Contours 71

Figure 31 Sections of J826 H-point Machine and Subjects Contours 72

Figure 32 Sections Through the ASPECT and UMTRI Contours with Postures and Contact Edges 74

Figure 33 Measured Back Contours 75

Figure 34 Contour Sections Up the Seat Back 76

Figure 35 Comparison between ASEPCT and UMTRI Back Contour 80

Figure 36 ASPECT Symmetrical Buttocks and Thigh Contours 82

Figure 37 Torso Length Scaled In Z-Direction 84

Figure 38 Measured Contour Curves 87

Figure 39 Measured Back Contours Between Upper Lumbar Joint 88

Figure 40 Average Back Contour And Posture Side View 89

Figure 41 Average Back Contour Left Rear View 90

Figure 42 ASPECT Back, Buttocks and Thigh Contour Surfaces 91

Figure 43 ASPECT Manikin 92

Figure 44 Tested and Scaled Subject 1's Contour Curves, rear view 102

Figure 45 Tested and Scaled Subject 1's Contour Curves, oblique view 103

Figure 46 Tested and Scaled Contour Curves at Each Section of Small Female Subject 1 104

Figure 47 Measured and Scaled Subject 1's Contour 115

Figure 48 Measured and Scaled Subject 1's Contour 116

Figure 49 Tested and Scaled Contour Curves at Each Section of Large Male Subject 1 117

Figure 50 Typical Difference Curves between Scaled and Measured Contour. 129

Figure 51 Typical Difference Curves between Scaled and Measured Contour. 133

Figure 52 Typical Bar Charts of Coefficient of Correlation 142

Figure 53 Typical Corridor Plots at Mid Thorax, Lumbar, Pelvis, and Thigh of Large Males 146

Figure 54 Typical Corridor Plots at Mid Thorax, Lumbar, Pelvis, and Thigh of Small Female 150

Figure 55 Pelvis Region Not Well Supported in Seat 156

Figure 56 Female Subject 2 Rear View 167

Figure 57 Small Female Subject 2 Iso View 167

Figure 58 Scaled and Measured Curves of Small Female Subject 2 168

Figure 59 Small Female Subject 3 Rear View 171

Figure 60 Small Female Subject 3 Iso View 171

Figure 61 Scaled and Measured Curves of Small Female Subject 3 172

Figure 62 Small Female Subject 4 Rear View 175

Figure 63 Small Female Subject 4 Iso View 175

Figure 64 Scaled and Measured Curves of Small Female 4 176

Figure 65 SmalFemale Subject 5 Rear View 179

Figure 66 Small Female Subject 5 Iso View 179

Figure 67 Scaled and Measured Curves of Small Female Subject 5 180

Figure 68 Small Female Subject 6 Rear View 183

Figure 69 Small Female Subject 6 Iso View 183
Figure 70 Scaled and Measured Curves of Small Female Subject 6 184
Figure 71 Small Female Subject 7 Rear View 187
Figure 72 Small Female Subject 7 Iso View 187
Figure 73 Scaled and Measured Curves of Small Female Subject 7 188
Figure 74 Small Female Subject 8 Rear View 191
Figure 75 Small Female Subject 8 Iso View 191
Figure 76 Scaled and Measured Curves of Small Female Subject 8 192
Figure 77 Small Female Subject 9 Rear View 195
Figure 78 Small Female Subject 9 Iso View 195
Figure 79 Scaled and Measured Curves of Small Female Subject 9 196
Figure 80 Large Male Subject 2 Rear View 200
Figure 81 Large Male Subject 2 Iso View 200
Figure 82 Scaled and Measured Curves of Large Male Subject 2 201
Figure 83 Large Male Subject 3 Rear View 204
Figure 84 Large Male Subject 3 Iso View 204
Figure 85 Scaled and Measured Curves of Large Male Subject 3 205
Figure 86 Large Male Subject 4 Rear View 207
Figure 87 Large Male Subject 4 Iso View 207
Figure 88 Scaled and Measured Curves of Large Male Subject 4 208
Figure 89 Large Male Subject 5 Rear View 211
Figure 90 Large Male Subject 5 Iso View 211
Figure 91 Scaled and Measured Curves of Large Male Subject 5 212
Figure 92 Large Male Subject 6 Rear View 215
Figure 93 Large Male Subject 6 Iso View 215

Figure 94 Scaled and Measured Curves of Large Male Subject 6 216
Figure 95 Large Male Subject 7 Rear View 219
Figure 96 Large Male Subject 7 Iso View 219
Figure 97 Scaled and Measured Curves of Large Male Subject 7 220

LIST OF TABLES

Table 1 Specifications of the Contour Chair....29
Table 2 Subject's Feet Positions....32
Table 3 Subjects Selection Criteria....46
Table 4 Calculation of Hip Joint Center....60
Table 5 Calculation of Lower Lumbar Joint....62
Table 6 Average Differences (mm) between Scaled and Measured Data....137
Table 7 Standard Deviations (mm) of the Differences....138
Table 8 Average Differences (mm) between Scaled and Measured Data....139
Table 9 Standard Deviations (mm) of the Differences....140
Table 10 Coefficients of Correlation....143
Table 11 Coefficients of Correlation....144
Table 12 Body Dimensions for Large Male Scaling....164
Table 13 Body Dimensions for Small Female Scaling....165

CHAPTER 1 INTRODUCTION

1.1 Background and Literature Review

Seating comfort is a growing issue in both automotive and office seat design. Comfort is also a vague and ubiquitous term, and comfort has no clear and operational definition. Comfort is influenced by several factors such as vehicle package factors, seat factors, an occupant's sitting posture, and seat contour. Seat factors include the geometric dimensions and mechanical responses of seats to test manikins and to human beings, as well as the layout of the vehicle interior components, also called vehicle package factors. The positions of the vehicle components affect a driver's location in the vehicle seat and can also affect the driver's postures. Therefore, a driver's posture results from compromises between comfort and restrictions from interior layouts and driving tasks. During driving, a driver may change his posture from time to time in order to make himself comfortable. When sitting, a person's body contours either conform to the seat contours or the seat will not be in contact with and support the person's body. The contours of the seat determine the possible contours of the body and the compatibility of seat and body contours influence contact pressures and sitting posture. Hence, seating comfort is directly related to seat contour, including lumbar support location and amount of lumbar prominence, associated with permissible ranges of sitting postures.

To achieve desired seat comfort, accurate and efficient tools are needed for both seat design and evaluation. To comply with the Society of Automobile

Engineer (SAE) Handbook Recommended Practice J826 [1] used since the early 1960's, seat dimensions and shapes are determined by using an SAE J826 two-dimensional H-point template, and an SAE J826 three-dimensional H-point

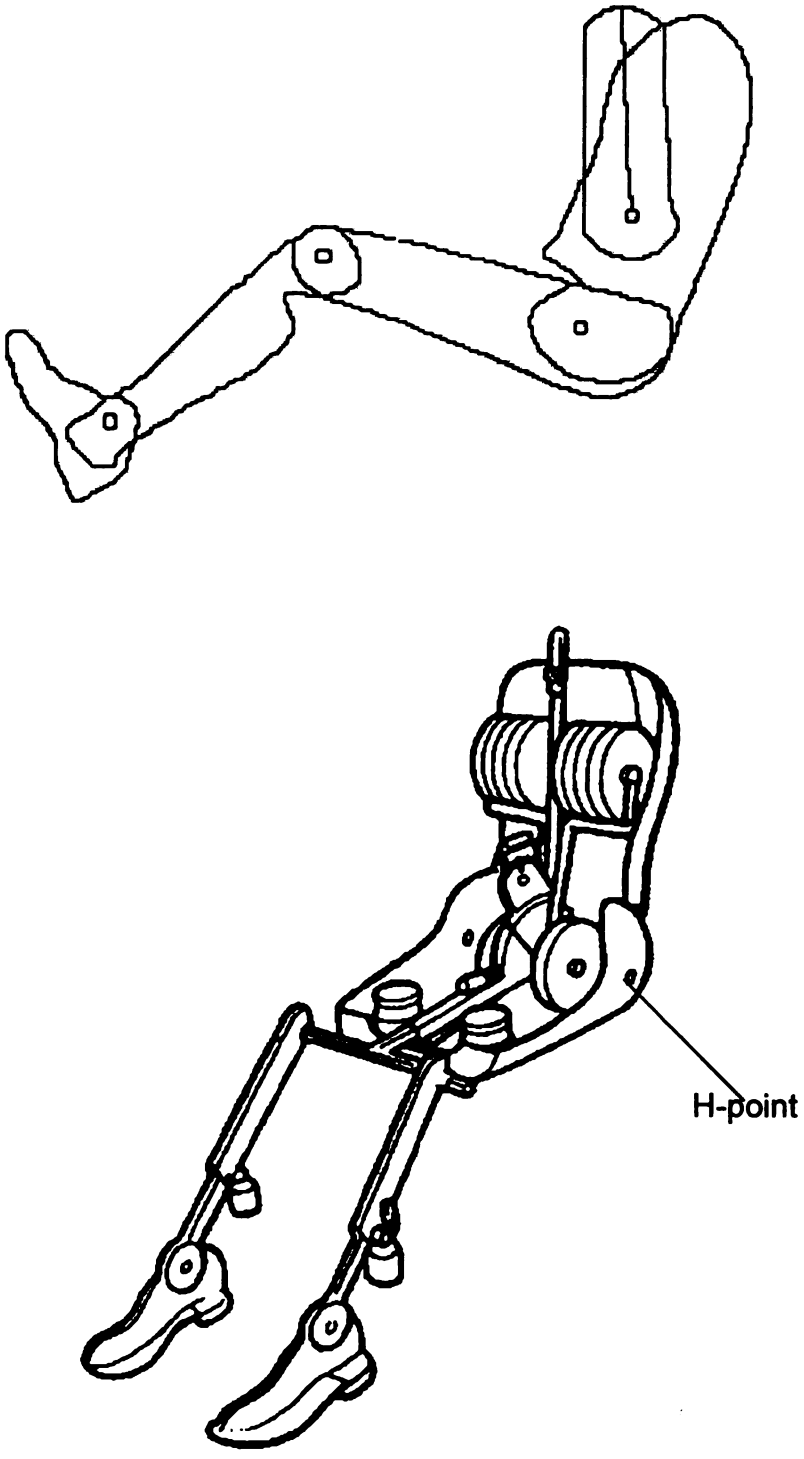

Figure 1 J826 Two-Dimensional H-point Template and Three-Dimensional H-point Machine

machine, known as the J826 manikin (Figure 1). The H-point in the SAE J826 tools is a representation of the average man's hip joint center (HJC). The SAE handbook also specifies measurements for dimensions, adjustability, and configuration of auto seating.

It is simple and practical to use physical tools in designing, confirming and evaluating the desired comfort. The survey [2] conducted by the Automotive Seat and Package Evaluation and Comparison Tools (ASPECT) program found a strong need for a physical tool like the J826 H-point machine. However, the J826 2-D H-point template and 3-D H-point machine were originally developed for locating occupants in an automobile seat within a vehicle interior. Hubbard [3] pointed out that the misuse of the J826 2-D H-point template and 3-D H-point machine resulted in a slumped posture and affected the comfort of seated occupants for more than two decades.

The J826 machines simulate the mid-size male body segments by simulating the combined pelvis and thighs, a segment of combined thorax and lumbar, and the two feet and legs, which can be adjusted to the 10^{th}, 50^{th} and 95^{th} percentile male adult's leg and thigh lengths. The torso and butt-thigh segments can articulate about a lateral axis through the H-points. The 3-D H-point machine is usually used to determine the H-point of a seat and seat back angle following methods specified in the SAE Handbook.

Normal human motion in a seat is very complicated, and includes, among other factors, lumbar curvature changes as well as, thorax and pelvis articulation around spinal joints, associated with changes in spinal curvature. The structure

of the 3-D H-point machine has a slumped posture with a straight lower back does not represent a normal human postures change in vehicle seats. The 3-D H-point machine does not fit into seats that have highly contoured shapes with large amount of lumbar prominence. If the J826 manikin is placed in a contoured automobile seat with lumbar support and its lower lumbar and pelvis area is held against the seat back, its upper torso is in a forward position without contacting the seat back. If its upper torso is pushed against the seat back, its H-point slides out away from the seat back.

From the point view of seating design and analysis, it is very important to describe human posture and contour as precisely and correctly as possible. There were two very important studies in this area. One was conducted by Haas and Hubbard at Michigan State University. They developed a two dimensional, sagittal computer model [4], which represents the average adult male's geometry, including the shape and relative position of the head, thorax and pelvis, and spinal motion. The head, thorax, and pelvis in the Haas model were connected by a series points representing joint centers in the cervical, thoracic, and lumbar spinal regions, as seen in Figure 2. In this model, the thorax and pelvis articulate around upper and lower lumbar joints respectively, with one-to-one opposite rotation. This computer model program is known as JOHN to recognize the support from Johnson Controls, Inc.

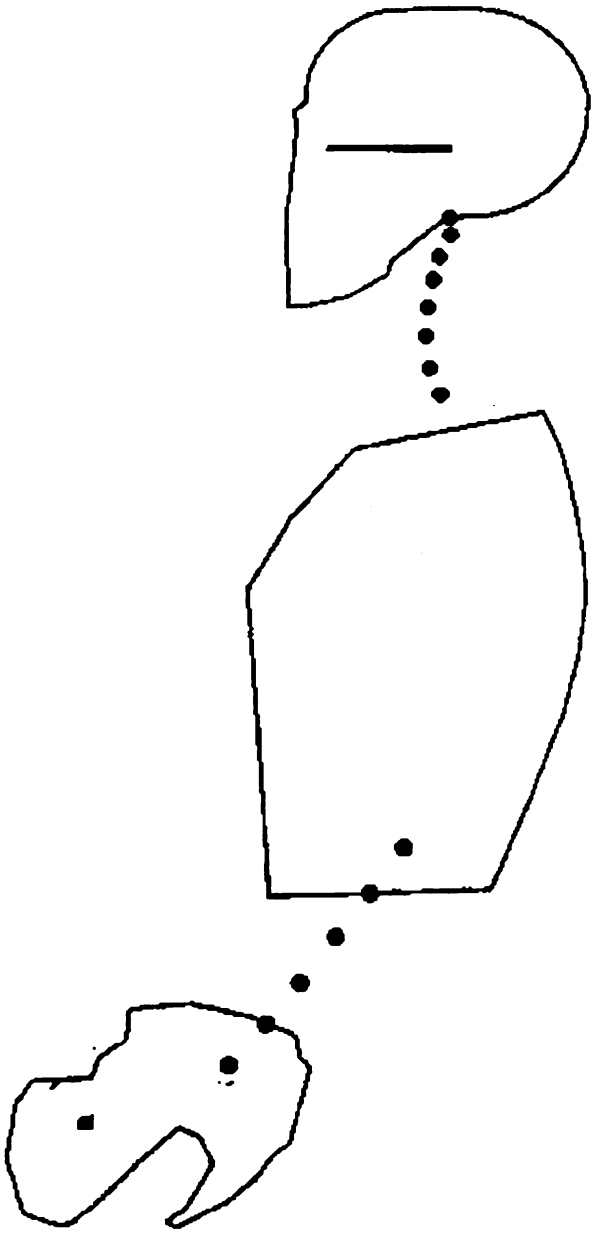

Figure 2 Two-Dimensional JOHN Model

Another important anthropometric study was performed at the University of Michigan Transportation Research Institute (UMTRI) [5] for crash dummy development by determining how a driver is positioned within an automobile. It was the best data resource at that time and was partially adopted in the JOHN program. In their study, UMTRI placed subjects in production auto seats in car interior layout environments. A combination of seat surface casting strips and photographs of external landmarks on subjects' skin was used to determine both exterior contour and landmark locations. Subjects were placed into three subgroups: mid-sized male, small female, and large male. The limitations of UMTRI contours are as follows: 1) the production seats were used in the study and the shape of the seat affected subject's contours, especially in the posterior thigh area, where soft tissue deformed substantially. The production seats were designed and evaluated by the 2-D H-point template and 3-D H-point machine, therefore, the shortcomings of the tools still influenced the UMTRI data; 2) the study did not consider the lumbar curvature and foot positions, which are crucial for seating design; 3) in Haas's study he pointed that the UMTRI contour's pelvis was positioned too high. Apparently the 46 mm soft tissue under ischial tuberosities on the bottom of the pelvis when one sits in a seat was unreasonable.

Development of computer model programs has rapidly advanced and cannot be overstressed in the area of seat design and computer-aided evaluation to achieve optimal design. Also, computer modeling can reduce expensive design and validation cycles. There are several available anthropometric

computer models for possible application to automotive seating design, which are briefly described below.

RAMSIS [6] is a three-dimensional, ergonomic computer program developed by TecMath (now Human Solutions), GmbH in Kaiserslautern, Germany, to represent people seated within automotive interior layouts for analysis and design. RAMSIS includes a posture prediction algorithm based on data of subjects seated in vehicle packages. The human sizes and shapes are fit to video images of individual subjects, and they are based on anthropometric data. Thus, the RAMSIS model is positioned in a seat based on the video images of individual subjects. Because video cameras are incapable of capturing the deformed body segments that are contacting a seat surface, the contour is not realistic. Therefore RAMSIS is not being used for seat comfort design or evaluation. This present study is being performed to provide TecMath the deformed back, buttocks, and posterior thigh contours.

JOHN has been developed under the direction of Professor Hubbard at Michigan State University with the support of the Automotive Systems Group of Johnson Controls, Inc. JOHN program is based upon Haas's human model [4], which represents the movement between the ribcage and pelvis with selected values of lumbar curvature and the torso recline angle to describe seated postures. JOHN represents the geometry of the skeleton, major muscles, and back skin surfaces of a 50^{th} percentile male.

There were several major phases in JOHN development worth mentioning here.

For his model [4], Hass defined two geometric variables to determine the relative positions of body segments. Torso recline angle (TRA) was defined as the angle measured from a vertical line passing through the twelfth thoracic/first lumbar vertebrae (T12/L1) and the fifth lumbar/first sacral (L5/S1) spinal joint centers. Total Lumbar Curvature (TLC) was defined as the total amount of curvature of the lumbar region in the sagittal plane. TLC is zero when the lumbar joints are aligned on a straight line. TLC is the angular position change of the thorax relative to the pelvis and is positive with lordosis (concave lumbar curvature). Both TRA and TLC are as shown in Figure 3 and Figure 4.

Boughner [7] created a three-dimensional model program for the 50^{th} percentile adult male using solid modeling techniques. The models of major skeletal structures were established by using the data from several anatomy texts and the data from the UMTRI study [5]. This model also represents the posterior thigh muscle geometry to calculate hamstring muscle length.

Bush [8] modeled the shapes of the erector spinae muscles and the external skin contours of the JOHN program by using data from the cadaver studies of Koritké and Sick [9]. Bush rotated the 0° TLC contours about the lumbar spinal joint centers to achieve other contours with respect to selected values of TLC, -10°, 0°, 10°, 20°, 30°, and 40°.

Frost [10] developed new contours for the JOHN models by using both the Bush and UMTRI data [5]. These contours could be articulated to any specified amount of TRA and TLC in the sagittal plane. Then, by using scaling factors for the individual dimensions of the thoracic, lumbar, and pelvic segments, Frost

created back skin contours for 5th percentile adult females as well as 50th, and 95th percentile adult males.

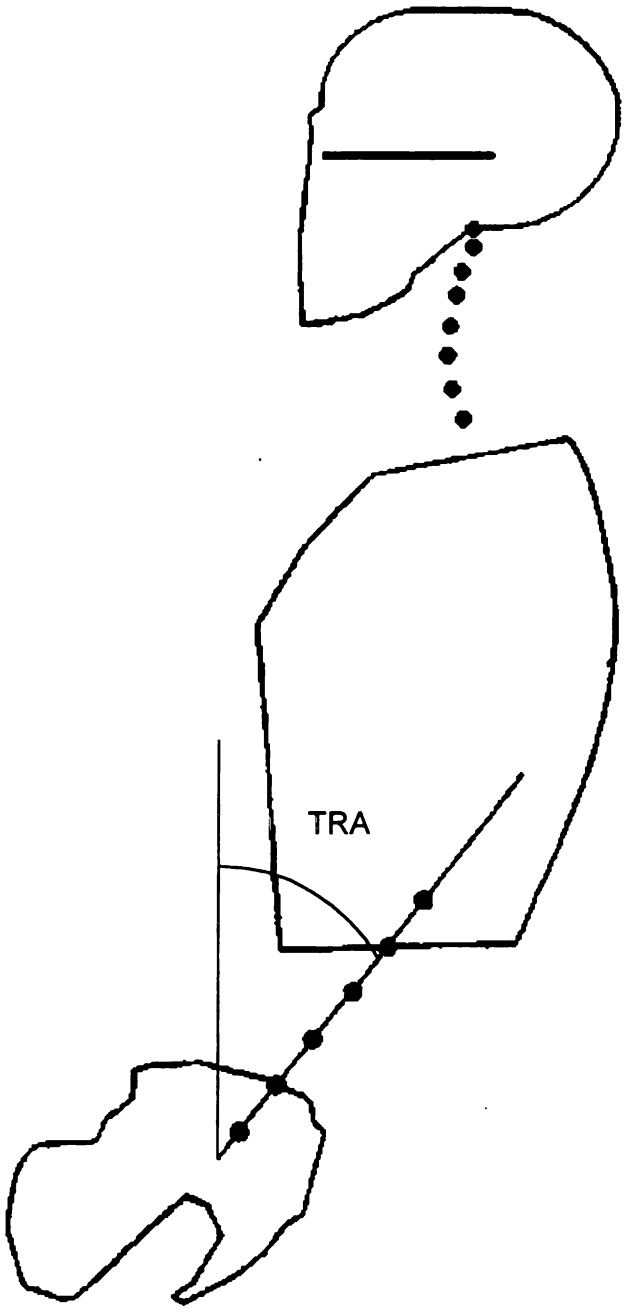

Figure 3 Definition of TRA

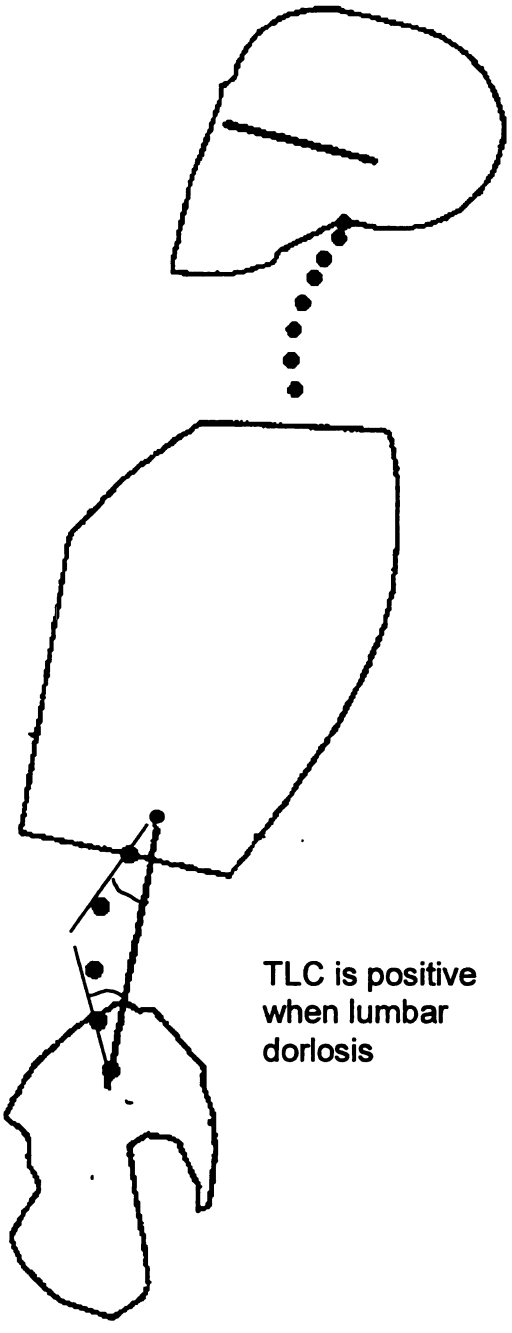

Figure 4 TLC

1.2 Statement of The Problem

The shape of the seat has a strong influence on the posture and comfort of the seat user. Because the body articulates when a person sits in a seat, his body changes posture so that his body surfaces against the seat conform to the seat shape. Thus, the shape of the seat strongly influences the shape and posture of the seat user. If the seat shape is not compatible with possible or preferred shapes of the person, then there is geometric mismatch between the seat and sitter. This mismatch can reduce the area of contact, increase local pressures, and be perceived as discomfort. Some postures may be preferred by the seat user to function in the seated environment, such as seeing instruments or operating controls in an automobile. Also, some postures are more healthful, such as postures with some concave lumbar curvature (lordosis), which allows the upper torso to rotate rearward and the head to be over the base of the neck. This lumbar curvature reduces spinal disc pressures, and this head position reduces neck and shoulder muscle tension to maintain head position. The shape of the interface surface between the seat and the user is significant for comfort support and posture.

1.3 Objectives

The general goal is to define seated contours for people in typical driving postures. The more specific objectives of this study are as follows:

1. Collect data of seat contact surface contours and postures for representative subjects of the 5th percentile small adult female, 50th percentile average adult male and 95th percentile large adult male.
2. Develop contours based on analyzed measurement data that could be used for the JOHN and RAMSIS programs.
3. Develop a methodology to represent seated contact surface contours for diverse driver populations.

CHAPTER 2 ANATOMICAL BASICS AND TARGETED BONY LANDMARKS

2.1 Introduction

In a sitting position, human body weight is mainly transferred to certain areas of ischial tuberosities of the pelvis and their surrounding soft tissues, and also the feet [11, 12]. The weight distribution is related to seating comfort, and soft tissue fatigue and is usually determined by sitting posture and the supporting seat contour. To better understand sitting posture and comfort, a brief review of the anatomy of spine, pelvis, and thigh is presented.

2.2 Posture Descriptions

The representation of sitting posture adopted in this research was developed in the ASPECT program [2]. It is based on a kinematical model of the human body, in which the human body is modeled as an open chain of straight-line segments connected at major joints [4]. The segment lengths, the orientation of the segments, and the location of the joints have to be determined by means of a combination of photography and calculation [2], as seen in Figure 5.

To collect posture data, the choice of appropriate bony landmarks has to be made based upon both the data acquisition method and human anatomy [2]. The bony landmarks of interest have to be palpable and easily located. It is crucial for targets at the selected landmark locations to be visible to multiple

video cameras so that their positions can be recorded and calculated to determine the joint centers of interests.

A typical presentation of a targeted subject and his posture data is shown in Figure 5 and Figure 6.

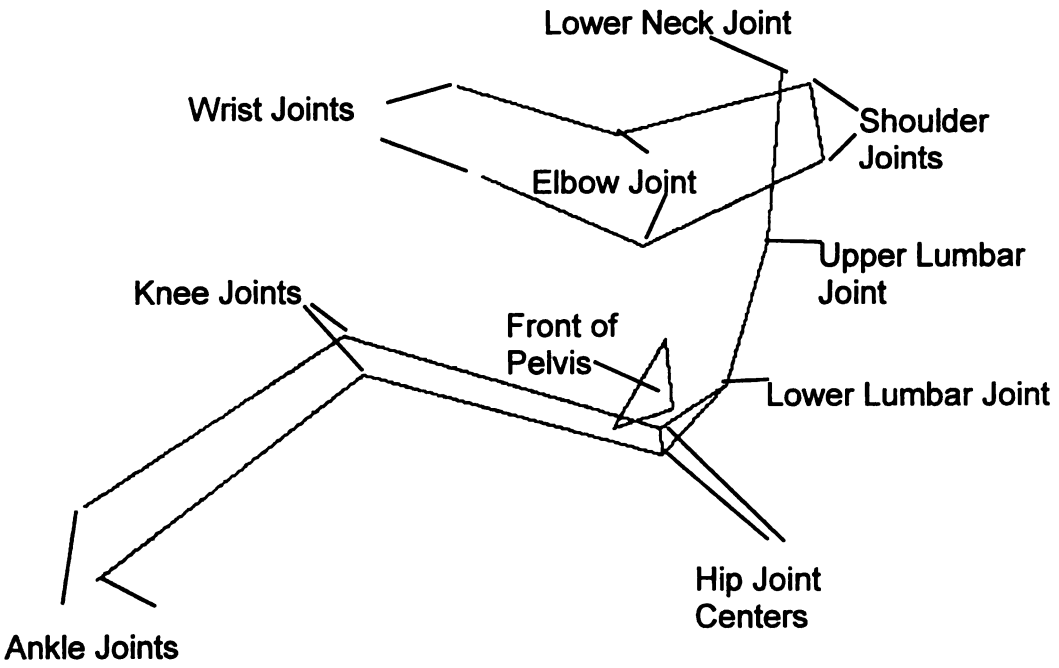

Figure 5 A Typical Posture Model

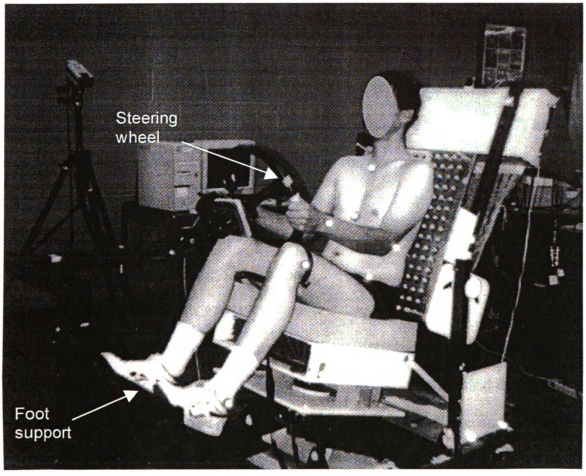

Figure 6 Subject in Contour Measurement Chair

2.3 Positional Terminologies

The term "superior" is used to express the direction toward the top of the head, and "inferior" toward the feet. The direction toward the front of the body is defined as "anterior", and toward the back of the body as "posterior".

There is a central mid-sagittal plane of symmetry passing through the head and trunk that separates the right from left sides. On either side of the central plane, the direction pointing to the plane is referred to as "medial", and the direction away from the plane is referred to as "lateral".

A plane perpendicular to the long axis of the body and dividing its superior portions from inferior is named the transverse or horizontal plane.

2.4 Upper Limb

In the performance of tasks and reaching controls, the positions of the shoulders and the upper limbs influence spinal postures and comfort during driving. Therefore, arm and shoulder positions must be taken into account for posture [7, 13]. The three bony landmarks targeted or probed on each side were the acromian process, lateral epicondyle, and mid-wrist (a midpoint of styloid process of radius and ulna) to locate the shoulder joint, elbow joint, and mid-wrist skin points, respectively. Figure 7 shows that the acromion process, lateral epicondyle, and mid wrist were targeted or probed.

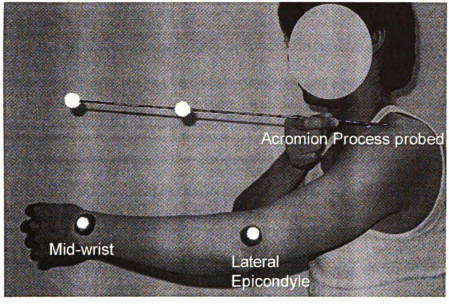

Figure 7 Targets at Lateral Epicondyle, Mid-wrist, and Acromion Probed

2.5 Spine

The spine is very important in biomechanical aspects of sitting, especially the lumbar region. The spinal column consists of five segments of cervical, thoracic, lumbar, sacral, and coccygeal vertebrae, as shown in Figure 8. There normally are thirty-three vertebrae stacked on top of one another in a spinal column for a normal person. Each vertebra is named with respect to its relative position in the spine column from top to bottom, such as C1-C7 for the seven

vertebrae in the cervical region, T1-T12 in the thoracic region, and L1-L5 in the lumbar region.

Among these five segments, only cervical and lumbar vertebrae have significant mobility. Because the cervical vertebrae are responsible for head movement, they are of less importance for sitting postures. In the thoracic spine, the mobility is limited because of the connection to the rib cage [13]. The sacrum is effectively part of the pelvis with 5 vertebrae fused together, and the coccyx (4 vertebrae) does not have meaningful function for seating posture. There are natural curvatures in the vertebral column: cervical lordosis, thoracic kyphosis, and lumbar lordosis resulting from the vertebrae and discs structural characteristics when standing erect, as shown in Figure 8. In this study, markers of the spinous processes of C7, T8, and sacrum were used to determine the spine posture. By palpating the most posterior aspect of the spinous process, these vertebral landmarks can be found, especially the prominent C7 vertebral process.

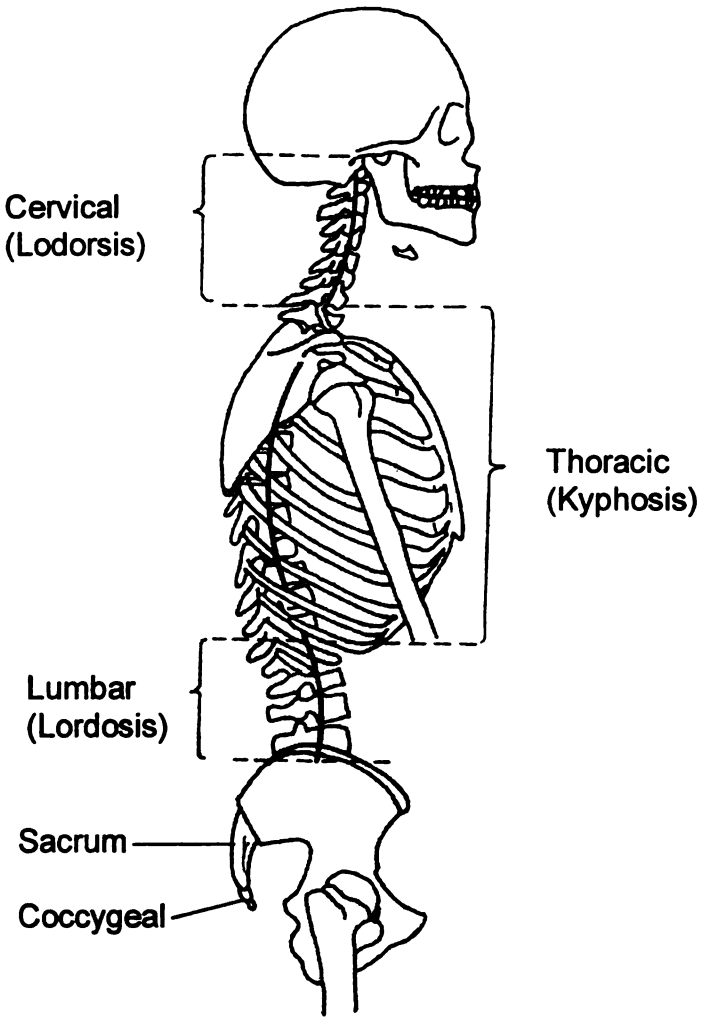

Figure 8 The Spine Column, Adapted from Chaffin [13]

2.6 Thorax

Thoracic vertebrae articulate with each other and with the rib cage, so their mobility is limited [13]. This is why the thorax is considered to be a rigid body in posture analysis [2]. The top end of the sternum is named the manubrium. The inferior tip of the sternum is called the xiphoid process, Figure 9. Together with the landmarks on the vertebral column, these two sternal landmarks are used to determine the thoracic shape and position in posture analysis.

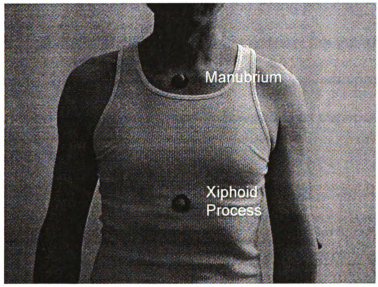

Figure 9 Targeted at Manubrium and Xiphoid Process

2.7 Pelvis

When seated, the body is mainly supported in the area of the ischial tuberosities of the pelvis and their surrounding soft tissues [13]. In this sense, the pelvis is really a base for the trunk when sitting. The sacrum transfers most of the weight from the lumbar spine through the pelvis to the ischial tuberosities and its surrounding soft tissues when a person sits. The pelvis also articulates at hip joint centers with the femurs of the thighs. The pelvis consists of two hipbones, or coxal bones. Each hipbone derives from three separate irregular bones: the illium, ischium, and pubis. The illiac crest is anteriorly prominent at the right and left anterior superior illiac spines (ASIS), which can be palpated and targeted easily. The most inferior prominence of each ischium is known as ischial tuberosity, which supports the pelvis in the sitting position. The pubic symphysis is located where the two pubic bones connect the left and right hipbones anteriorly. During the tests, the pubic symphysis was probed to determine its location. Also, the mid-point of two posterior superior illiac spine (PSIS) was targeted as shown in Figure 10.

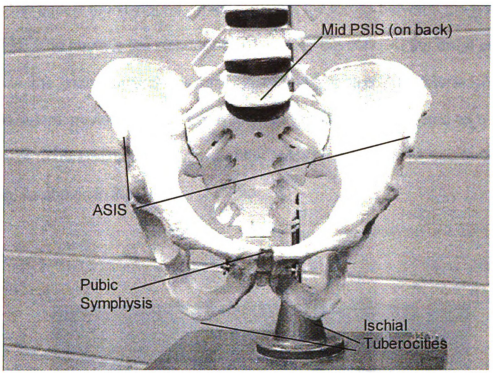

Figure 10 Pelvis: illium, ischium, pubic symphysis

2.8 The Lower Limbs

The spherical head of the femur inserts into the acetabulum of the pelvis to form the hip joint center. The neck of the femur then extends to the greater

and lesser trochanters. At the distal end of the femur, there are the medial and lateral femoral condyles of the knee.

The tibia is the shinbone, which transfers the forces between the knee and the ankle. The fibula is the slender bone lateral to the tibia. At the distal end of the fibula, the lateral malleolus is easily seen and palpated. The lateral femoral condyle, lateral malleolus, and approximate ball of foot were selected as bony landmarks to determine the locations of the ankle joint, knee joint, and foot position, as shown in Figure 11.

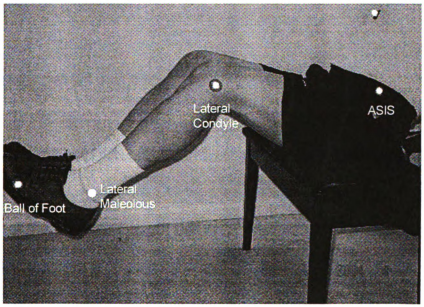

Figure 11 Targets on Lower Limbs

CHAPTER 3 MEASUREMENT OF SEATED HUMAN CONTOURS AND POSTURES

3.1 Introduction

The goal of this research is to experimentally determine seat contact surface contours for selected subgroups of driver populations in certain permissible ranges of sitting postures within typical vehicle interior geometries. To simplify anthropometric issues, two measurements that account for most of the variance of body dimensions (height and weight) [14,15] were chosen to classify the subgroups of driver populations. In this section, the details related to measurement will be discussed.

3.2 Experimental Device and Setup

3.2.1 Contour Test Chair

To acquire the seat/sitter contact surface data, a special contour test chair was designed and built, Figure 12. To represent a typical mid-sized sedan, the specifications of the contour chair were used. See Table 1. The seat pan angle and the seat back angle were measured by following the SAE J826 procedure described in [1].

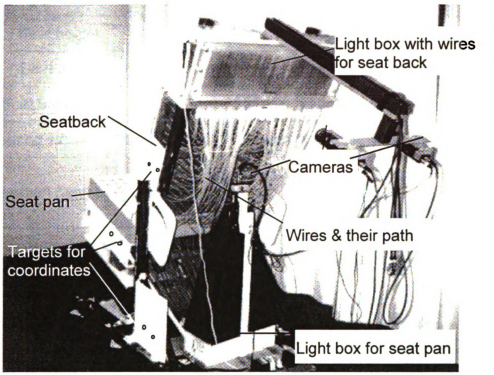

Figure 12 Contour Chair with Targets for Local Coordinate System

Table 1 Specifications of the Contour Chair

Seat height	280 mm from foot support surface to H-point
Seat angle	15° with respect to horizontal
Seat back angle	23° with respect to vertical
Steering wheel angle	20° with respect to vertical
Cushion foam size	500 mm X 500 mm X 100 mm (Width by Depth by Thickness)
Seat back size	580 mm X 650 mm X 100 mm

3.2.1.1 Seat Pan

In the contour chair, there was a flat seat pan with a foam block having dimensions of 500 mm by 500 mm by 100 mm. A hundred stainless steel wire cables were evenly distributed over the 500 mm x 500 mm area in a matrix of 10x10 with the wires 45 mm apart. These wires moved smoothly within plastic tubes when one of the cable ends was displaced via soft plastic discs of 25 mm in diameter that were on the foam surface. The other ends of these wires were led through the plastic tubes to channels in a light box where they were aligned in parallel channels. By means of video cameras and computer interface, the positions of the wire ends in the light box shown in Figure 13 could be digitized

accurately and rapidly with a Visual Basic program. An original reference position file (before deformation) of these ends was taken separately with respect to the displaced position file (after deformation). Thus the deformation of the seat pan and seat back can be recorded and further processed.

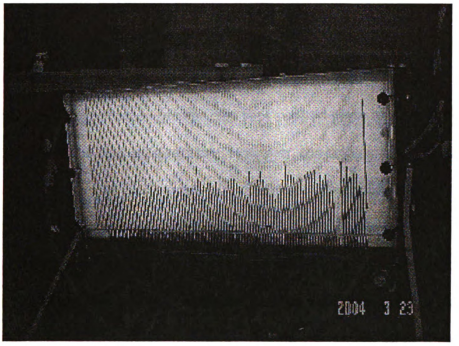

Figure 13 Light Box

3.2.1.2 Seat Back

On the seat back there is a 13 x 16 matrix of steel cables, 45 mm apart. A maximum of four inches of working distance can be set for the wires on the seat back. No foam pad was needed for the seat back because there was sufficient friction in the matrix of measurement wires to support the torso in the selected posture. The seat back was flat to eliminate the influence on the measured back contour from the shape of the back support. The data acquisition principles were the same as those for the seat pan.

3.2.1.3 Foot Support Plate and Steering Wheel

To fit the different sized groups, the foot support plate and steering wheel were adjustable in the fore-aft direction. However, the angles were fixed. The selected angle value was 20 degrees with respect to horizontal for foot support plate, vertical for steering wheel, respectively. Refer to Figure 6.

The horizontal distance from the heel to H-point could be changed to adjust the relative deformation of the thighs into the seat foam, and let the subject determine his preferred position by altering the horizontal position of the foot support plate. Also, the design foot position was analyzed. The distances for small size female, mid size male, and large male were listed in the Table 2.

The steering wheel was adjusted horizontally and vertically for the subject to feel comfortable as in his normal driving condition, and the angle of the steering wheel was fixed. Refer to Figure 6.

Table 2 Subject's Feet Positions

	Mid-male	Small Female	Large Male
Foot Position	900 mm	800 mm	1000 mm

3.2.1.4 Measurement Contour Chair Accuracy

To determine the accuracy of the contour chair, two methods were employed to obtain the outer shape of the SAE manikin. First, the shell of the SAE manikin was scanned by a probe. This shell could be considered as an accurate one. Secondly, the SAE manikin was put into the measurement contour chair and the shape was recorded in the system. Then, the second shell shape was compared to the first measurement from the scanning at the same locations. The results showed the system error was within 3 to 5 mm.

3.2.1.5 Seat Foam Stiffness Selection

After the primary mechanism of the contour test seat was built, a preliminary comparison study between softer and stiffer foams was performed for the same subjects to evaluate the effects of foam properties on measured thigh contours. The results are shown in Figure 14. In the regions directly under the femurs, the deformed thigh shapes were almost the same for both stiffer and softer foams owing to the mechanical restrictions from the femur and the presence of the hamstring muscles. For the softer foam, more of the subjects'

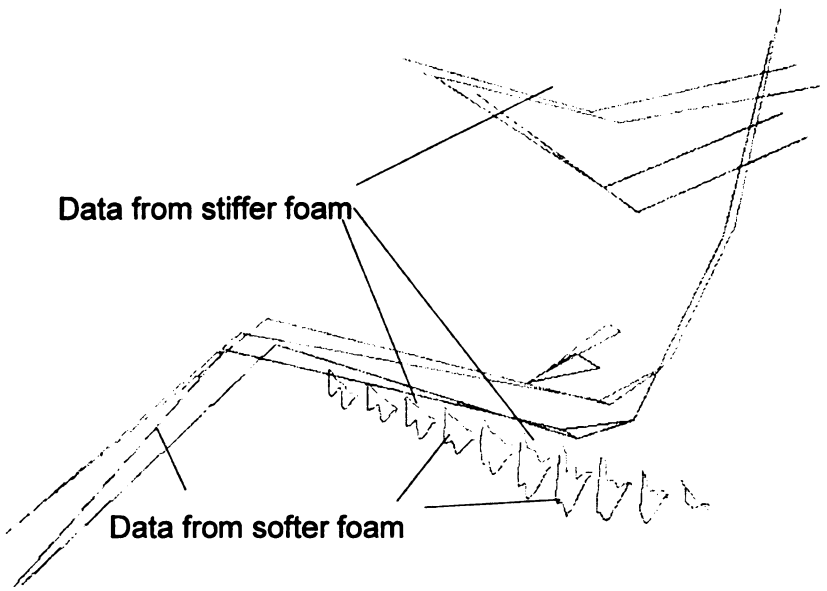

Figure 14 Same Subject Measured on Stiff and Soft Foams

body shapes were recorded because the foam deformed more. These findings were also verified by Setyabudhy's finite element model [16]. On the other hand, the foam shape itself as a seat factor was also considered. A flat, soft block of foam was selected as seat pan cushion to minimize the influence of seat pan shape on the contour shape and to obtain more of the subjects' body shapes.)

3.2.2 Test Lab Space

The testing space was approximately 6m X 6m X 3m. A five-camera MacReflex Qualysis high-speed video system [17] was carefully set up in the space so that each target could be visible simultaneously at least for two cameras, as required by the software used for calculation of the three dimensional coordinates [17]. Through calibration of the camera system, a right-handed SAE vehicle Cartesian system was defined in the space, with positive X-axis pointing rear ward, Y-axis from subject's left to right, and the Z-axis upward vertically.

3.2.3 Measurement Targets and Probe

Measurement targets were spherical wooden beads of 16 mm diameter covered with 3M retro-reflective tape [18], shown in Figure 15, as required by the camera system. The reflective bead was then glued to a square piece of vinyl with approximate 20 mm by 20 mm in dimension. By means of double-sided tape and medical tape, the target was secured to the subject's skin over the skeletal landmark of interest.

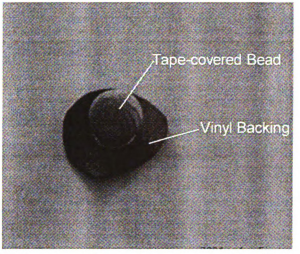

Figure 15 Measurement Target

A measurement probe used in the testing is shown in Figure 16. There were two targets fixed on a steel rod of 4 mm diameter. The centers of the targets were on the rod centerline. Whenever it is difficult to apply the targets in some region or for two cameras to capture a target, the probe can be used to locate the skeletal landmark.

The landmark location could be calculated from the measured centers of bead 1 and bead 2, and the lengths of the steel rod as follow.

$$L_{12} = \sqrt{(x_1 - x_2)^2 + (y_1 - y_2)^2 + (z_1 - z_2)^2} \qquad (1)$$

$$X = \frac{L \cdot x_2 + (L - L_{12})x_1}{L_{12}}$$

$$Y = \frac{L \cdot y_2 + (L - L_{12})y_1}{L_{12}} \qquad (2)$$

$$Z = \frac{L \cdot z_2 + (L - L_{12})z_1}{L_{12}}$$

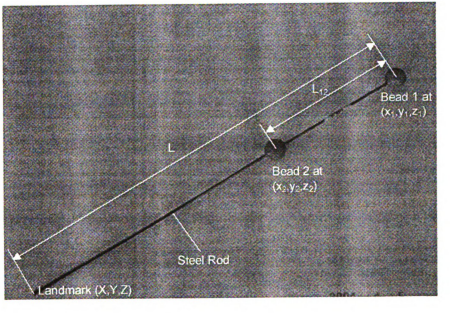

Figure 16 Measurement Probe

3.2.5 Reference Chair

When a subject sits in the contour chair, any targets on his back will not be visible to the cameras. To collect the position data of C7, and T8, a non-deformable thorax was assumed. This makes it possible to gather the position data of C7 and T8 relative to the manubrium and xyphoid in a so-called reference seat, or hard seat as presented in Figure 17.

There is a 70 mm opening down the centerline on the seat back, which provides visibility to the targets on the subject's spine for the cameras. The seat angles were determined based on SAE standards J826 [1]. The first target on the edge is 120 mm forward of the seat back, and the second target 225 mm apart from the first one in the rearward direction. The two targets provided a reference coordinate system.

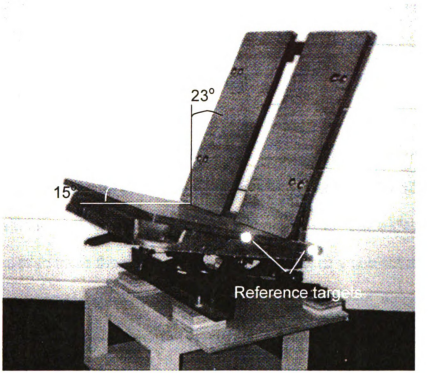

Figure 17 Reference Chair

3.2.6 Contour Data Acquisition

A reference position of the contour chair was collected to record the initial positions of the ends of the steel cables when the seat pan foam was not deformed. While the subject was sitting on the contour chair, the positions of the displaced ends of the steel cables were gathered. The differences between the two positions of the steel cables illustrated the deformed interface between the seat foam surface and the subject.

In the collected seat contour data, only the contact region between a subject and the seat can be taken for a subject's body contour. To differentiate the subject's body contour from the non-contact part of the seat surface, a testing probe was used to trace the border of the contact areas of a subject and the seat. The positions of the two balls on the probe were recorded, since the lengths of the probe were known, the tip positions of the probe could be computed.

Ten mid-sized male subjects were measured and 9 out of 10 subjects' data analyzed for the ASPECT manikin contour [16]. Ten of small female and another ten large male subjects were measured and the data were analyzed.

The testing protocol is attached. The subject measurement is pictured in Figure 6.

3.2.7 Posture Data Collection

The representation of sitting posture adopted in this experiment was developed in the ASPECT program [2]. This kinematic model of the human body is modeled as an open chain of straight-line segments connected at major joints. The segment length, the orientation of the segments and the location of the joints have to be determined by means of a combination of photography and calculation. Reflective balls of 16 mm diameter were placed at the selected skin landmarks on subjects. The posture data were collected in both the reference hard seat (Figure 16) and the contour test chair in Figure 6 or 11.

A five-camera MacReflex Qualysis high-speed video system was used to gather the motion measurement data in the approximately 6 m x 6 m x 3 m testing space [17]. Each camera contains an optical filter, which cuts off the visible part of the light spectrum. Each camera is equipped with an infrared light to illuminate the measurement area, and light is reflected from the targets back to the camera. These infrared lights help to suppress the ambient light and only the target balls can be seen and recorded. There is a video processor to calculate the center of the ball coming with each camera. The MacReflex software provides the tool to read data from the camera system and to distinguish one target from another among all the targets in the image by using direct linear transformation from the object space to the image space. Each camera can only read only two of the three coordinates in a three-dimensional space, so any marker must be seen by two cameras to form an over-determined system of four equations for the three coordinates in the three-dimensional space. Before data

collection, all the cameras were calibrated to gather all the set-up constants for the direct linear transformation. Finally the MacReflex converts the data to a format proper for the subsequent processing, such as a CSV format in our case.

During the measurement, the acromions were probed because of the visibility to the cameras. Owing to the personal privacy and sensitivity concern, the pubic symphysis was probed by the subject after instructions was given.

3.3 Testing Protocol

1) Instruct a subject about the measurement procedures. Have the subject sign the consent form (IRB#96-765) approved by University Committee on Research Involving Human Subjects (UCHRIS).

2) Target subject for the reference chair

The landmarks C7, T8, T12, Sacrum, sternal notch, xyphoid process; right and left ASIS, right and left lateral femoral condyle, maleolous, ball of foot on left side were targeted by the taped wooden beads on vinyl backing. The pubic symphysis will be probed by the subject.

3) Take the reference file of the body in the reference chair in Figure 16. Measure the distance between the ball of foot target and heel point for the calculation purpose.

4) Target subject for contour chair

Surface landmarks sternal notch, xyphoid process; right and left lateral humeral condyle, right and left Wrist, right and left ASIS, right and left femoral lateral condyle, right and left maleolous and ball of foot on left side and two seat pan targets, two seatback targets and two test frame targets.

Surface landmark acromion will be probed by a tester and pubic symphysis will be probed separately by the subject during the measurement process.

5) Decide steering wheel position

Position subject at the desired distance between H-point and foot support bar, placing hands at 3 and 9 o'clock position (during all measurements), adjust the steering wheel fore or aft for a comfortable position by the subject.

6) Decide preferred foot position

Set the distance between manikin H-point and foot support bar to designed distance 1, let subject sit in the contour chair and select a comfortable position 1 by moving foot rest forward, then subject leaves chair.

Set the distance between manikin H-point and foot support bar to designed distance 2, let subject sit in the chair and select a comfortable position 2 by moving foot rest rearward.

Decide Preferred foot position (the mid-point 3 between positions 1 & 2).

7) Gather posterior contour of thigh and buttocks

Set the distance between manikin H-point and foot support bar to designed driving distance with the seat pan in normal position, let subject sit into the chair with back flat against seat back.

At designed driving position, wait for 20 sec., and then gather the data for contour and posture (one file with Acromian probed, the another with Pubic Symphysis probed).

Move the foot support to designed driving position 2, wait for 20 sec.; gather the data of contour, posture, and perimeter.

Move the foot support to preferred position, wait for 20 sec., gather the data of contour, posture.

Move the foot support to designed driving position 3, wait for 20 sec., gather the data of contour, posture.

Redo step 7) twice.

8) Gather posterior contour of back, thigh and buttocks

With 0 lumbar prominence, pull the back wires out and set the distance between manikin H-point and foot support bar to designed driving position with the seat pan in a forward position, let subject sit on the seat pan, move the seat pan back into the seat back support using power track, have subject sit in the chair with back flat against seat back and wait for 20 sec., gather data of contour, posture.

Redo step 8) twice.

3.4 Subject Selection Criteria

Based upon data from U. S. population study by Abraham, [15], body mass and stature range from 5th percentile small female values are 47 kg (104 lbs.) and 151 cm (59.5 in.) to 95th percentile large male values of 102 kg (225 lbs.) and 187 cm (73.5 in.), respectively. A decision was made that three size groups would be used, they are 5th percentile small female, 50th percentile average male, and 95th percentile large male within the U. S. population,. The ranges of mass and stature are given in the Table 3.

Table 3 Subjects Selection Criteria

Subject Categories	Large Male (95%)		Mid-sized Male (50%)		Small Female (5%)	
Range	Min	Max	Min	Max	Min	Max
Body Mass kg/(lb)	76.5 (170)	108 (240)	67.5 (150)	78.75 (175)	45 (100)	56.25 (125)
Stature (height) cm / (in)	178.9 (73)	186.2 (76)	164.2 (67)	171.5 (70)	144.6 (59)	151.9 (62)

3.5 Subject Anthropometric Data Acquisition

To detail information of participating subjects' body dimensions, it was necessarily to obtain anthropometric data. These data were collected by using the definitions and methodologies specified in 1988 Anthropometric Survey Of U.S. Army Personnel [14]. The list of the following anthropometric items was gathered.

ANTHROPOMETRIC DIMENSIONS MEASURED

Definitions cited from ANSUR [18], as follow.

Stature (99, reference number in [18])

Weight (124)

Sitting Height (93)

Biacromial Breadth (10)

Mid-shoulder Height, Sitting (78)

Hip Breadth, Sitting (66)

Waist Height, sitting (121)

Bispinous Breadth (14)---------- Inter-ASIS Width

Waist Breadth (112)

Chest Breadth (32)

Chest Depth (36)

Interscye II (70)

Interscye I (71)

Waist Depth (115)

Waist Back Length (Natural indentation)(110)

Waist Back Length (Omphalion)(111)

Waist Height,sitting (Natural Indentation)(120)

Waist Height,asitting (Omphalion)(121)

Chest Circumference (33)

Chest Circumference at Scye (34)

Chest Circumference below Breast (35)

Waist Circumference (Natural indentation)(113)

Waist Circumference (Omphalion)(114)

Inter-PSIS Width

Hip Breadth (65)

Hip Breadth,sitting (66)

Buttock Depth (24)

Buttock Circumference (23)

Thigh Circumference (103)

Knee Circumference (71)

Buttock height (25)

Buttock-knee length (26)

Buttock-popliteal length (27)

CHAPTER 4 DATA ANALYSIS APPROACHES AND RESULTS

4.1 Introduction

The recorded posture data were tracked by using MacReflex software [17] and exported in a format of CSV files. During data processing, the data were transformed from intermediate coordinate systems to the global coordinate system.

Because of the complexity of comparing the three-dimension data plots, the contour data were converted into two dimension curves for analysis purposes by creating planes relative to skeletal landmarks to intersect the contour surfaces. In this section the methods of data analysis are discussed. Some of the representative results are presented and discussed.

4.2 Initial Raw Data Treatment

Based on the posture descriptors defined by the ASPECT program [2], key skin landmarks on both sides of the subjects were targeted to reflect the subject's real sitting postures in the present study. The tracked data for target location were input to the spreadsheet program [19] that has been revised for this application to calculate the joint centers coordinates of interest. After coordinate transformation and the contour surface data file format was changed to IGES files, the data were imported into the I-DEAS program package [20]. First, the data points (see Figure 18) from the seat pan and seat back were splined into

curves, then these curves were lofted to create the three-dimensional contour surface as seen in Figure 19.

4.2.1 Data Transformation Among Coordinate Systems

There were four coordinate systems used: 1) a global coordinate system in the testing space set by the camera system, 2) one local coordinate system on the seat pan, 3) one local coordinate system located on the seat back, and 4) a local coordinate system on the contour chair frame. The systems 2, 3 and 4 are as shown in the Figure 12. All the back, buttocks and posterior thigh data from the local coordinate systems on the seat back and seat pan were transformed into the global coordinate system [21].

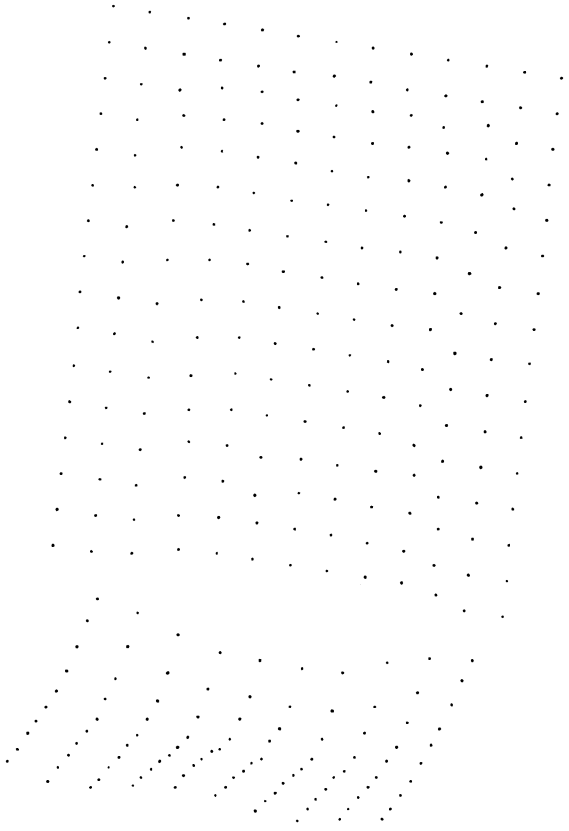

Figure 18 Transformed Data Points

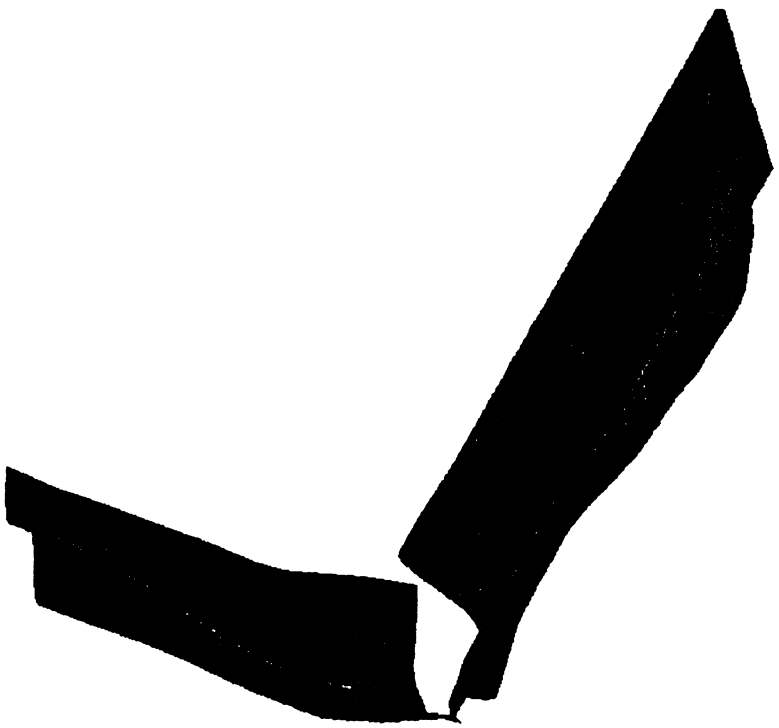

Figure 19 Lofted Data Surface

4.2.1.1 Translation

Data point $[U]=\begin{bmatrix} x_1 \\ x_2 \\ x_3 \end{bmatrix}$ in coordinate system $Ox_1x_2x_3$ was translated to a new coordinate system $O'x_1'x_2'x_3'$ as $[U']=\begin{bmatrix} x_1' \\ x_2 \\ x_3' \end{bmatrix}$. See Figue 20. The distance between the two origins O and O' are $[D]=\begin{bmatrix} a \\ b \\ c \end{bmatrix}$, and the following relation will hold:

$$U' = U + D = \begin{bmatrix} x_1 \\ x_2 \\ x_3 \end{bmatrix} + \begin{bmatrix} a \\ b \\ c \end{bmatrix} \qquad (3)$$

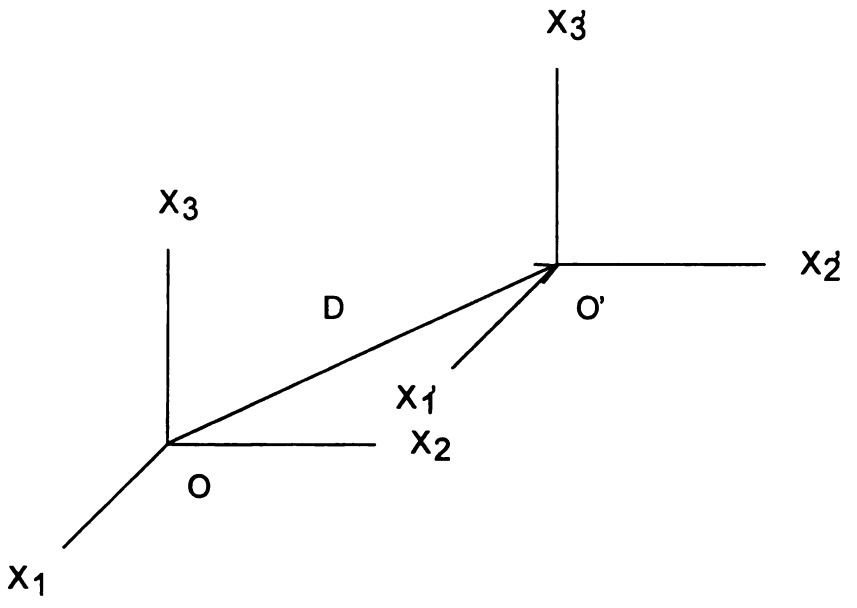

Figure 20 From Coordinate System $Ox_1x_2x_3$ Translated to $Ox_1'x_2'x_3'$

4.2.1.2 Rotation

Suppose that two rectangular Cartesian coordinate systems $ox_1x_2x_3$ and $ox_1'x_2'x_3'$ originate at the same point o, as shown in Figure 21, and the angle between unprimed and primed axes is defined by

$$A_{ij}=(x_i', x_j) \qquad i,j=1,2,3 \qquad (4)$$

and the direction cosines a_{ij} are given by

$$a_{ij}= \cos(x_i', x_j) \qquad i,j=1,2,3 \qquad (5)$$

so the transformation matrix $[a_{ij}]$ is

$$[a_{ij}]=\begin{bmatrix} a_{11} & a_{12} & a_{13} \\ a_{21} & a_{22} & a_{23} \\ a_{31} & a_{32} & a_{33} \end{bmatrix} \qquad i,j=1,2,3 \qquad (6)$$

Write translated position vector U' as $[U']=\begin{bmatrix} x_1' \\ x_2 \\ x_3' \end{bmatrix}$ and the rotated same point U as

$[U]=\begin{bmatrix} x_1 \\ x_2 \\ x_3 \end{bmatrix}$, the following relation will hold,

$$[U']=[a_{ij}]\cdot[U] \qquad i,j=1,2,3 \qquad (7)$$

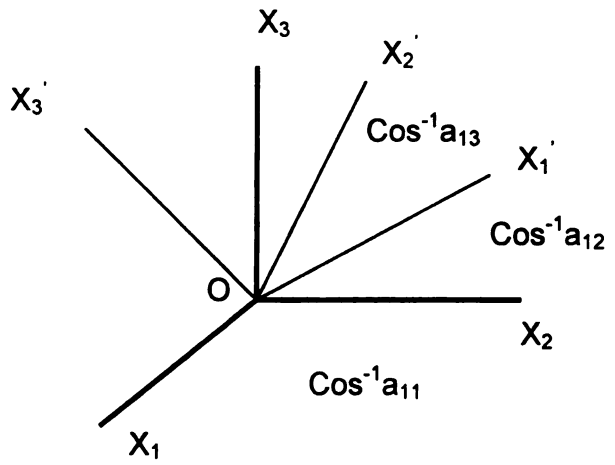

Figure 21 Cartesian Coordinate System $Ox_1x_2x_3$ Rotated to $Ox_1'x_2'x_3'$

4.2.2 Generating Contour Surface from Measurement Data Points

A contour surface was generated from the measurement data points of a subject after the raw data were initially treated, including file format change, coordinate system transformation, etc. The I-DEAS program was employed in the surface generation. First, the primary curves were in the lateral direction, as in Figure 19. The measurement points in the lateral direction were B-splined into curves. These primary curves describe the major features of the contour [14]. The secondary direction in surface generation was engaged in lofting the primary curves into a contour surface, as shown in Figure 19.

4.3 Seated Posture Calculations

One of the goals of this study was to represent subjects' seated surface contours relative to their bone structures. To accomplish this goal, the subjects' sitting postures were estimated by using both targeting landmarks and available scaling data [2]. Once the locations of target centers were recorded, actual bony landmark locations could be calculated by constructing a vector from the center of the target to the location of the actual bony landmark on the skin surface. The length of this vector $L_{T->L}$ was as follow:

$$L_{T->L} = \frac{1}{2}D_t + T_b + T_t \qquad (8)$$

Where D_t: the diameter of the target,

T_b: the thickness of the target backing,

T_t: the tissue thickness at the targeted location.

To determine the direction of the vector from the target center to a joint center, another adjacent landmark target was chosen to create a line between the two target centers. Usually the direction of the vector would be toward the joint under the skin landmark and perpendicular to the line. For a second method to determine a joint center, three landmark targets were needed to yield a plane with three points. The direction of the vector was chosen to be perpendicular to the plane, and pointing to the joint by the landmark.

4.3.1 Lower Neck Joint

The location of the lower neck joint was determined using the C7 and suprasternal surface landmarks. See Figure 22. The vector R from C7 to suprasternal was rotated counter clockwise 8^{o} and became R'. The lower neck joint was the point on vector R', away from C7 at 55 percent of the R length.

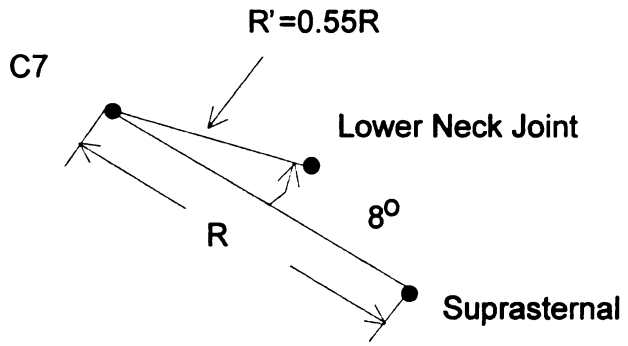

Figure 22 Calculation of Lower Neck Joint

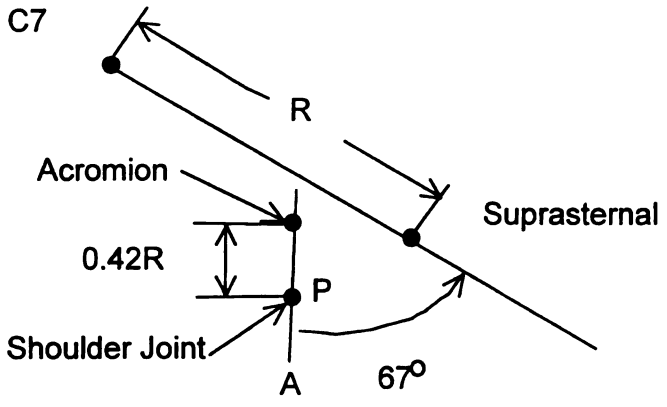

Figure 23 Calculation of Shoulder Joint

4.3.2 Shoulder Joints

The surface landmarks C7, suprasternal, and acromion were used to calculate the shoulder joint. The Y coordinate of the shoulder is the same as that of the acromian landmark. Through the acromion, a vector A was created to form an angle of 67° with the vector R, as shown in Figure 23. The shoulder joint is located on the vector A at P, which is 42 percent of the length of C7 to suprasternal from the acromian. From the position of this point, the joint coordinate X and Z could be decided. Because the ASPECT posture was defined as sagittal symmetry, another shoulder joint could be reflected in the 3-D space.

4.3.3 Upper Lumbar Joint

The upper lumbar joint was calculated from the T8 and T12 positions, as shown in Figure 24. The vector T8-T12 was rotated counter-clockwise 94° to form vector UL, and the upper lumbar joint was located on the vector UL at 52 percent of the length of C7 to suprasternal from the T12.

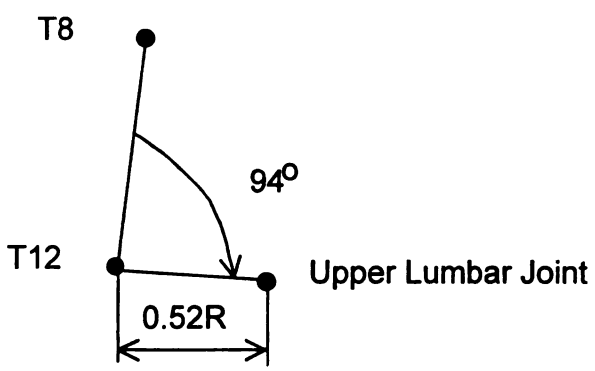

Figure 24 Calculation of Upper Lumbar Joint

4.3.4 Lower Lumbar and Hip Joints

The right and left anterior-superior iliac spine (ASIS) landmarks, the pubic symphysis (PS) landmark, and the posterior-superior iliac spine landmark (PSIS) were used to calculate the lower lumbar joint and hip joint centers. A pelvis coordinate system was created to calculate the lower lumbar joint and hip joint centers, as shown in Figure 25. The Y-axis passes through both right and left ASIS on bone. The Z-axis was perpendicular to Y-axis and passes through the pubic symphysis and the mid-point of right and left ASIS. The X-axis was mutually perpendicular to the Y and Z-axes.

To locate the hip joint center (HJC) in the pelvis coordinate system, the method exploited by Seidel, et al [22], was adopted in this study. The HJC coordinates were scaled from subjects' pelvic width (PW), pelvic height (PH), and pelvic depth (PD) as tabulated in the Table 4. The computed HJC coordinates were then transformed into the global coordinate system for further analysis.

Table 4 Calculation of Hip Joint Center

Coordinate	Measurement	Calculation
X	Pelvic depth PD	0.34*PD
Y	Pelvic width PW	± 0.36*PW
Z	Pelvic height PH	- 0.79*PH

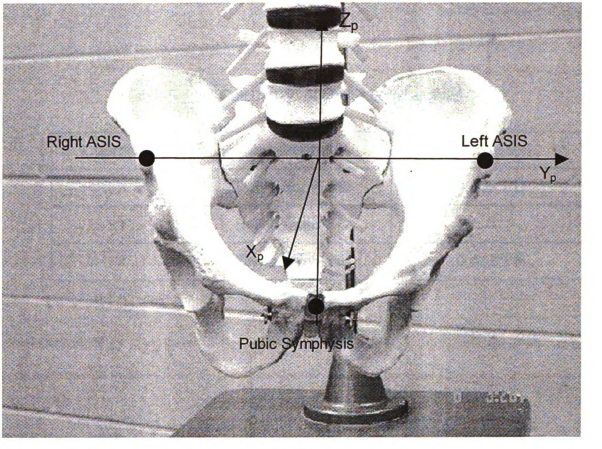

Figure 25 Pelvis Coordinate System

The method developed by Reynolds, et al [23] was used to locate the lower lumbar joint center in the bone pelvis coordinate system [2] as illustrated in Table 5.

Table 5 Calculation of Lower Lumbar Joint

Coordinate	Measurement	Calculation
X	Pelvic depth PD	0.399*PD
Y	Pelvic width PW	0
Z	Pelvic height PH	0.432*PH

4.3.5 Knee Joints

To determine the knee joint locations, the landmarks at the lateral maleolus and lateral condyle along with the calculated hip joint location were utilized to create a plane. At the measured lateral femoral condyle landmark, a vector was constructed perpendicular to this plane. The knee joint location was on the vector medial to the landmark by a distance of 11.8 percent of the measured length between lateral maleolus and the lateral femoral condyle landmarks. See Figure 26.

4.3.6 Ankle Joints

The ankle joint could be calculated from Figure 26. At the lateral maleolus landmark, a vector was created perpendicular to the described plane. The ankle joint was located medial to the landmark by a distance equal to 8.5 percent of the distance between the lateral maleolus and the lateral femoral condyle landmarks.

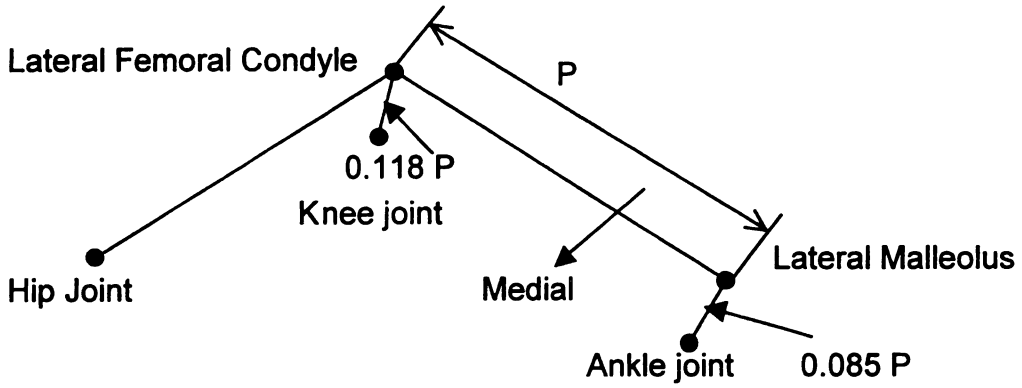

Figure 26 Calculation of Lower Limbs Joints

4.3.7 Wrist Joints

For this application, the wrist landmarks were adequate for accuracy. The measured wrist point was just a mid skin point between the radial and ulnar styloid process.

4.3.8 Elbow Joints

In Figure 27, the landmark on the lateral humeral condyle, mid wrist, and calculated shoulder joint were used to yield a plane for calculating the elbow joint. A vector was created passing through the lateral humeral condyle landmark, perpendicular to the plane mentioned above. The elbow joint was located on the vector medial to the lateral humeral condyle a distance at 15.5 percent of the length between the lateral humeral condyle and wrist landmarks.

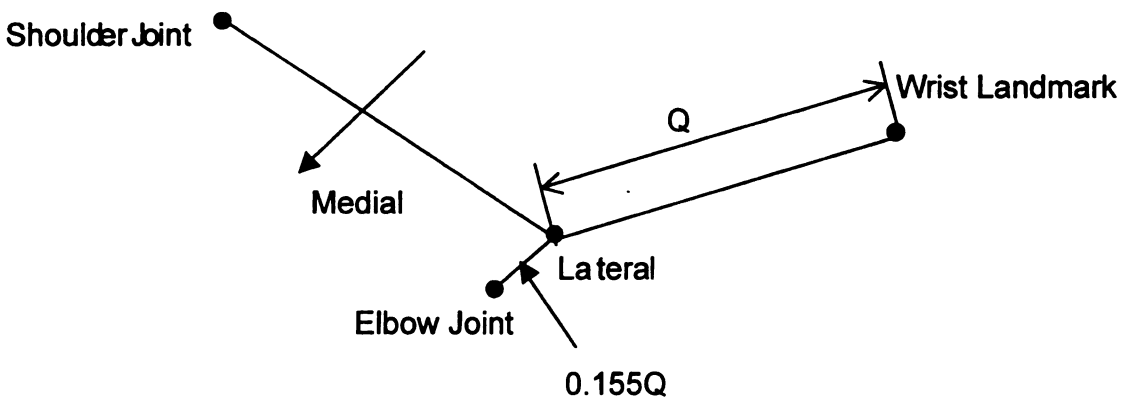

Figure 27 Calculation of Upper Limbs Joints

4.4 Deformed Contours Data Analysis

4.4.1 Methods

To compare different subjects' body shapes, the three-dimensional data were converted to two-dimensional curves as shown in Figure 28.

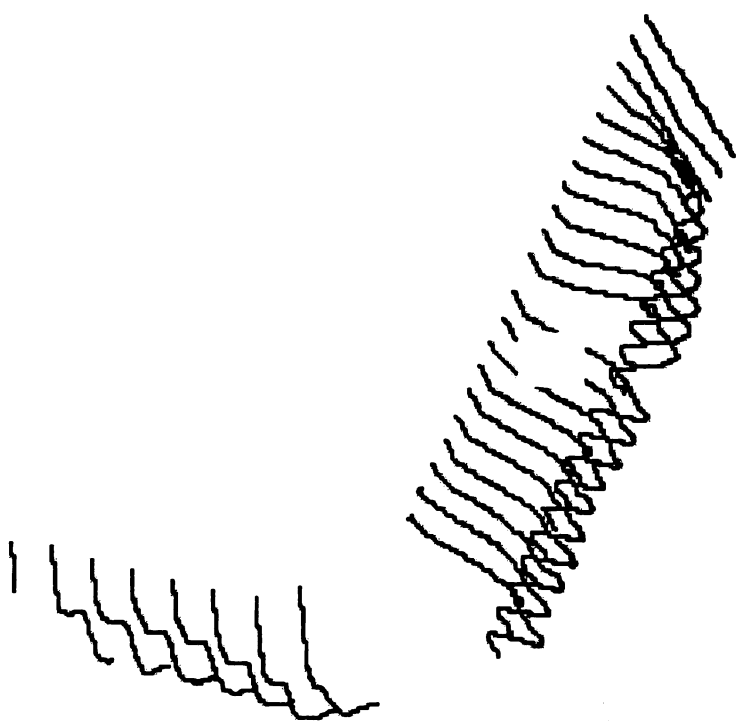

Figure 28 Sliced Thigh Curves (Relative to Left Femur Axis) and Back Curves

4.4.1.1 Analyzing the Thigh and Buttocks Data Surface

After examining the left and right sides of the measured data, it was found that the differences between both sides were within the resolution range of the contour chair, which is 5 mm. So a decision was made to section the left thigh. A local coordinate system was created with its origin at left HJC and x-axis through the knee joint center after the transform of the HJC together and alignment of the left thigh axes for this purpose. Although the subjects were from the same mid-size male subgroup, each of their body parts was not exactly proportional to their stature. Therefore, the thigh axis was defined as from HJC to knee joint center on the same side of the body, and evenly divided into 10 sections for the comparison. Planes that were perpendicular to the left thigh axis started from the left HJC towards knee joint center were created at ten percent of their thigh length (HJC to knee joint) apart from each other to intersect the three-dimensional contour surface. See Figure 29. Because of the limitation of the length of the seat pan of the contour chair, there was seven sections on each subjects' data, and the seventh usually is not long enough to provide all the information needed.

The other way to section the contour surface is by using the vertical plane through the thigh axis to intersect the contour surface to investigate the shape change in the longitudinal direction of the thigh.

The same procedure was applied to the data of the J826 H-Point machine.

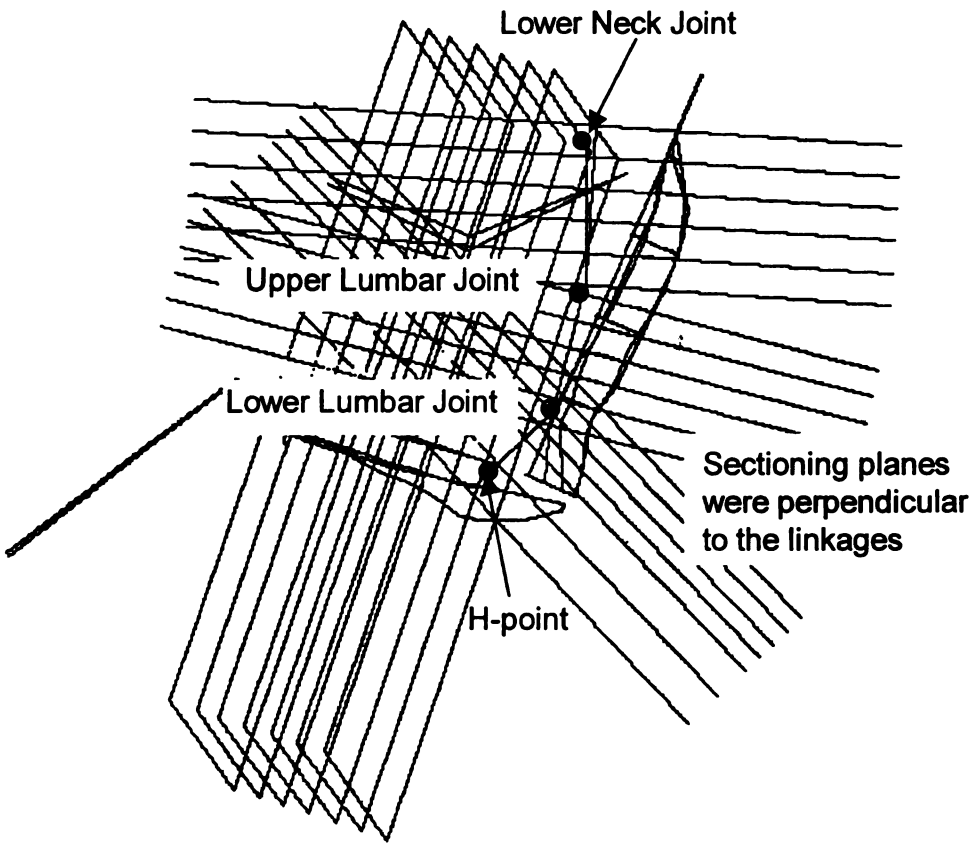

Figure 29 Contour Surface Analyzing Scheme

4.4.1.2 Analyzing the Back Data Surfaces

The anatomical aspects of the back and its motion are much more complicated than the thigh. Future applications of the processed back contour data for input into JOHN program were considered. Sectioning planes were created to intersect the back contour surfaces that were perpendicular to the joint linkages, such as the linkage between lower neck joint and upper lumbar joint of the thorax, or the linkage between upper lumbar joint and lower lumbar joint of the lumbar region. In the pelvic region, the linkage of the hip joint center (the mid-point of right and left HJC and lower lumbar was used as the intersection planes were created. The intersection planes were spaced at a distance of ten percent of the linkage length as seen in Figure 29. Due to the differences in linkage orientations caused by the different postures, using this sectioning method sometimes left a gap between two adjacent regions as can be seen in Figure 28. According to the thoracic and pelvis shape and their relative position to the joint centers, the linkages were extended and a few more planes were created to intersect the back surface to fill the gaps in such a case. Meanwhile these planes also intersected the skeletal links in the torso and lumbar to create the points of intersection with the torso and lumbar links.

4.4.2 Comparing Measured Data and J826 H-point Machine

Based on the measurement data of nine mid-male subjects, a comparison between the J826 machine and measurement data was conducted.

4.4.2.1 The Thigh and Buttocks Data

At each thigh section, there were typically nine curves (from nine mid-sized male subjects) together with the intersection points of the thigh axis to be analyzed. In order to compare the thigh shape relative to the skeletal linkage, the lowest points on the curves to the left buttocks and thigh were determined by creating straight horizontal lines tangent to the curves at the lowest Z position in the coordinate Y-Z plane in the thigh coordinates where X was along the thigh axis. One of the nine lowest points was chosen as a reference point (usually one near the center of the distribution). Then all the curves along with the corresponding intersection points on the thigh axes were translated to coincide with all the lowest points on the curves. From here the relative positions of the intersection points on the thigh axes was calculated and further statistic analysis performed.

These sectioning and analysis methods were employed to compare the measured data of the mid-sized subjects and J826 H-Point machine. The following are the brief results of that part of the study as an example here.

In Figure 30, (A) are the sections under the hip joint center (HJC). The H-point of J826 H-point machine and the average HJC of human subjects were positioned on the same Z level. There is 5 mm difference between the lowest

points on the curves of J826 H-point machine and subjects, i.e., the H-point location of J826 H-point machine is 5 mm higher than the mean location of the subjects' HJC. From (B) and (C) it can be seen that the subject's thigh contours were more symmetrical, flatter and the thigh axes closer to the bottom of the curves compared to the J826 H-point machine. Moreover, the subjects' contours are more prominent under the ischial tuberosities in the medial region.

To study the contours along the length of the thigh, the thigh axes and HJC of all subjects and the J826 H-point machine were overlaid. After the lowest points on all curves were determined and marked, all curves were translated to coincide with the mean lowest point and the marks left in the original positions (Figure 31). This data verified that the H-point of J826 H-point machine was higher than the mean HJC location of human subjects. There is a 10 mm vertical distance between the lowest points of the J826 H-point machine and the mean location of subject contours. The bigger difference occurred near the knees on the curves. The main reason for this is that the subjects' leg lengths are different. The shorter the subjects' lower leg, the more the thigh penetrates the seat pan. The testing protocol controlled the horizontal distance between the H-point and toe-bar on the contour chair.

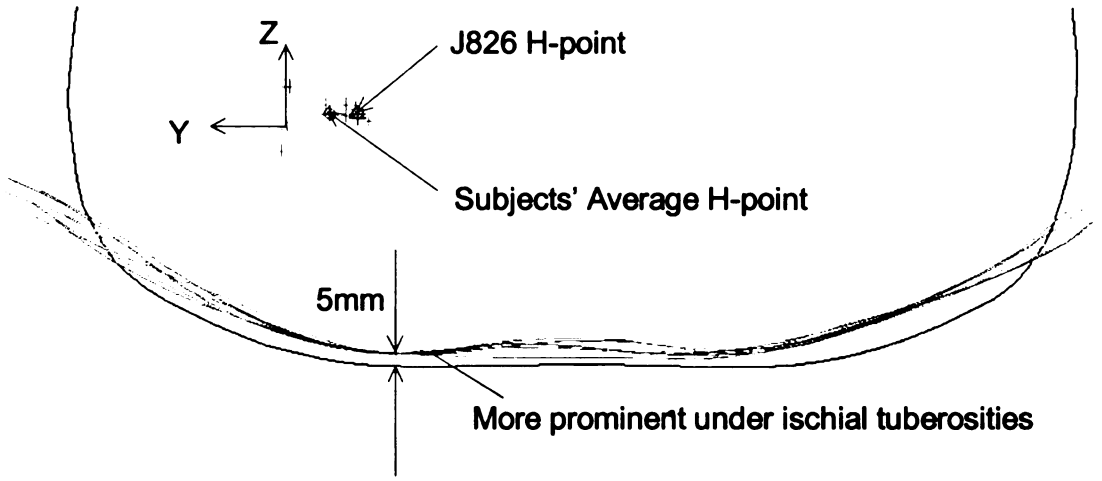

(A) Sections Right Under H-point

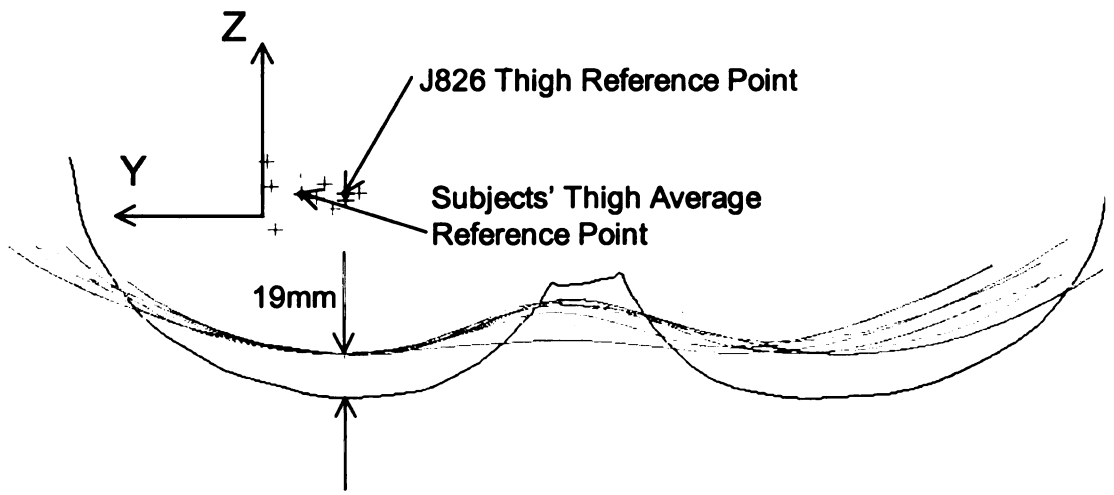

(B) The Fourth Sections from H-point

Figure 30 Sections of J826 H-point Machine and Subjects Contours

(Planes perpendicular to thigh axes)

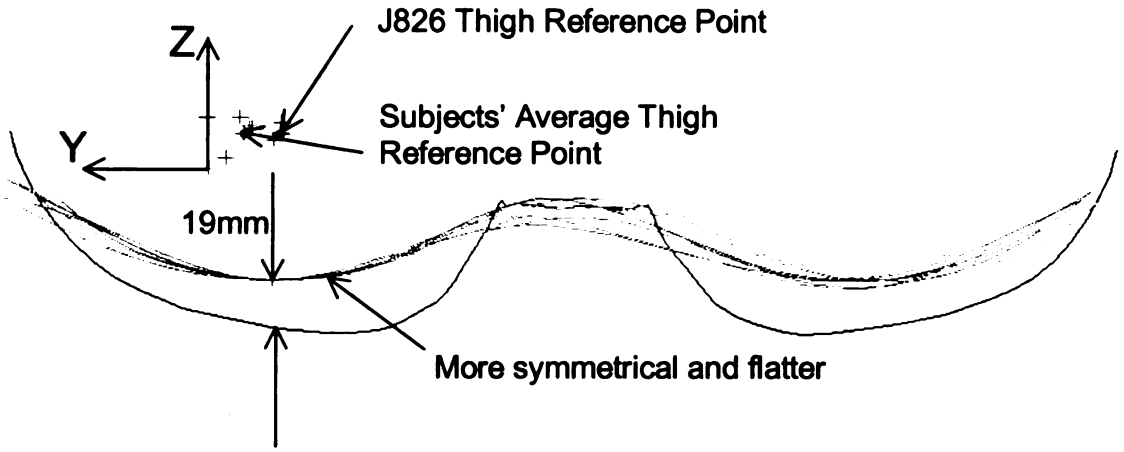

(C) The Sixth Sections from H-point

Figure 30 Continued

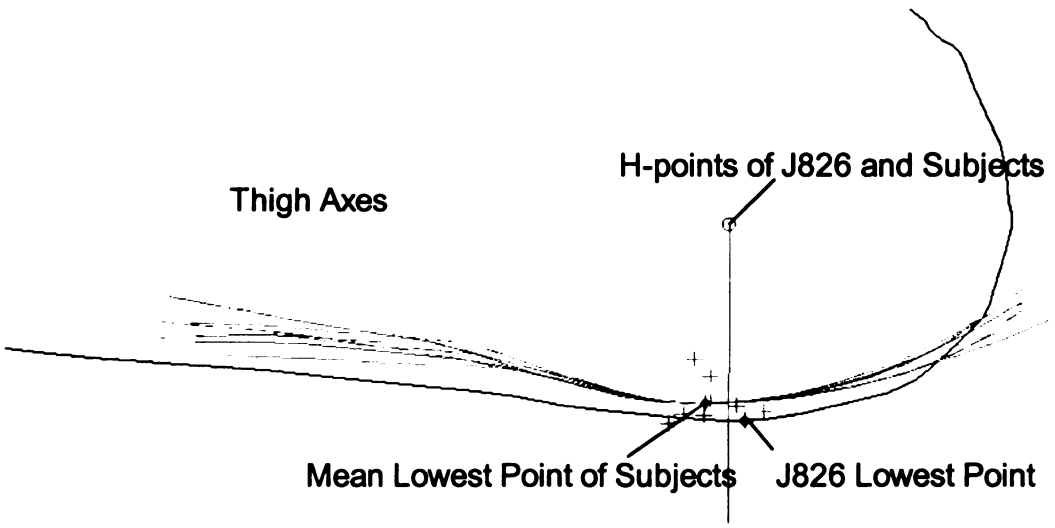

Figure 31 Sections of J826 H-point Machine and Subjects Contours

(Planes vertical through the thigh axes)

4.4.2.2 The Back Contour Data

The approach used to analyze the thigh and buttocks contours was also applied to the back contours. The comparisons between human subject data, the J826 H-point machine, and the UMTRI data [5] were performed.

Figure 32 shows a view from the left upper front of sections at 30 mm intervals above the HJC of the average data from this study for the ASPECT program (so named as ASPECT contour data) and the UMTRI back contours with the limits of seat contact marked for each contour. The limit of seat contact for the UMTRI contours was selected at the divergence of the UMTRI shell and seat contours measured in this study. The region of measured seat contact for the ASPECT contour was wider than with the UMTRI back (Figure 32).

The side views of the ASPECT and SAE back contours are very close (Figure 33). Compared to the ASPECT back contour, the side view of the UMTRI crash dummy seat-shell contour was convex (Figure 33).

Compared to the average posture of the ASPECT subjects, the angle from UL to LN in UMTRI posture was 6 degrees forward. The UMTRI torso seat-shell shape was rotated rearward about its UL joint to provide a composite back contour such that the original UMTRI contour was rearmost below the UL and the rotated UMTRI contour was rearmost above the UL. The side view of this adjusted UMTRI back contour was very close (within a few millimeters) to the ASPECT and the J826 back contours (Figure 34).

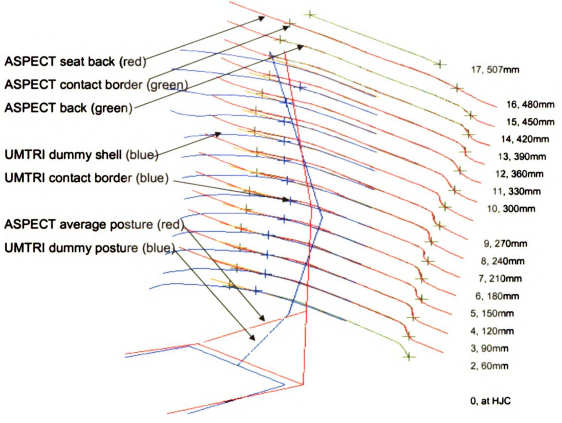

Figure 32 Sections Through the ASPECT and UMTRI Contours with Postures and Contact Edges

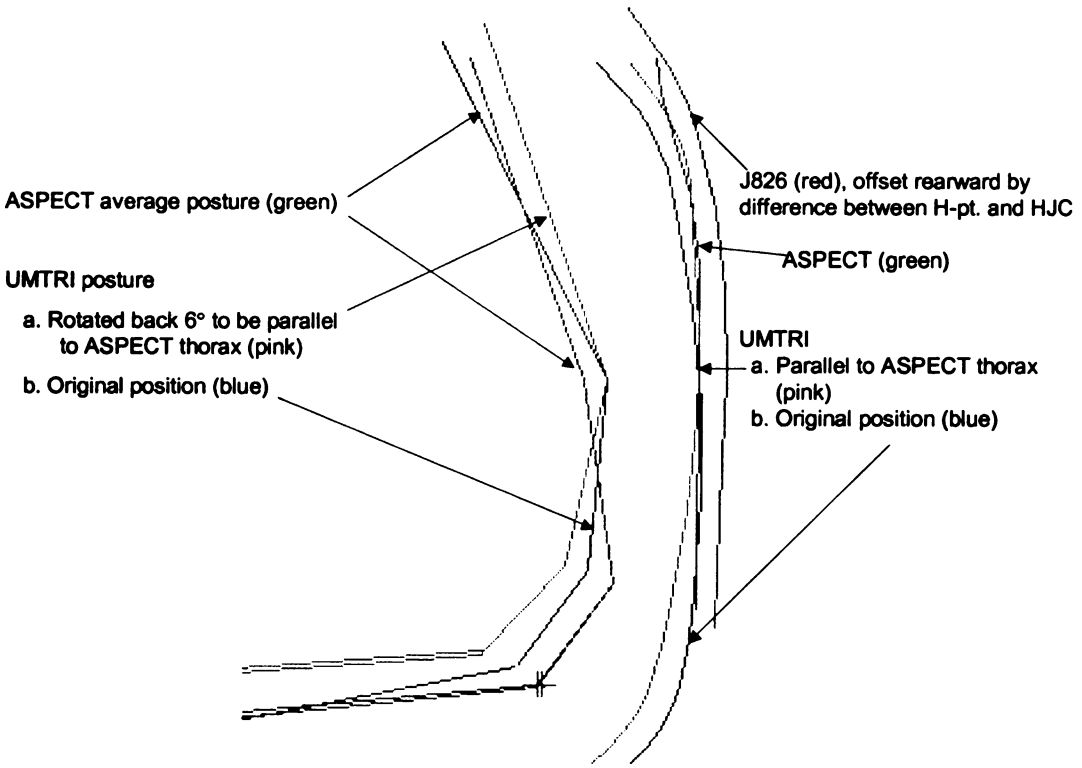

Figure 33 Measured Back Contours

Between Upper Lumbar and Lower Neck Joint

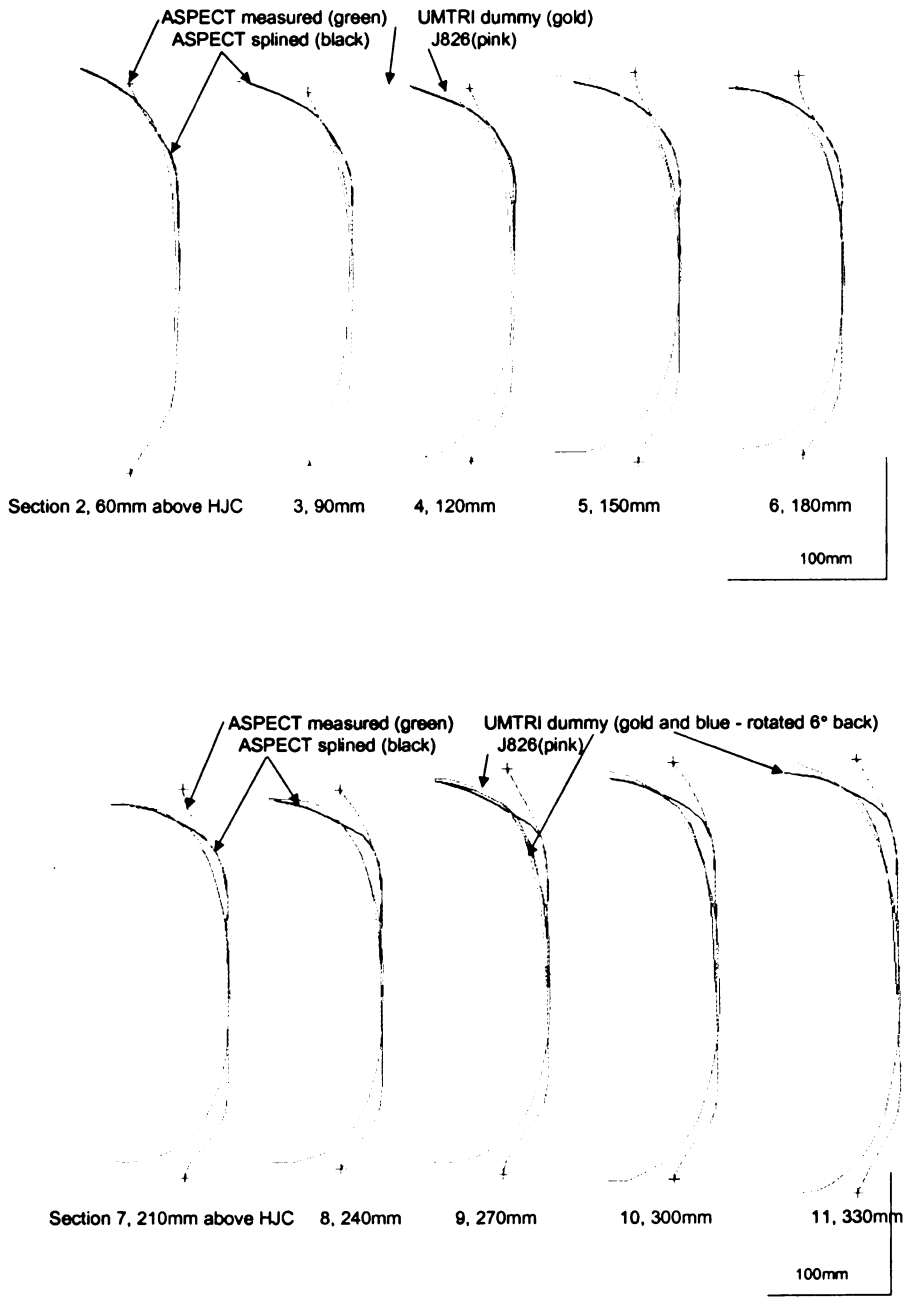

Figure 34 Contour Sections up the Seat Back

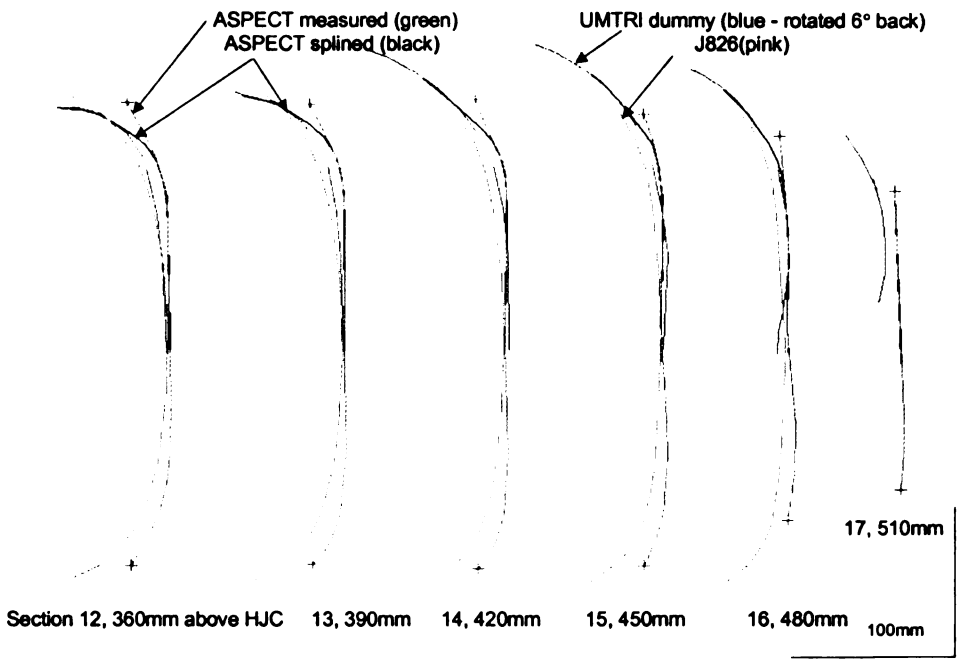

Figure 34 Continued

With the side view back contours aligned as above, X-Y (transverse) sections of the ASPECT back contour were compared to sections of the UMTRI composite torso. A series of sections at 30 mm intervals above the H-point or HJC through the ASPECT, UMTRI, and SAE back contours are shown in Figure 34. Section 2 is the first section shown and it is 60 mm above HJC. For Sections 3 – 7 and 14 – 16, the sides of the UMTRI sections generally appeared to be continuous with lateral parts of the ASPECT contours near the 50 mm X-direction limit of the ASPECT back measurements. In the region of the shoulder on the

sides of Sections 8 – 13, the UMTRI contours were forward of the ASPECT contours probably because of difference in arm placement. For the UMTRI contours the hands were on a steering wheel while the ASPECT contours were measured with the arms closer to the torso. The middle part of the ASPECT measured contours (within approximately Y = ±90 mm) were nearly flat because of the flat seat back of the measurement chair, while the UMTRI contours were more rounded (Figure 34).

In the sections of Figures 34 and 35, the sides of the J826 back contour become apparent in section 4, which is 120 mm above H-point and HJC. Up to section 8 at 240 mm above HJC, just above the upper lumbar pivot, the J826 is more rounded than the ASPECT measured contour or the UMTRI dummy shell, yet the widths of the J826 and UMTRI contours are similar. Above the upper lumbar pivot, the J826 contours continue to be more rounded than the ASPECT contours and the UMTRI contours are generally between J826 and ASPECT. As stated above, the difference between the shape of the ASPECT and UMTRI contours above section 10 was probably due to the forward UMTRI hand position to reach the steering wheel.

As described in the next section, the sides of the UMTRI dummy shell torso were added to the measured ASPECT back contours to provide the ASPECT manikin torso contour. The following is a comparison of the back widths of the J826 torso and ASPECT torso (which uses the sides of the UMTRI dummy shell torso).

The narrowest part of the J826 back is 306 mm at 230 mm above H-point. Comparable dimensions of the UMTRI dummy shell are the width lateral to the bottom of the 10th rib which is 312 mm at 160 mm above HJC and the abdominal breadth of 325 mm and waist breadth at the umbilicus 314 mm. These dimensions indicate that J826 is approximately 6 mm narrower than the new ASPECT back.

The widest part of the J826 back is 392 mm at 430 mm above H-point. On the UMTRI dummy shell, the width between the rear upper margins of the armpit (posterior Scye landmark) is 394 mm wide at 370 above HJC. This is nearly the same as the J826 widest part. The dimensional differences between J826 and UMTRI back widths are small, and the ASPECT back is flatter in cross-section (seen below in Figure 35).

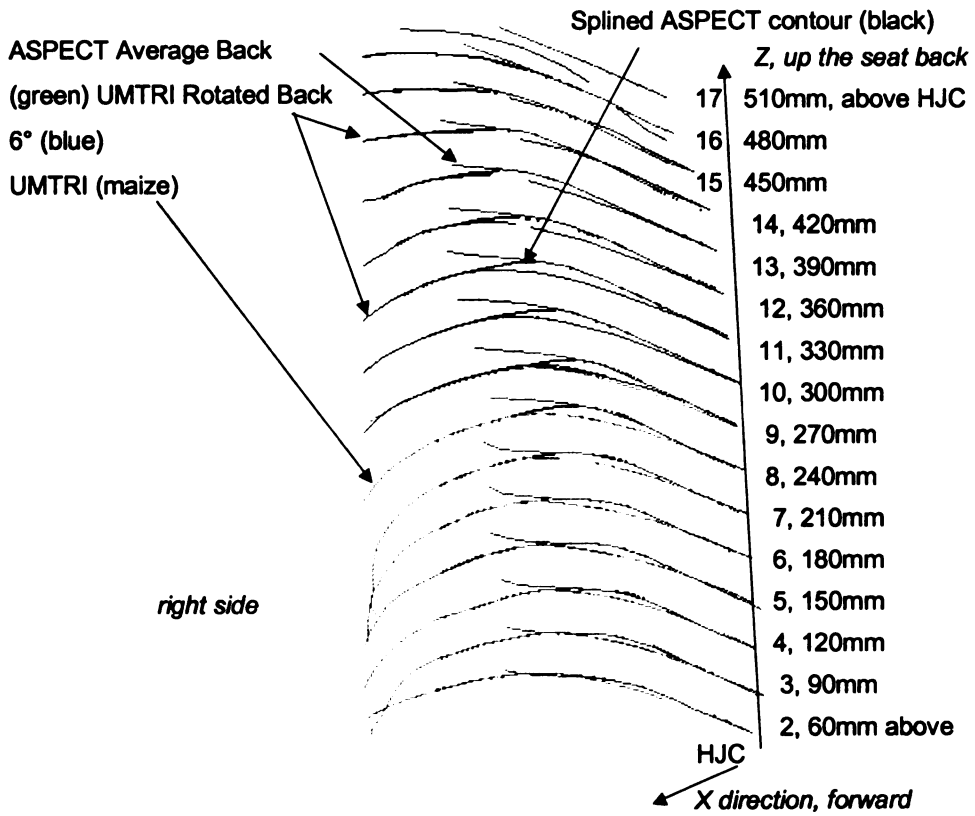

Figure 35 Comparison between ASEPCT and UMTRI Back Contour

4.5 Defining Mid-male Contour

Even though humans are not precisely symmetrical, the posture and contours for manikins or the computer models ought to be symmetrically defined [24]. By creating a central, mid-sagittal plane of symmetry, the contour surfaces were separated into right and left sides. The right side and its reflection were used for the development of the manikin contours. After the right side of the contour was reflected about the plane of symmetry, the right and left sides were nearly identical, with a difference of only approximately ±1 mm. This small difference is less than measurement accuracy and supports the decision to develop symmetrical contours.

There were two versions of mid-male contours that were defined in this section, and they were ASPECT mid-male and TecMath mid-male contours.

4.5.1 Defining The ASPECT Mid-male Contours

In the ASPECT program, there was a need to reevaluate and revise the J826 hardware and procedures as stated earlier in the Chapter 1. Because the contact contours of the new manikin were very important in determining the interactions with seat pans and resulting measurements of H-point location and seat pan angle, a study of the contact contours between subjects and the seat support surface was carefully conducted, which resulted in the creation of the new ASPECT manikin contour of mid-male size.

4.5.1.1 Thigh and Buttocks Contours

The thigh and buttocks surface contour of the new manikin was defined by selecting one of the mid-male subject's contours that was consistently in the middle of the small range of variation of the nine subjects' contours. The contour then was separated right from left; the right side and its reflection were used in the ASPECT thigh and buttocks contours. An averaged contour would have been similar to, yet may not be as realistic as, this single subject's contour. The ASPECT thigh and buttocks contours are shown in Figure 36.

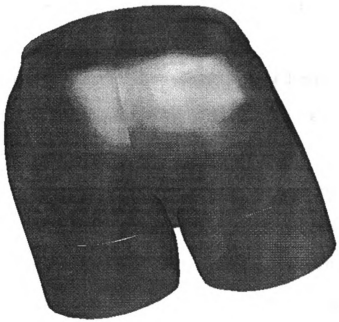

Figure 36 ASPECT Symmetrical Buttocks and Thigh Contours

4.5.1.2 Back Contour

Compared to the buttocks and thigh, back posture and contours are more complex because there are a greater number of mobile segments, leading to greater potential for postural and contour variability.

Although the subjects were chosen to be mid-size males, there were variations in their skeletal anthropometric dimensions and postures. To reduce the effects of these variations and to analyze the subjects' back contours for the generation of the single manikin contour being developed, the following analysis steps were accomplished:

1. The measured back contour data for each subject were splined to yield a surface.
2. The splined back contour for each subject was rotated and translated so that the mid-HJC was aligned on the same axis and the LN was in the same plane.
3. A coordinate system was established (Figure 37) such that:
    a. The X-axis was forward and perpendicular to the seat back plane of the measurement chair. The posture data for each subject was positioned so that the point midway between the hip joint centers (mid-HJC) was on the X-axis. The origin of the axis system was in the plane of the seat back of the measurement chair.
    b. The Z-axis was upward in the seat back plane. The posture data for each subject was positioned so that the perpendicular projection

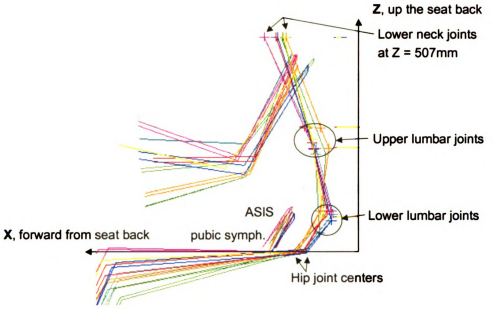

Figure 37 Torso Length Scaled In Z-Direction

of the lower neck joint (LN) to the seat back plane was on the Z-axis.

c. The Y-axis was perpendicular to X and Z, in the seat back plane, and to the left.

In this coordinate system, the mid-HJC of each subject was placed on the X-axis and the lower neck joint (LN) was placed in the X-Z plane.

4. The Z distance from the mid-HJC to the LN was averaged (Z_{av} = 507 mm), and the Z values of the posture and splined contour data for each subject were scaled to the average.

By these steps, the mid-HJC of each subject was at (X_i, 0, 0) where X_i was X-coordinate value of each subject's HJC. The LN of each subject was (X_j, 0, Z_{av}) where X_j was the X-coordinate value of each subject's LN and Z_{av} is the average Z coordinate value for all the subjects. The Y coordinate values were not altered but were within a few millimeters of zero.

The X values of the HJC and LN were averaged and the X, Y, and Z values of the LL and UL were averaged to yield an average torso posture for the back contour subjects.

The lower backs of the subjects' were all against the flat seat back of the measurement chair so that their measured contours in this region were very similar (Figure 38). In the upper torso (Figure 39), the contours varied because

the upper torso postures of the subjects varied primarily due to different angles of their thorax from vertical.

The depth of ASPECT back contour measurements was limited to 50 mm in the X direction perpendicular from the flat seat back. The measured and splined seat back contours for each subject were sectioned with X-Y (transverse) planes that were 30 mm apart in the Z-direction starting 60 mm above HJC, which was near the bottom of the measured back data. At seventeen points (sixteen segments) equally spaced along each contour section, the X and Y values of the contours for each section were averaged to generate an average back contour. There were very small differences within two millimeters in the Y values between subjects, and these were averaged by this procedure. The average contour sections are shown in Figures 40 and 41. The ASPECT back, buttocks, and thigh contours are shown in Figure 42. ASPECT manikin is illustrated in Figure 43.

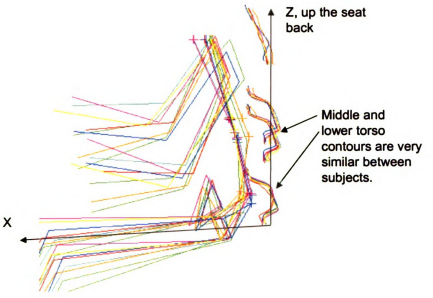

Figure 38 Measured Contour Curves
from Mid Thorax to End of Lumbar

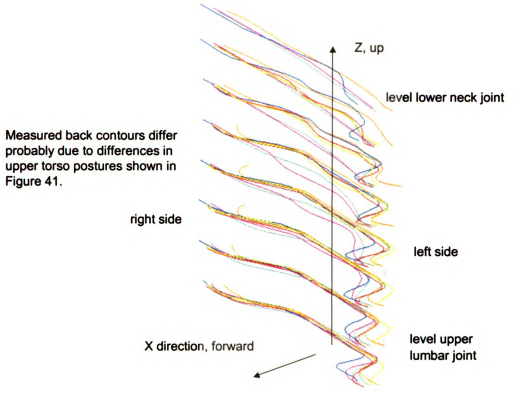

Figure 39 Measured Back Contours between Upper Lumbar Joint And Lower Neck Joint

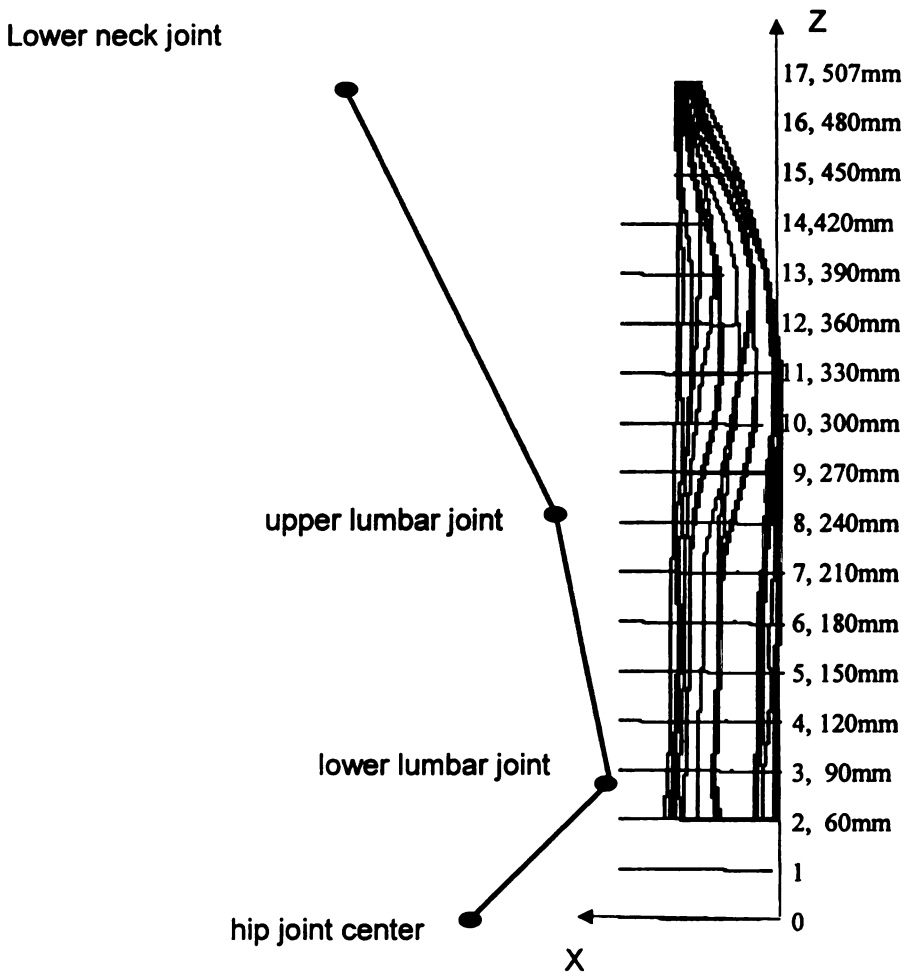

Figure 40 Average Back Contour And Posture Side View

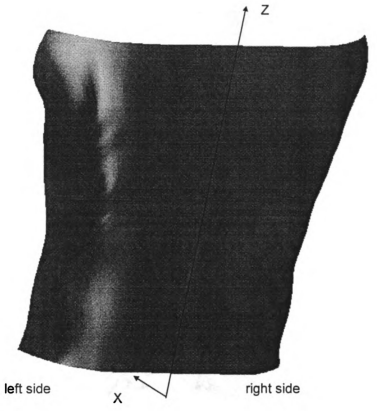

Figure 41 Average Back Contour Left Rear View

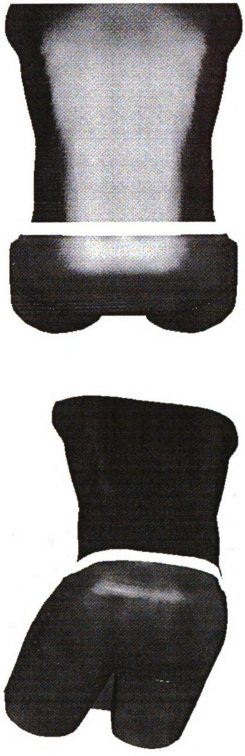

Figure 42 ASPECT Back, Buttocks and Thigh Contour Surfaces

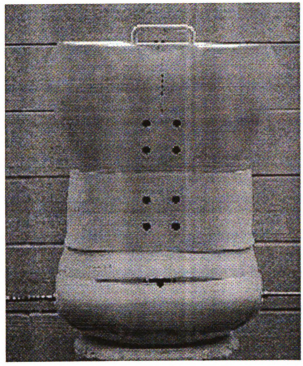

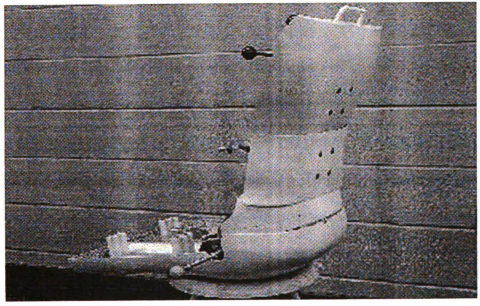

Figure 43 ASPECT Manikin

To define the edge of contact between the seat and body, points on the contour sections were chosen that were the first points from the sides with an X value that was clearly less the maximum X value for that section. The X-value of the chosen point was typically near 40 mm. Actual contact was between this chosen point and the next point to the side, which was at the maximum measurable X value (near 50 mm). The contours lateral to these chosen points would be affected by inclusion of some points that were not in contact with the subject. However, contours splined to the edge of known contact were found to be less than 1 mm different in X-value when compared to contours splined with points beyond the contact edge. The contact edge for the average ASPECT back contours is shown in Figure 32 with the edge of seat back contact for the UMTRI dummy shells.

4.5.2 Defining The RAMSIS Mid-male Contours

Boughner [7] developed a three-dimensional skeleton that represented mid-size males and was based on the UMTRI dummy anthropometrics [5] and articulated according to the work of Haas [4]. To his skeletal model, Boughner added shapes to represent major muscle groups. To represent the mid-size male, Frost [10] added skin surfaces to the Boughner model so the skin surfaces articulated with the skeletal linkage. In developing this contour, Frost considered both the skeletal and muscle geometries of Boughner [7] and the surface contours of UMTRI [5]. So, the Frost contours included transverse section curvatures that were believed to be more representative of people's back than

the flatter UMTRI contour that was based on the shape of an automobile seat in contact with their human subjects. Frost also scaled the mid-male contour based on anthropometric dimensions to represent small women and large men.

Because the ASPECT contour of this study was based on data measured in a flat-backed seat fixture, the resulting contours appeared to be flat. For aesthetics in the development in this study of the contours for the RAMSIS model [6], the ASPECT contours were adjusted by a few millimeters, less than measurement variability. For this, the contours from Frost [10] and UMTRI [5] and the APSECT contours from this study were considered. The side view (sagittal plane) shape of the Frost and UMTRI contours were nearly identical but the Frost contour was thought to have more human-like transverse contours, so the Frost contour was selected. To develop the RAMSIS contour, the postural linkages for the Frost and ASPECT contours were aligned and the differences between these contours were averaged to produce the RAMSIS contour.

CHAPTER 5 CONTOUR SCALING FOR LARGE MALE AND SMALL FEMALE

5.1 Introduction

Since the early 1960s, both physical and digital models of mid-sized males, such as SAE practice J826 [1] and the JOHN model [7], have been extensively used in seat design and evaluation. However, there are needs for tools representing other groups of people in different height and weight ranges. Among those most needed are models of 5th percentile small female and 95th percentile large male for applications to confirm that seats will accommodate these extreme sizes of people. Because of the extensive and prevailing application of the mid-sized male models, it became very meaningful to explore the correlations or the relations between mid-male and small female, and mid-male and large male. Frost [10] and Robbins [5] used the scaling method to create contour models for small females and large males from the mid-male data, but the scaling method was never validated by data from human subjects. Therefore in this study, mid-male contours from experimental data were employed to create contours for small females and large males by scaling. Furthermore, the measured data of large males and small females were utilized to validate the scaling methodology.

If a feasible scaling system could be established, then the contours of any percentiles could be created from the mid-sized male contours by using the scaling method. This would be a very efficient way to create a contour for any size individual.

5.2 Development of Scaling Factors

The seat contact contours of three groups of human subjects (small women, mid-size men, and large men) were measured in this study along with anthropometric dimensions for these three size groups. As described previously, a seat contact contour was developed to represent mid-size men and was used in the development of the ASPECT manikin and for RAMSIS model development [6].

In computer modeling, it is easily possible to scale the size of shapes so that seat contact contours for different size people could be generated based on their sizes. In this section, scaling factors are described for the purpose of scaling the mid-size male contours to the size of the contours for small women and large men. These scaling factors were based on values of anthropometric dimensions measured on the surfaces of the human subjects and internal skeletal linkage dimensions that were based on the external anthropometric dimensions. The approach to evaluating agreement between the contours scaled from the mid-size male to the other size people was to compare the scaled contour for each individual subject to the measured contour for that subject.

Scaling factor F in one specific body direction was defined as the individual subject's body dimension D_s divided by mid-sized male body corresponding dimension D_m, i.e.,

$$F = \frac{D_s}{D_m} \qquad (9)$$

There were three scaling factors for each body segment corresponding to scaling in length, depth, and breadth directions, for instance, F_l, F_d, and F_b, respectively.

5.2.1 Thoracic

In the thorax area, three scaling factors are defined for body dimensions in breadth as F_{tb}, in depth as F_{td}, and in length as F_{tl}.

$$F_{tb} = \frac{D_{stb}}{D_{mtb}} \tag{10}$$

$$F_{td} = \frac{D_{std}}{D_{mtd}} \tag{11}$$

$$F_{tl} = \frac{D_{stl}}{D_{mtl}} \tag{12}$$

Where D_{stb}, D_{std}, and D_{stl} are subject's chest breadth (reference number 32 in [14]), chest depth (36), and chest length, respectively. The chest length here is the average distance between the lower neck joint and upper lumbar joint. D_{mtb}, D_{mtd}, and D_{mtl} are the chest breadth, chest depth, and distance between the lower neck and upper lumbar joint of the mid-male contour, respectively.

5.2.2 Lumbar

To scale the mid-sized male contour to the desired subject's contour in this area, scaling factors F_{lb}, F_{ld}, and F_{ll} are used for the lumbar area scaling.

$$F_{lb} = \frac{D_{slb}}{D_{mlb}} \quad (13)$$

$$F_{ld} = \frac{D_{sld}}{D_{mld}} \quad (14)$$

$$F_{ll} = \frac{D_{sll}}{D_{mll}} \quad (15)$$

In equations 13 to 15, D_{slb}, D_{sld}, and D_{sll} stand for subject's waist breadth (112), waist depth (115), and length between the upper and lower lumbar joints, D_{mlb}, D_{mld}, and D_{mll} for the waist breadth (112), waist depth (115), and the distance between the upper and lower lumbar joints of the mid-male contour in that order.

5.2.3 Pelvis

In the same fashion as for the thorax and lumbar areas, three scaling factors are defined for the pelvic area as F_{pb}, F_{pd}, and F_{pl}.

$$F_{pb} = \frac{D_{spb}}{D_{mpb}} \quad (16)$$

$$F_{pd} = \frac{D_{spd}}{D_{mpd}} \quad (17)$$

$$F_{pl} = \frac{D_{spl}}{D_{mpl}} \quad (18)$$

Where D_{spb}, D_{spd}, and D_{spl} are used for subject's sitting hip breadth (66), buttocks depth (24), and the distance between the lower lumbar joint and the midpoint of HJCs, and D_{mpb}, D_{mpd}, and D_{mpl} for the sitting hip breadth (66), buttocks depth (24), and distance between the lower lumbar joint and midpoint of HJCs of the mid-male contour, correspondingly.

5.2.4 Thigh

For the thighs, scaling factors F_{thib}, F_{thid}, and F_{thil} are defined for the thigh breadth, depth, and length in the following way:

$$F_{thib} = \frac{D_{spb}}{D_{mpb}} \tag{19}$$

$$F_{thid} = \frac{D_{spd}}{D_{mpd}} \tag{20}$$

$$F_{thil} = \frac{D_{sthil}}{D_{mthil}} \tag{21}$$

In the equations 17-19, D_{sthil} is the average distance between the HJCs and knee joints of a subject, D_{mthil} is the distance between the HJC and knee joint of the mid-male contour. For the thigh region, the pelvis's breadth and depth are utilized to scale the thigh shape for both the subject and the RAMSIS mid-male.

5.3 Scaling Procedures and Results

Once the scaling factors for each body segment had been defined, the values of the scaling factors were calculated and are tabulated in Table 12 for large males and in Table 13 for small females in Appendix A.

Before the scaling procedures started, there were four local coordinate systems to be defined.

1) Thorax coordinate system was originated at upper lumbar joint, positive X-axis pointing to lower neck joint, positive Y-axis from left to right. The Z-axis was determined by the existing axes by the right-hand rule.

2) Lumbar coordinate system started with the X-axis from lower lumbar joint toward upper lumbar joint, Y-axis pointing to right from left, and the X and Y directions decided the Z-axis by the right-hand rule.

3) Pelvic coordinate system origin was located midway between the two hip joint centers with X-axis pointing to lower lumbar joint, Y-axis pointing from left to right, and the Z-axis was then decided by these two X and Y axes.

4) Thigh coordinate system was originated at the mid point between right and left hip joints. Positive X-axis pointing toward the midway of the two knee joint centers, positive Y-axis pointing from left to right, and Z-axis was decided by the X- and Y-axes.

5.3.1 Small Female

In the scaling process, the RAMSIS mid-sized male contour and posture were scaled down to each small female subject's contours.

First the thorax contour of the RAMSIS mid-male was translated to coincide with the upper lumbar joint for the subject. Then the mid-male thorax contour and the skeletal linkage were scaled down to the small subject's contour in the local thorax coordinate system using the previously defined scaling factors.

Finally the scaled body segment and the posture linkage were aligned with the subject's linkage connecting lower neck joint and upper lumbar joint.

The lumbar contour of the RAMSIS mid-male contour was repositioned at the lower lumbar joint of the small female subject. In the local lumbar coordinate system, the lumbar contour of the mid-male then was scaled down according to the small female subject's anthropometric data. The scaled lumbar and the posture were then rotated to the subject's posture linkage.

The pelvic contour and the posture linkage of the RAMSIS mid-male was relocated at the center of the right and left H-points. The pelvic contour and posture were scaled down to the small female subject's dimension. The contour and linkage were also rotated to align to the small subject's.

All of the scaled contour curves from small female subject 1 are presented together with the curves from measured contours for that subject in Figure 44 for a back view and in Figure 45 for an oblique view. The curve at each individual section is illustrated in Figure 46 in detail. By visual inspection, the differences between the two sets of contour curves are within less than 10 mm. Considering the accuracy of contour and skeletal landmark measurement, the two sets of curves match with each other to an acceptable degree. The rest of the small female subjects' results are documented in the Appendix B. The similarity of these curves is analyzed and discussed in section 5.4 below.

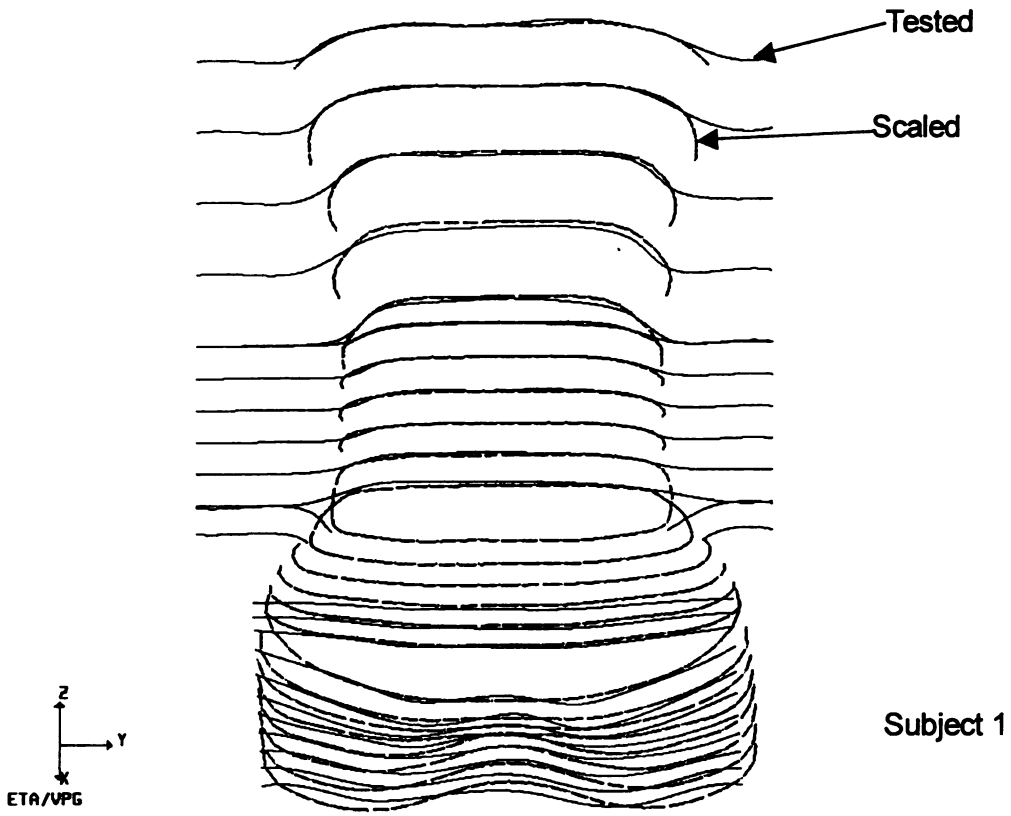

Figure 44 Tested and Scaled Subject 1's Contour Curves, rear view

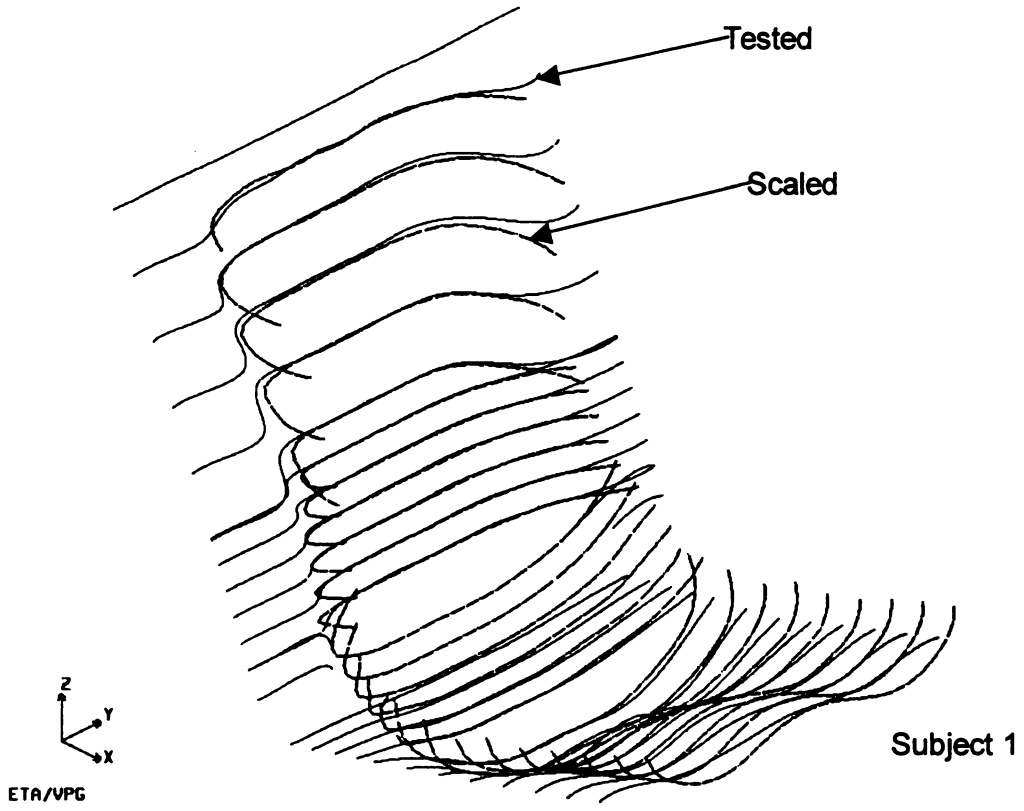

Figure 45 Tested and Scaled Subject 1's Contour Curves, oblique view

SF1 Thorax 2nd

SF1 Thorax 3rd

SF1 Thorax 4th

Figure 46 Tested and Scaled Contour Curves at Each Section of Small Female Subject 1

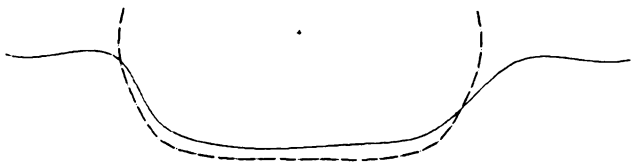

SF1 Thorax 5th

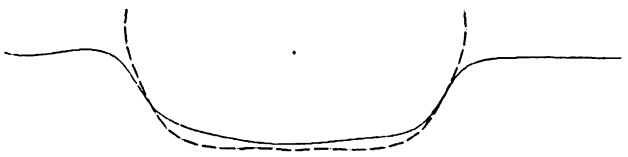

SF1 Thorax 6th

Figure 46 Continued

SF1 Lumbar 1st

SF1 Lumbar 2nd

SF1 Lumbar 3rd

Figure 46 Continued

SF1 Lumbar 4th

SF1 Lumbar 5th

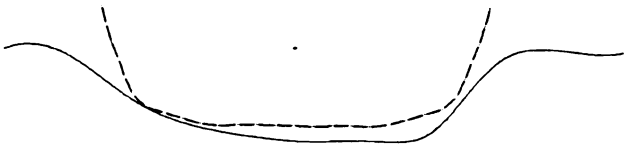

SF1 Lumbar 6th

Figure 46 Continued

SF1 Pelvic 1st

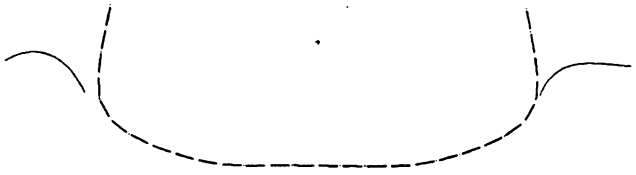

SF1 Pelvic 2nd

SF1 Pelvic 4th

Figure 46 Continued

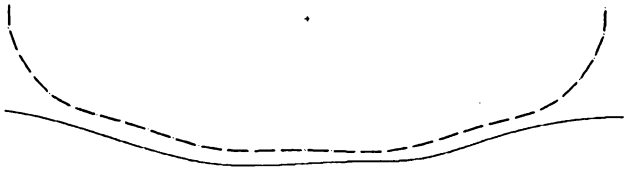

SF1 Pelvic 5th

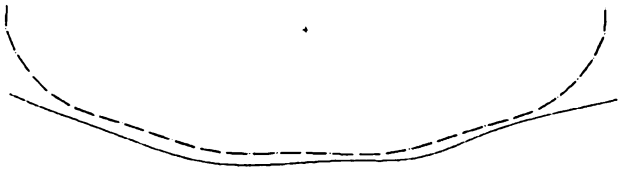

SF1 Pelvic 6th

Figure 46 Continued

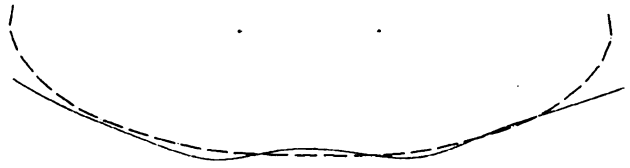

SF1 Thigh 1st

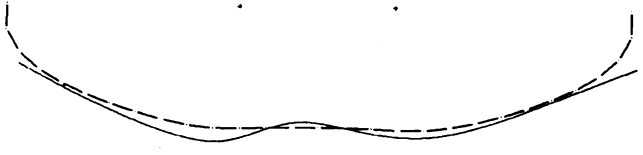

SF1 Thigh 2nd

SF1 Thigh 3rd

Figure 46 Continued

SF1 Thigh 4th

SF1 Thigh 5th

SF1 Thigh 6th

Figure 46 Continued

SF1 Thigh 7th

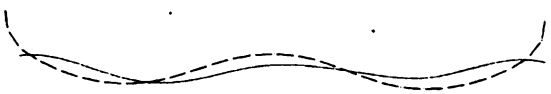

SF1 Thigh 8th

Figure 46 Continued

5.3.2 Large Male

In the scaling process, the RAMSIS mid-sized male contour and posture were scaled to each large male subject's contours.

First the thorax contour of the RAMSIS mid-male was translated to coincide with the upper lumbar joint of the subject. A local thorax coordinate system was created at upper lumbar joint, X-axis pointing from upper lumbar joint towards lower neck joint and Y axis in lateral direction. Then the mid-male thorax contour was scaled up to the large male subject's contour in the local thorax coordinate system, using the previously defined scaling factors. After this the scaled contour and posture were then aligned with the subject's thoracic skeletal axis system.

The lumbar contour of the RAMSIS mid-male contour was repositioned at the lower lumbar joint of the large male subject. In the local lumbar coordinate system, which was originated at lower lumbar joint and with X axis pointed from lower to upper lumbar joint center and Y axis goes laterally. The lumbar contour of the mid-male was then scaled up according to the large male subject's anthropometric data. The scaled lumbar and the posture were rotated to line up with the subject's posture linkage.

The pelvic contour of the RAMSIS mid-male was relocated at the center of the right and left H-points. Next, the pelvic contour was scaled up to the large male subject's dimension in the local pelvic coordinate system. The mid-point of the right and left H-points was the center of the local pelvic coordinate system, and its X-axis was in the direction of the mid point to lower lumbar joint, Y in the

lateral direction. Then the scaled pelvic contour and the posture were brought into the line of subject's posture linkage.

The rest of the other large males' results are documented in the Appendix C.

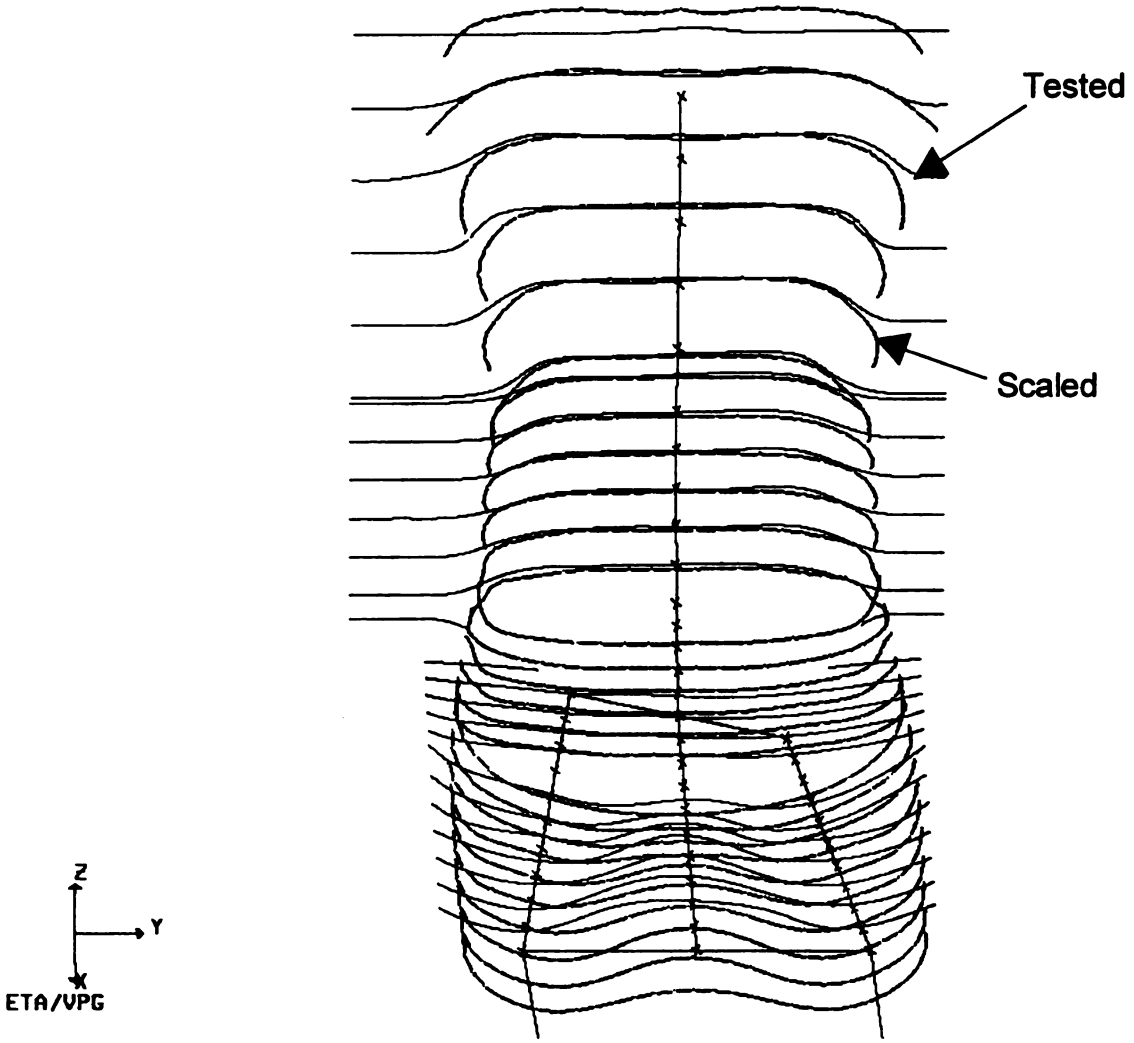

Figure 47 Measured and Scaled Subject 1's Contour

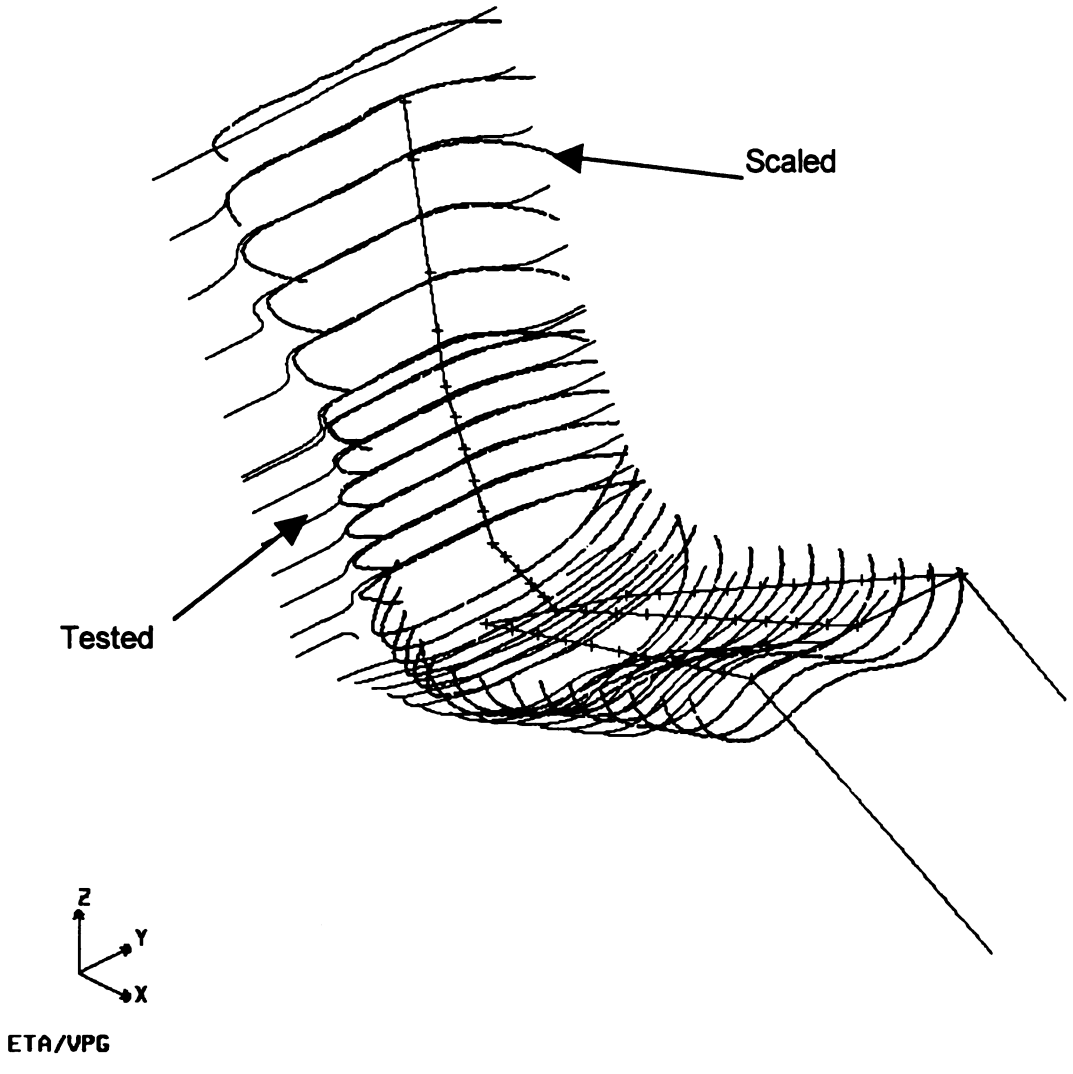

Figure 48 Measured and Scaled Subject 1's Contour

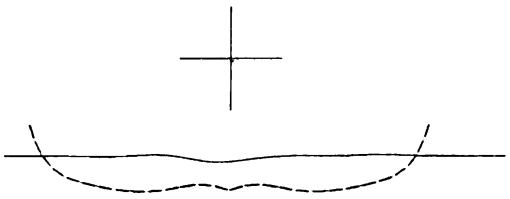

LM1 Thorax 1st

LM1 Thorax 2nd

LM1 Thorax 3rd

Figure 49 Tested and Scaled Contour Curves at Each Section of Large Male Subject 1

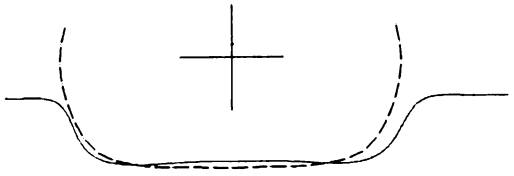

LM1 Thorax 4th

LM1 Thorax 5th

LM1 Thorax 6th

Figure 49 Continued

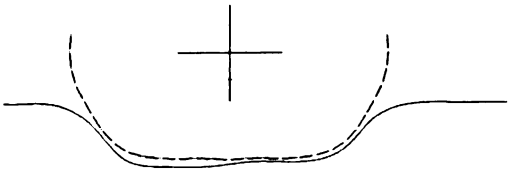

LM1 Lumbar 1st

LM1 Lumbar 2nd

LM1 Lumbar 3rd

Figure 49 Continued

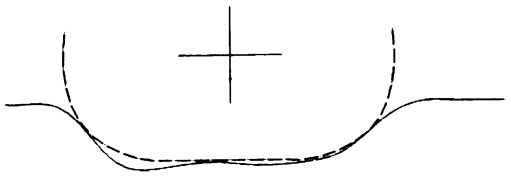

LM1 Lumbar 4th

LM1 Lumbar 5th

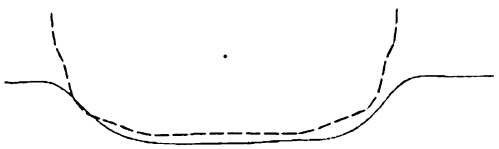

LM1 Lumbar 6th

Figure 49 Continued

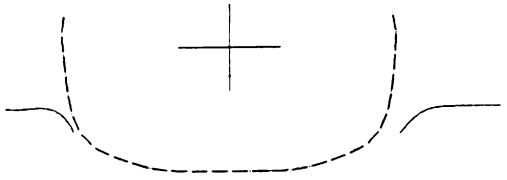

LM1 Pelvis 1st

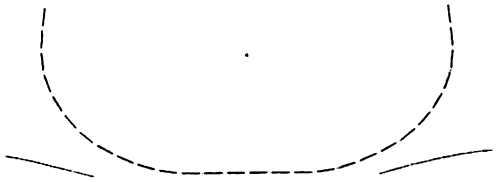

LM1 Pelvis 2nd

LM1 Pelvis 3rd

Figure 49 Continued

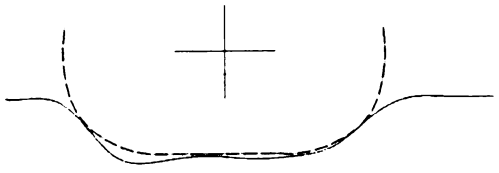

LM1 Pelvis 4th

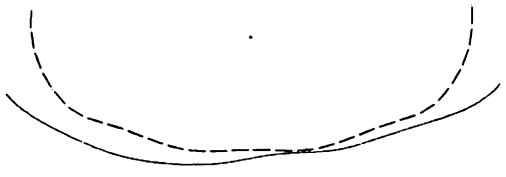

LM1 Pelvis 5th

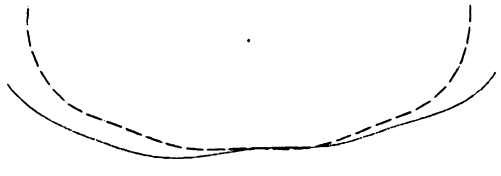

LM1 Pelvis 6th

Figure 49 Continued

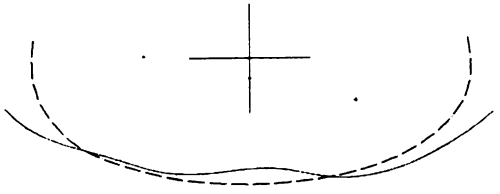

LM1 Thigh 1st

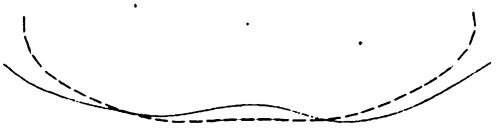

LM1 Thigh 2nd

LM1 Thigh 3rd

Figure 49 Continued

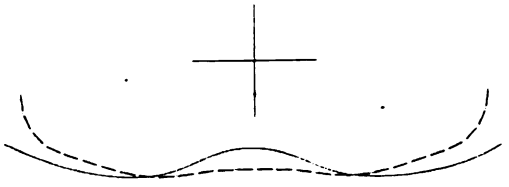

LM1 Thigh 4th

LM1 Thigh 5th

LM1 Thigh 6th

Figure 49 Continued

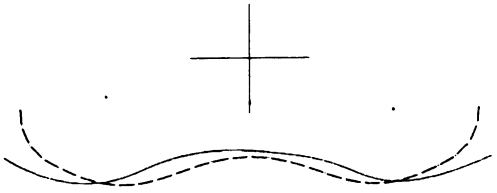

LM1 Thigh 7th

Figure 49 Continued

5.4 Correlation Comparison Between Measured and Scaled Contours

When comparing each pair of curves of measured and scaled contours, the scaled curves typically matched to the measured contours within less than 15 mm. A further numerical correlation analysis [25] was performed to assess the quantitative resemblance between the scaled and the tested contour curves at selected sections of the contours.

5.4.1 Methods

Three aspects of the geometric resemblance between the scaled and tested curves of the contours were considered. They were differences between scaled and tested curves, shape resemblances, and corridors with one and two standard deviations [26, 27]. The differences showed how far apart the curves were from each other numerically and graphically. The coefficient of the correlation was employed in the analysis of the shape resemblance as defined in the following section. The corridors with standard deviations described how closely the scaled contour curves were distributed in the space.

The scaled and tested curves have respective magnitudes X_S, and X_M. So the coefficient of the correlation between the scaled and tested curves was S_R defined as follows [26, 27]:

$$S_R = \frac{\int_a^b X_s X_M dx}{\sqrt{\int_a^b X_S^2 dx \int_a^b X_M^2 dx}} \qquad (22)$$

or,

$$S_R = \frac{\sum X_S X_M \delta x}{\sqrt{\sum X_S^2 \delta x \sum X_M^2 \delta x}} \qquad (23)$$

If $S_R = 1$, the curves with magnitudes of X_S and X_M had identical shapes. The values of S_R were between 1 and 0. When $S_R = 0$, it means that the two compared are not related to each other.

For simplicity of comparisons and reduction of the amount of computational work, curves from sections 3, 4, and 6 in the thoracic region, 2, 4, and 6 in the lumbar region, and 4, 5, and 6 in the pelvis region, and 1, 4, and 7 in the thigh region were quantitatively analyzed. The procedures (MatLab program) [28] were used to perform the correlation analysis.

5.4.2 Correlation of Large Male and Small Female Contours

5.4.2.1 Differences

The first comparison was to find out the difference, d, in the X direction between tested and scaled contour curves. Figure 50 and Figure 51 show typical plots of the difference (d) in the midsections of thorax, lumbar, pelvis, and thigh for large males and small females. In the measured region of the body contour, the contour data were linearly interpolated every millimeter apart to provide a continuous curve. Then, at the same corresponding locations, the differences between points on the measured contours and the scaled contours were found and plotted. Almost all the differences (d) were within 10 to 12 mm. The rest of

the difference results are in the Table 6 for large males and Table 8 for small females, and the standard deviations of the differences can be found in the Table 7 and Table 9 for large males and small females, respectively.

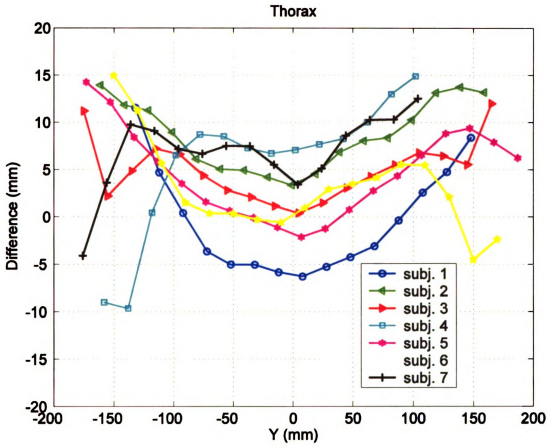

(A) At Mid Thorax – Large Males

Figure 50 Typical Difference Curves between Scaled and Measured Contour at Mid sections of Large Males

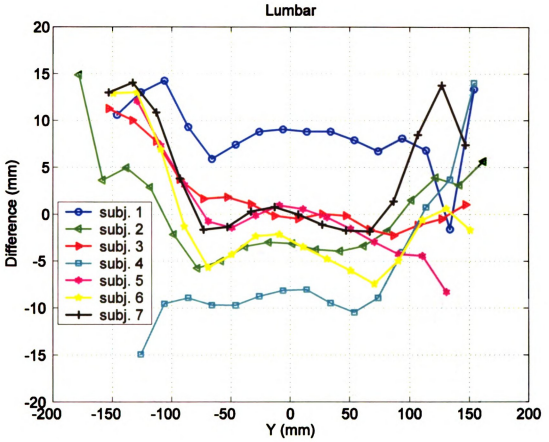

(B) At Mid Lumbar – Large Males

Figure 50 Continued

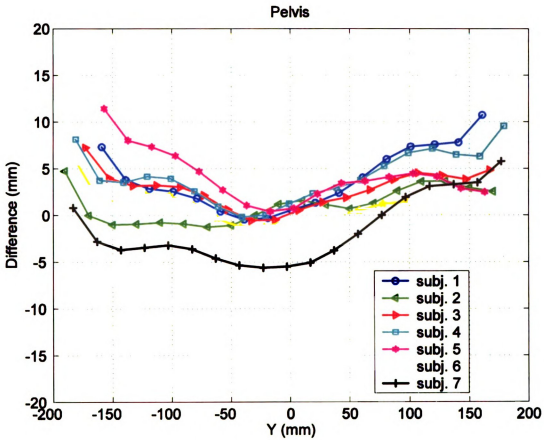

(C) At Pelvis – Large Males

Figure 50 Continued

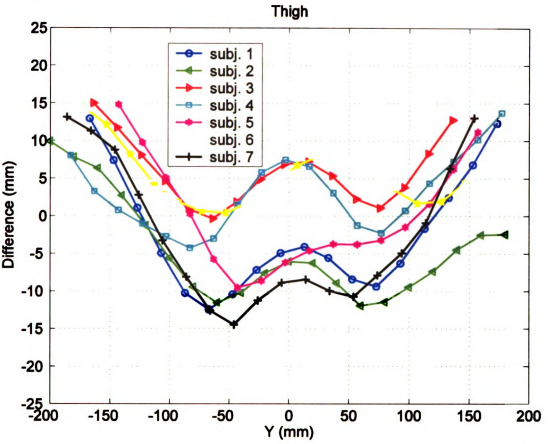

(D) At Mid Thigh – Large Males

Figure 50 Continued

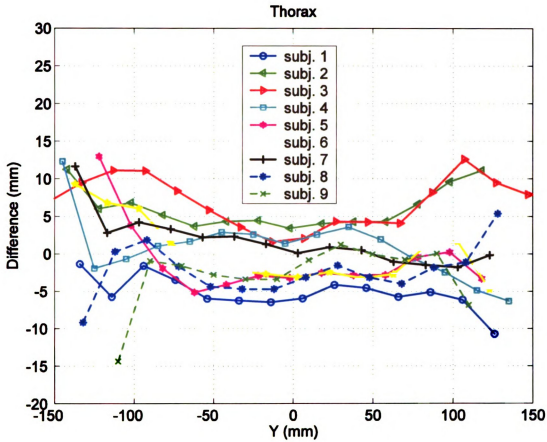

(A) At Mid Thorax – Small Females

Figure 51 Typical Difference Curves between Scaled and Measured Contour at Mid sections of Small Females

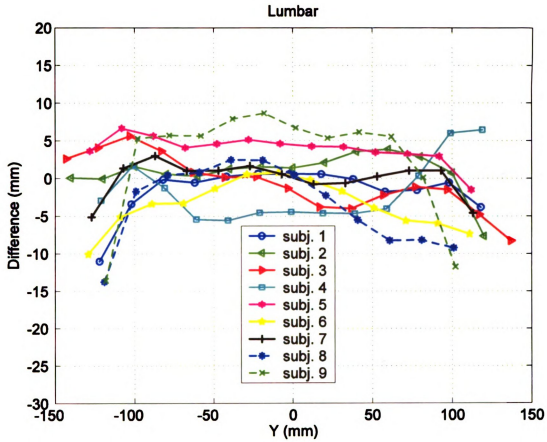

(B) At Mid Lumbar – Small Females

Figure 51 Continued

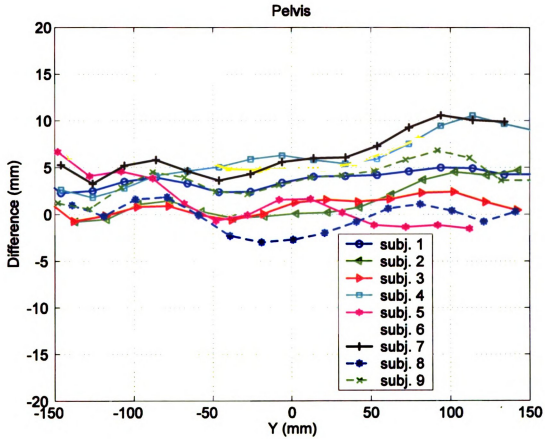

(C) At Mid Pelvis – Small Females

Figure 51 Continued

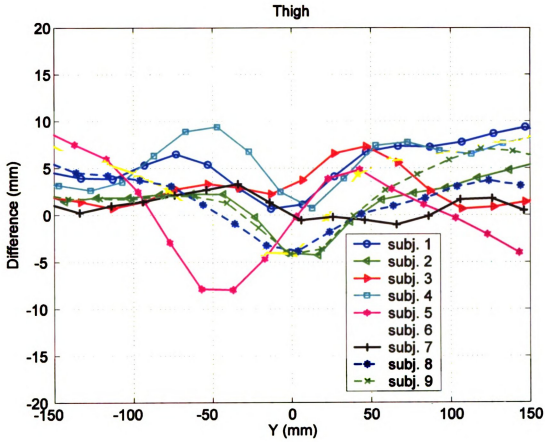

(D) At Mid Thigh – Small Females

Figure 51 Continued

Table 6 Average Differences (mm) between Scaled and Measured Data

-- Large males

	Subject 1	Subject 2	Subject 3	Subject 4	Subject 5	Subject 6	Subject 7	Average
Lumbar 1	6	5	3	2	5	7	5	6
Lumbar 4	4	4	3	12	4	7	5	6
Lumbar 6	9	6	3	10	6	6	6	6
Pelvis 4	6	2	7	5	6	4	3	5
Pelvis 5	5	2	5	4	6	3	3	4
Pelvis 6	4	2	3	4	4	1	4	3
Thorax 2	4	5	3	15	7	3	6	6
Thorax 4	6	10	5	10	5	5	9	7
Thorax 6	4	5	4	13	7	7	5	6
Thigh 1	7	4	7	13	7	7	5	7
Thigh 4	6	6	8	4	7	5	6	6
Thigh 7	8	6	10	3	8	7	8	7
Average	6	4	5	9	6	5	5	6

Table 7 Standard Deviations (mm) of the Differences

--Large male subjects

	Subject 1	Subject 2	Subject 3	Subject 4	Subject 5	Subject 6	Subject 7	Average
Lumbar 1	2	4	2	5	8	3	4	4
Lumbar 4	3	1	3	6	5	4	5	4
Lumbar 6	4	4	5	5	8	6	7	6
Pelvis 4	3	1	1	2	3	1	3	2
Pelvis 5	3	1	1	2	2	1	2	2
Pelvis 6	3	1	2	2	2	1	1	2
Thorax 2	3	2	2	5	2	2	3	3
Thorax 4	5	6	4	5	4	5	4	5
Thorax 6	3	5	3	7	9	4	4	5
Thigh 1	4	3	5	7	9	4	4	5
Thigh 4	4	3	5	2	6	4	4	4
Thigh 7	4	3	6	2	6	6	5	4
Average	4	3	3	4	5	4	4	4

Table 8 Average Differences (mm) between Scaled and Measured Data

-- Small females

	Subject 1	Subject 2	Subject 3	Subject 4	Subject 5	Subject 6	Subject 7	Subject 8	Subject 9	Average
Lumbar 1	2	3	3	3	5	3	4	2	5	3
Lumbar 4	2	2	3	4	4	4	2	5	7	4
Lumbar 6	9	4	3	4	4	3	9	2	7	5
Pelvis 4	7	5	3	7	5	9	12	3	10	7
Pelvis 5	5	3	2	9	3	9	9	1	7	5
Pelvis 6	4	2	1	6	2	6	7	1	4	4
Thorax 2	3	4	2	8	3	4	3	6	5	4
Thorax 3	2	4	3	3	2	3	2	3	5	3
Thorax 4	5	6	7	3	4	3	2	3	6	4
Thorax 6	6	5	3	5	3	3	6	2	10	5
Thigh 1	3	3	3	5	6	5	3	3	3	4
Thigh 4	6	3	3	6	4	5	1	3	3	4
Thigh 7	6	4	5	5	5	2	5	3	4	4
Average	5	4	3	5	4	4	5	3	6	4

Table 9 Standard Deviations (mm) of the Differences

--Small female subjects

	Subject 1	Subject 2	Subject 3	Subject 4	Subject 5	Subject 6	Subject 7	Subject 8	Subject 9	Average
Lumbar 1	2	3	2	2	3	1	2	2	6	2
Lumbar 4	2	3	2	2	1	3	2	4	5	2
Lumbar 6	4	3	2	5	4	3	5	2	3	3
Pelvis 4	2	2	1	2	3	2	3	1	2	2
Pelvis 5	1	2	1	3	2	2	2	1	1	2
Pelvis 6	1	2	1	3	2	1	3	1	2	2
Thorax 2	2	3	2	4	2	3	2	2	4	3
Thorax 3	2	3	2	2	1	3	2	3	6	3
Thorax 4	2	4	3	2	4	2	4	2	10	4
Thorax 6	3	7	3	4	5	4	3	2	7	4
Thigh 1	2	2	3	3	3	2	4	2	2	3
Thigh 4	2	1	2	2	3	2	1	1	2	2
Thigh 7	3	3	3	4	3	2	2	2	2	3
Average	2	3	2	3	3	2	3	2	4	3

5.4.2.2 Coefficients of Correlation

The coefficient of correlation analysis results S_R were falling in the range of 0.99 ~ 0.95 for almost all section curves, as presented in Table 10 for large male subjects, and Table 11 for small female subjects. The values of S_R indicated nearly identical shape of the pairs of scaled and measured curves.

Figure 52 shows the trends of the coefficients of correlation of subjects 1 of the large male and small female subjects.

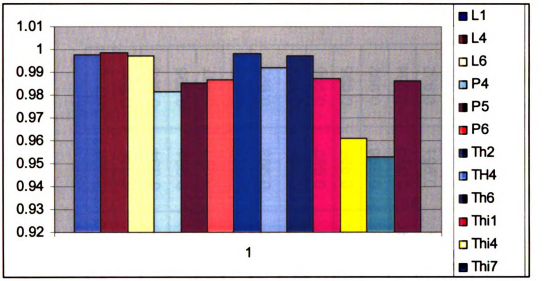

(A) Coefficient of Correlation -- Large Male Subject 1

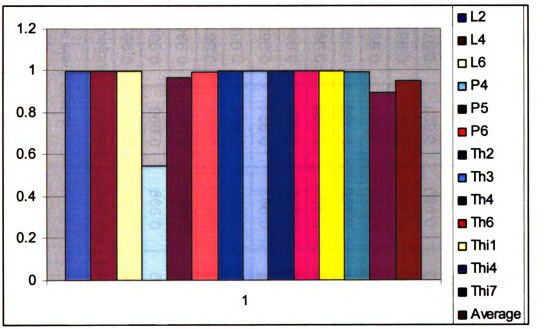

(B) Coefficient of Correlation -- Small Female Subject 1

Figure 52 Typical Bar Charts of Coefficient of Correlation

Table 10 Coefficients of Correlation

--Large male subjects

	Subject 1	Subject 2	Subject 3	Subject 4	Subject 5	Subject 6	Subject 7	Average
Lumbar 1	0.998	0.995	0.998	0.993	0.995	0.996	0.994	0.996
Lumbar 4	0.999	0.999	0.996	0.989	0.996	0.991	0.994	0.995
Lumbar 6	0.997	0.9944	0.996	0.996	0.996	0.991	0.991	0.995
Pelvis 4	0.981	0.997	0.983	0.981	0.977	0.995	0.994	0.987
Pelvis 5	0.985	0.997	0.994	0.988	0.993	0.997	0.993	0.992
Pelvis 6	0.987	0.997	0.994	0.988	0.995	0.998	0.993	0.993
Thorax 2	0.998	0.986	0.997	0.934	0.999	0.990	0.984	0.984
Thorax 4	0.992	0.991	0.998	0.995	0.996	0.996	0.997	0.995
Thorax 6	0.997	0.995	0.998	0.992	0.994	0.996	0.996	0.995
Thigh 1	0.987	0.996	0.981	0.992	0.994	0.996	0.996	0.992
Thigh 4	0.961	0.965	0.967	0.983	0.955	0.944	0.974	0.964
Thigh 7	0.953	0.980	0.827	0.974	0.967	0.861	0.961	0.932
Average	0.986	0.991	0.978	0.984	0.988	0.979	0.989	0.985

Table 11 Coefficients of Correlation
--Small female subjects

	Subject 1	Subject 2	Subject 3	Subject 4	Subject 5	Subject 6	Subject 7	Subject 8	Subject 9	Average
Lumbar 1	0.999	0.999	0.999	0.999	0.998	0.999	0.997	0.999	0.995	0.998
Lumbar 4	0.998	0.998	0.998	0.998	0.9995	0.997	0.998	0.996	0.991	0.997
Lumbar 6	0.997	0.997	0.999	0.997	0.997	0.998	0.997	0.999	0.998	0.998
Pelvis 4	0.543	0.904	0.994	0.997	0.579	0.998	0.762	0.989	0.326	0.788
Pelvis 5	0.968	0.991	0.999	0.711	0.972	0.873	0.973	0.9990	0.976	0.940
Pelvis 6	0.994	0.994	0.999	0.991	0.995	0.987	0.994	0.998	0.997	0.994
Thorax 2	0.998	0.996	0.996	0.994	0.999	0.995	0.998	0.999	0.997	0.997
Thorax 3	0.999	0.998	0.998	0.999	0.999	0.998	0.999	0.998	0.993	0.998
Thorax 4	0.999	0.999	0.998	0.999	0.998	0.999	0.998	0.999	0.989	0.998
Thorax 6	0.999	0.994	0.999	0.998	0.997	0.997	0.998	0.999	0.994	0.997
Thigh 1	0.996	0.998	0.994	0.993	0.995	0.993	0.996	0.995	0.997	0.995
Thigh 4	0.992	0.995	0.998	0.995	0.987	0.987	0.999	0.992	0.989	0.993
Thigh 7	0.895	0.941	0.943	0.917	0.981	0.981	0.877	0.976	0.914	0.936
Average	0.952	0.985	0.993	0.968	0.961	0.985	0.968	0.995	0.935	0.971

5.4.2.3 Corridors

There were always differences even though the contour curves were at the same relative sections and in one subgroup of subjects. Because the anthropometric dimensions were different from each other for the different subjects, the variability necessitates that corridors be created to represent the range of contour shapes at the interested sections.

The average of the tested contour curves were first calculated at each section of interest. Then at each point (1 mm apart), the standard deviations of the tested data were computed, and were added to the average curves to construct the corridors.

For the most of the scaled contour curves, they were within the corridors of tested average with $\pm\sigma$. See Figures 53, (A), (B), (C), (D), and Figure 54, (A), (B), (C), (D).

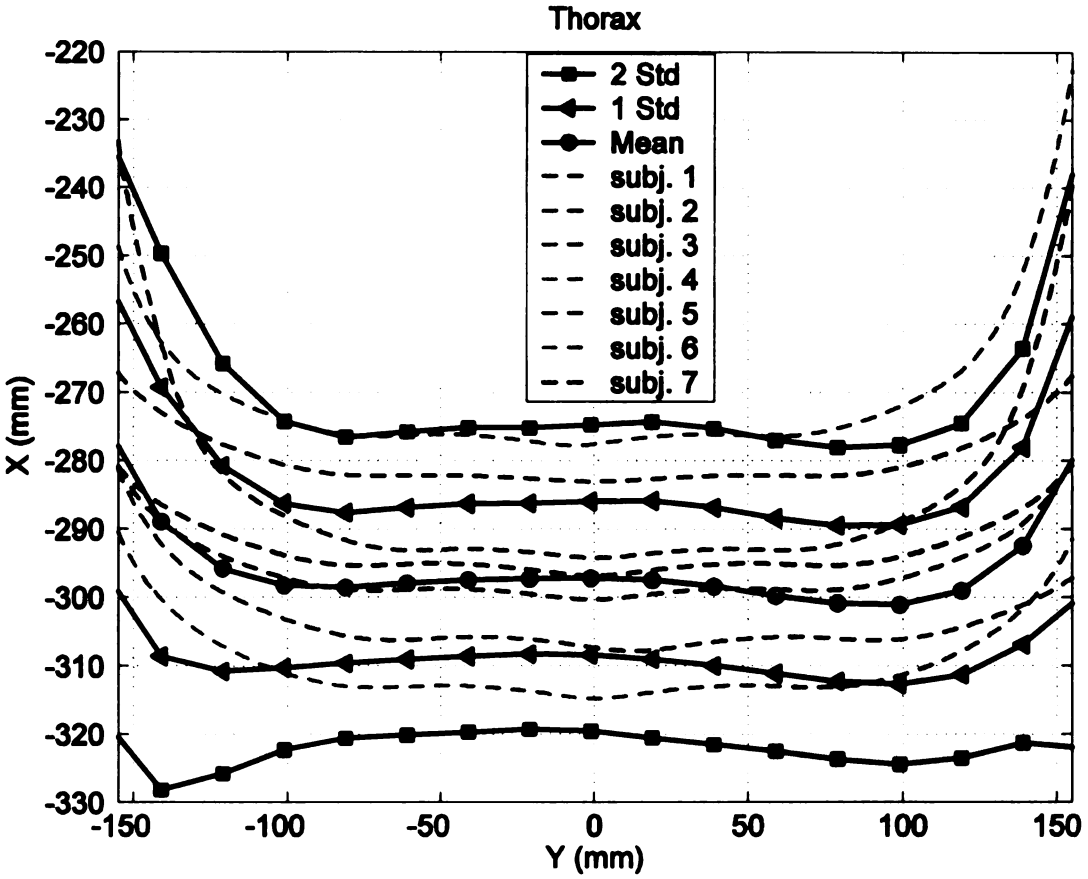

(A) Scaled Curves and Corridors at Mid Thoraxes – Large Males

Figure 53 Typical Corridor Plots at Mid Thorax, Lumbar, Pelvis, and Thigh of Large Males

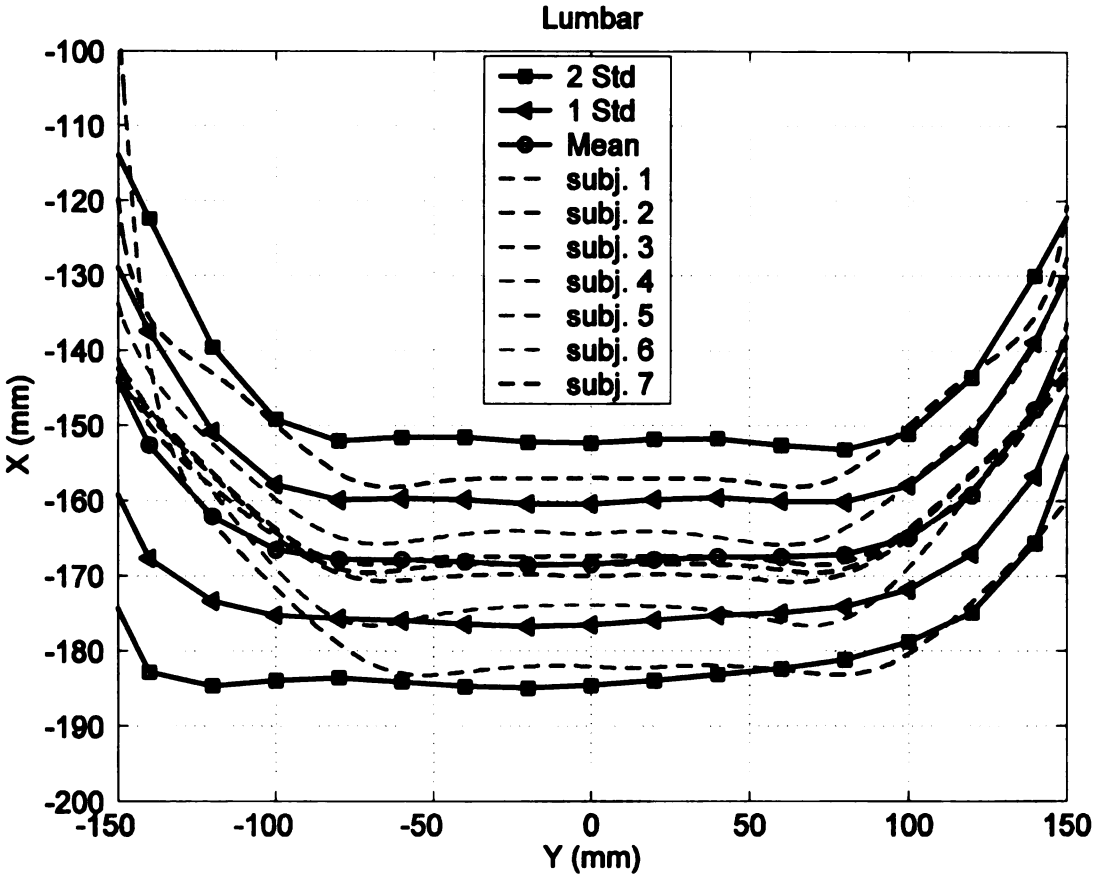

(B) Scaled Curves and Corridors at Mid Lumbar – Large Males

Figure 53 Continued

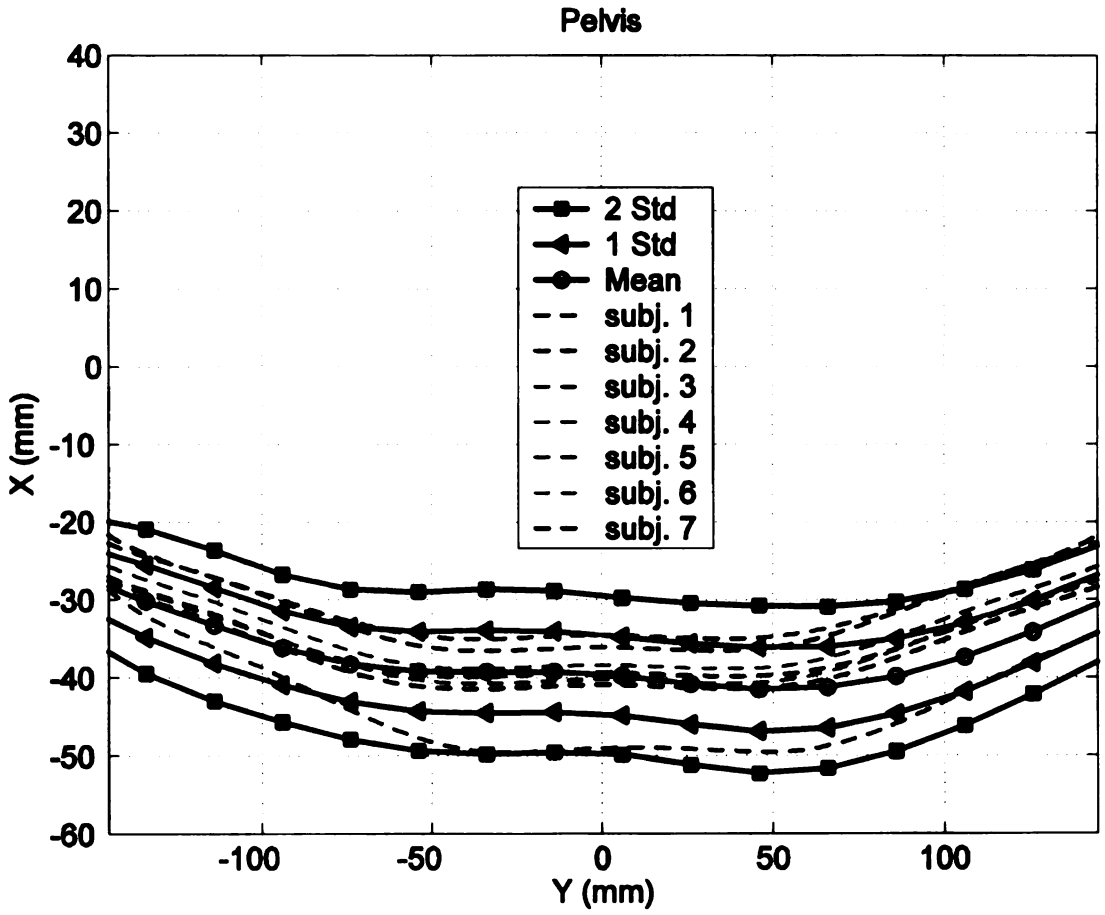

(C) Scaled Curves and Corridors at Mid Pelvis – Large Males

Figure 53 Continued

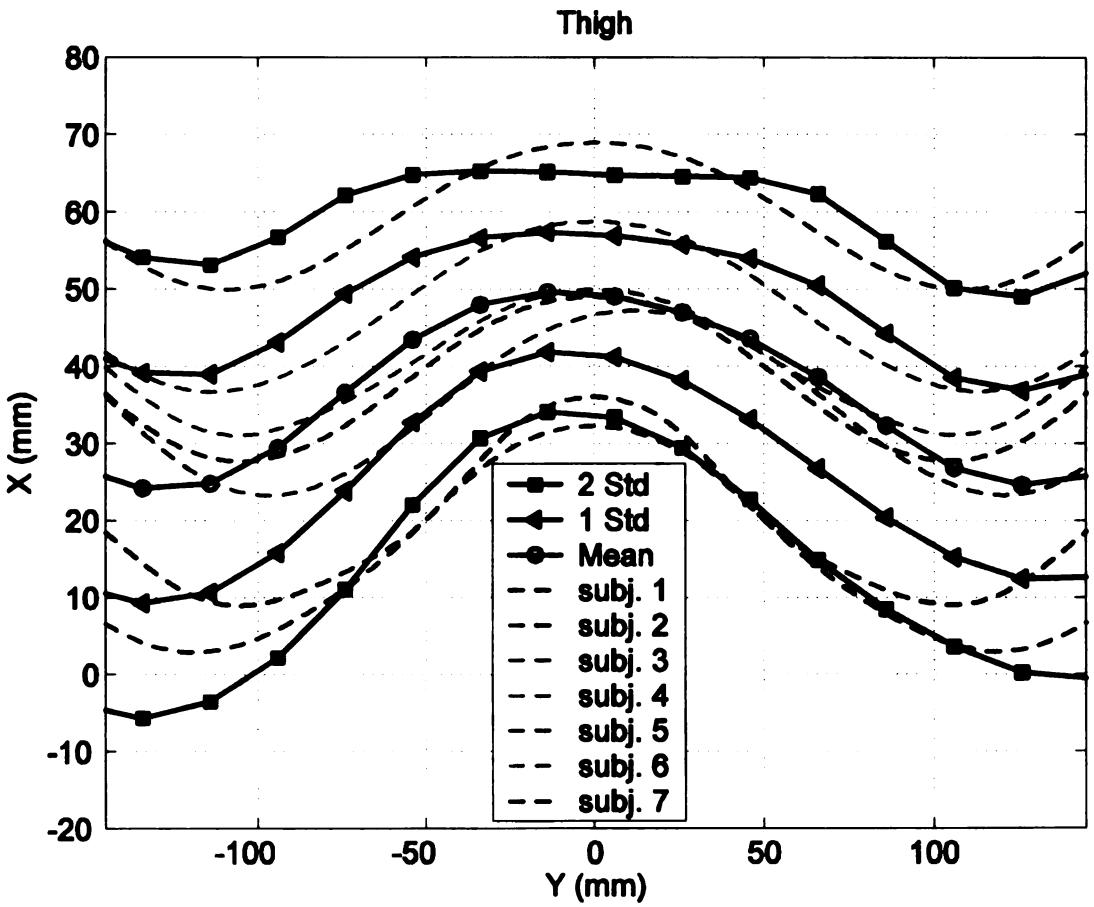

(D) Scaled Curves and Corridors at Mid Thighs – Large Males

Figure 53 Continued

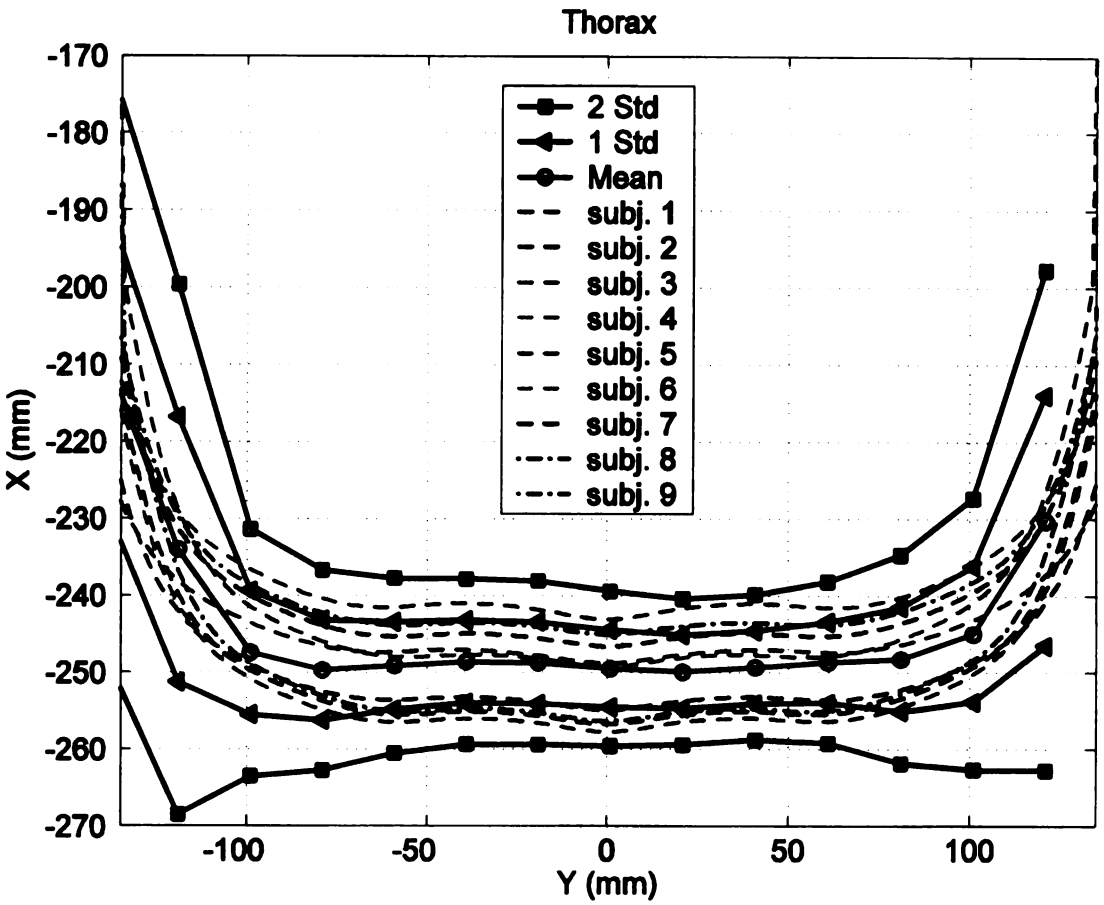

(A) Scaled Curves and Corridors at Mid Thoraxes – Small Females

Figure 54 Typical Corridor Plots at Mid Thorax, Lumbar, Pelvis, and Thigh of Small Female

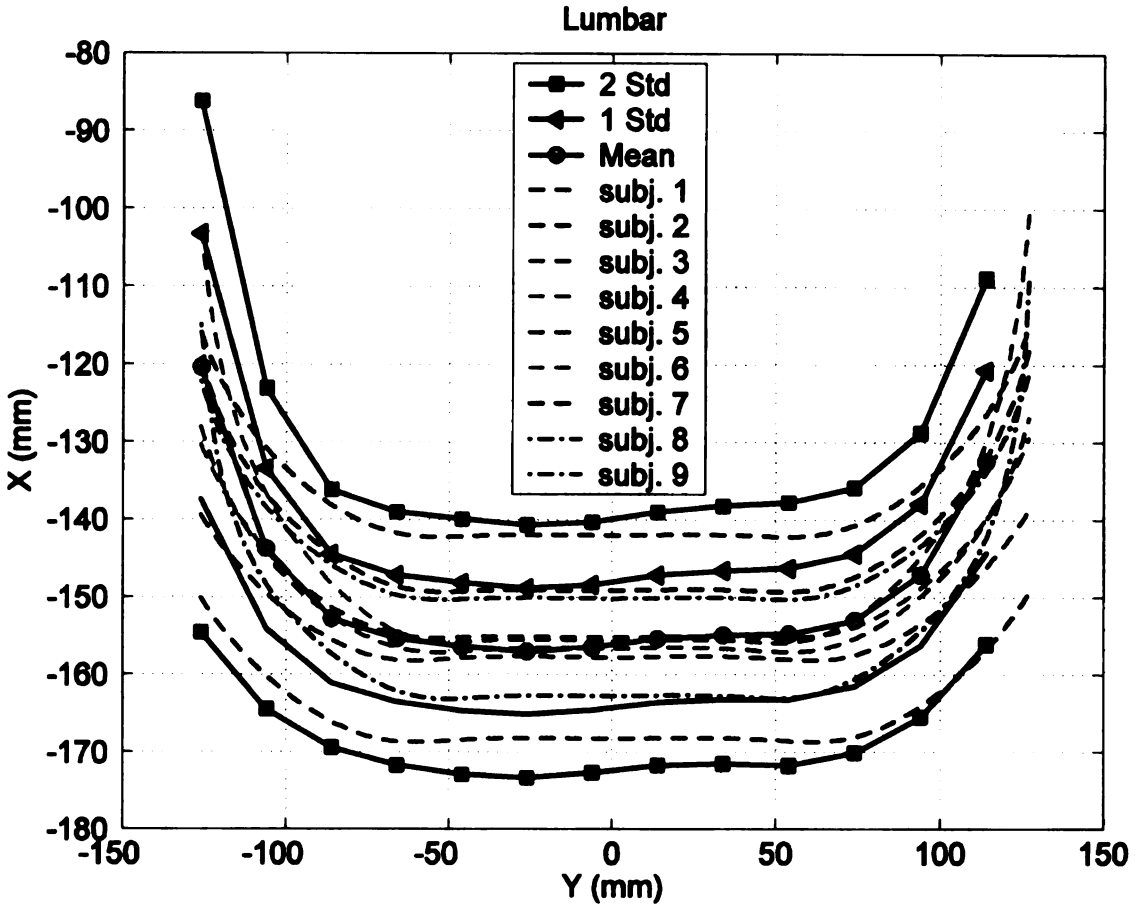

(B) Scaled Curves and Corridors at Mid Lumbars – Small Females

Figure 54 Continued

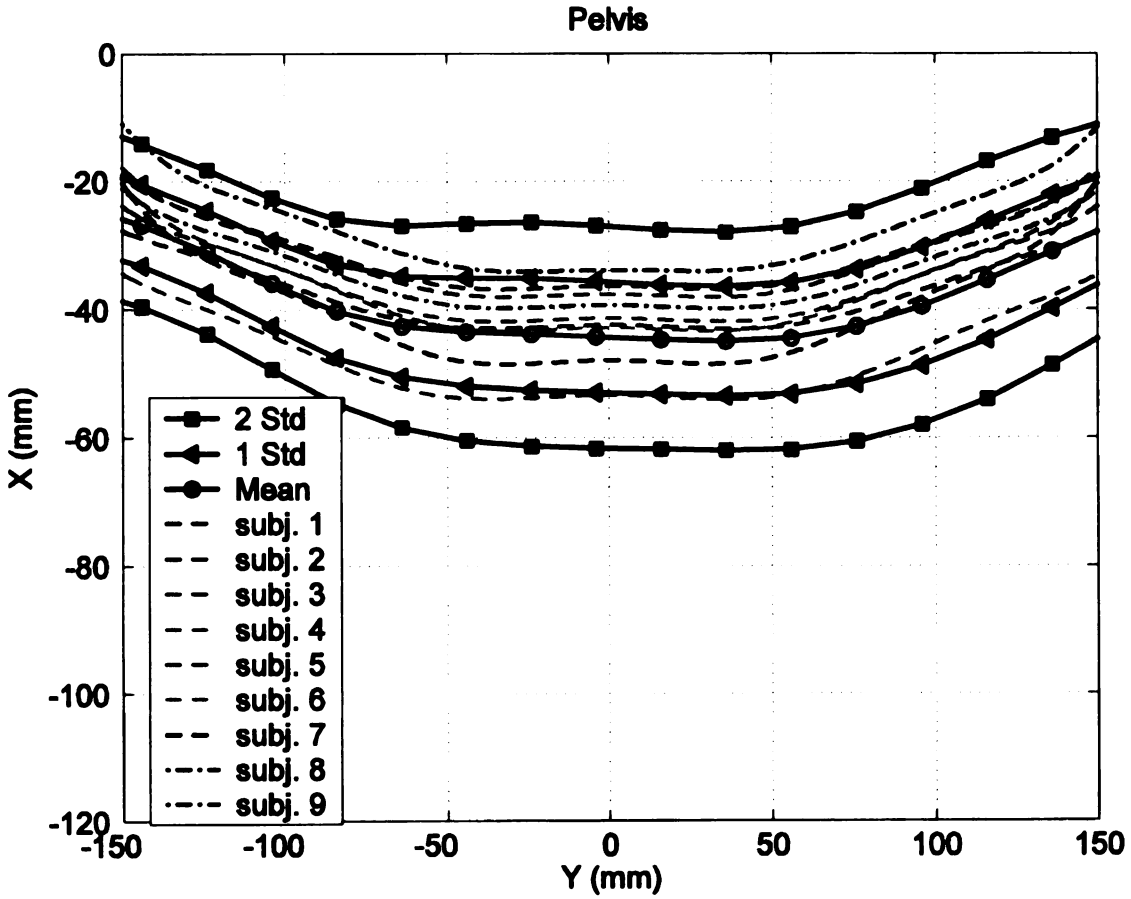

(C) Scaled Curves and Corridors at Mid Pelvis – Small Females

Figure 54 Continued

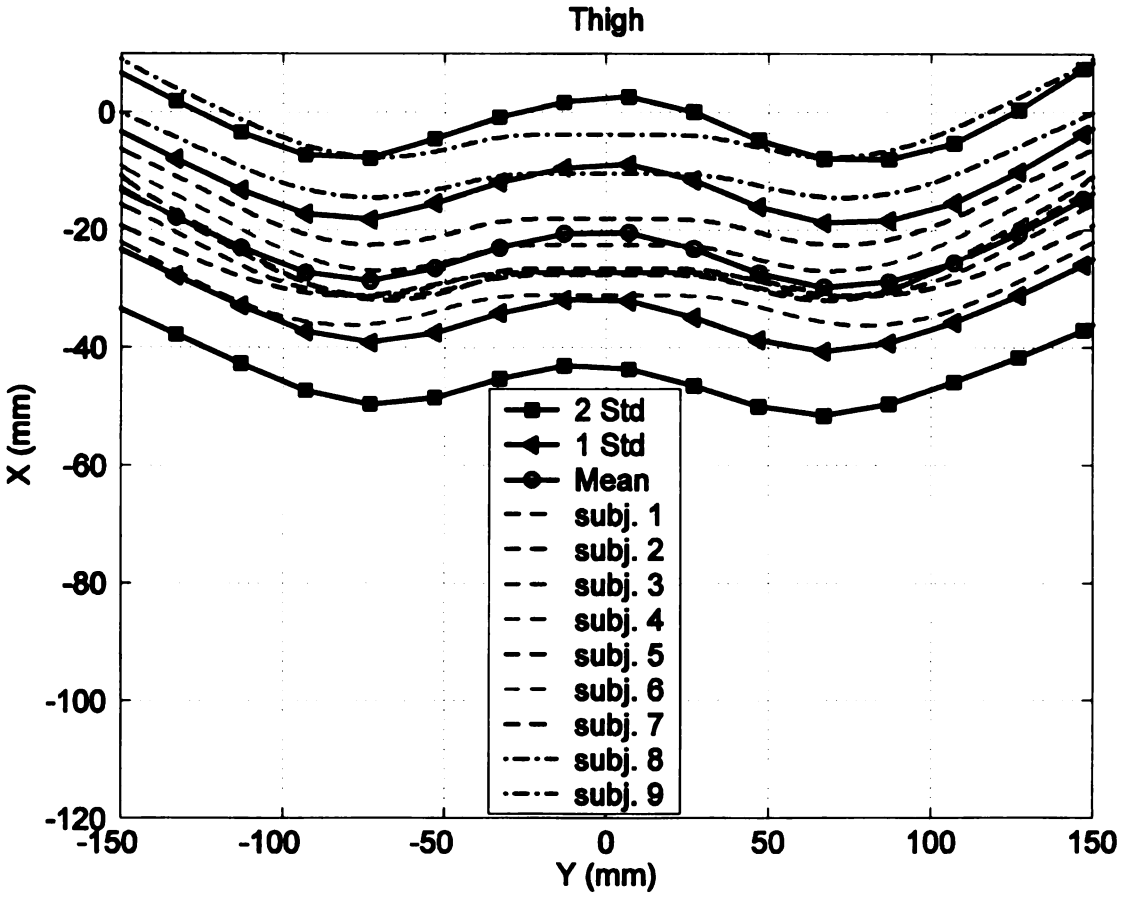

(D) Scaled Curves and Corridors at Mid Thighs – Small Females

Figure 54 Continued

5.5.1 Thorax

In this region, the subjects' backs came into contact with the chair usually after the 3rd section from the lower neck joints in this study. This is basically decided by the position of the lower neck joint with respect to the chair back. If the position of the lower neck joint is far away from the chair back, the subject's back starts contacting the chair back at a lower point vertically on the chair back. After the 4th section, the contour shapes were less affected by the sitting postures of the subjects as can be observed in the Figures 44,45, 46, 47, 48, 49, and the rest of the figures in Appendices B and C.

From the correlation analysis of the scaled and measured contour data, very good results could be seen from the 4th section down to the 6th section, which was the last section in this region.

The average difference (d) of between the scaled and measured contour curves, presented in the Table 6, and Table 8, show that the contour data agree within 15 mm with standard deviation less than 10 mm after the 4th section.

Table 10 and Table 11 list all the coefficients of the correlation of the correlation analysis between the scaled and measured data. For the thorax region, all the coefficients are more than 0.95, which means that the curves are very highly related or resemble to each other.

In the Figure 53 (A) and Figure 54 (A), most of the scaled contour curves are very close to the average measured curve within one standard deviation σ.

5.5.2 Lumbar

Because the bodies were in full contact with the chair back in the lumbar region, the back deformed shapes were well measured and well defined in this area, and the contour results were close to each other from the scaling and the testing. The differences between the scaled and measured contour curves were less than 12 mm and deviations less than 7 mm (Table 6 and 8). The correlation analysis results show that the contour curves have excellent resemblance, with the coefficient of correlation within the range of 0.989 to 0.999 (Table 10 and 11). The scaled contour curves were all within the corridors with 2 σ.

5.5.3 Pelvis

In the current seat, the body segment in this region is not well supported by the seat. Or in this region, the body is not contacting the seat. See Figure 55. Obviously the body shapes were not well recorded and defined. Only after the 5th section in this area did the contour curves reflect subjects' body shapes. That is why the coefficient of correlation started becoming close to 1 after the 4th sections as can be seen in the Table 10 and 11 for the small female data.

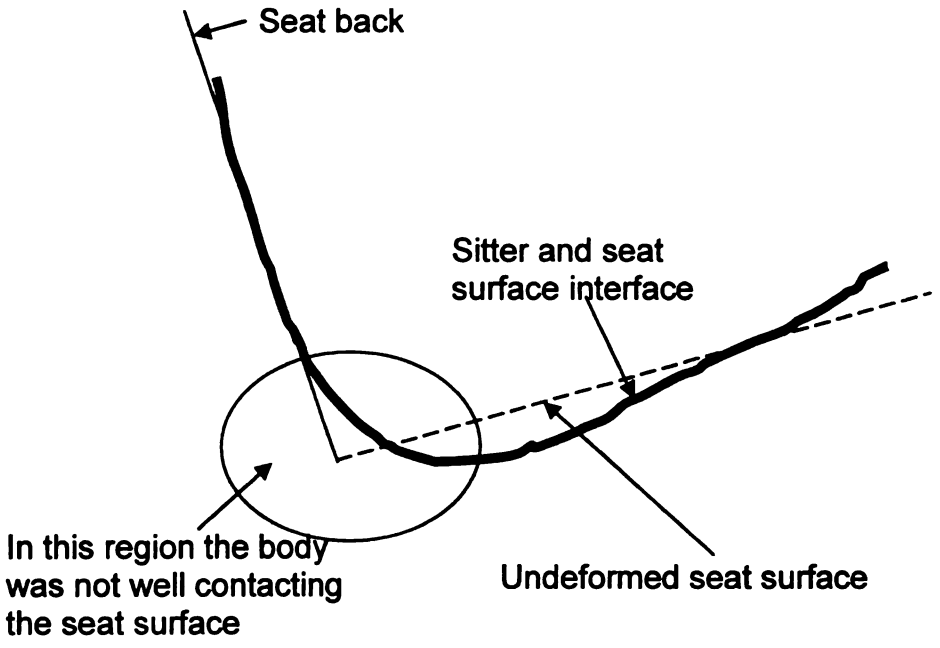

Figure 55 Pelvis Region Not Well Supported in Seat

5.5.4 Thigh

In this area, the interface between the chair and sitter were in good contact conditions for most of the contours because of the presence of the foam. See the Figures 44, 45, 46, 47, 48, 49, and the rest of the figures in Appendices B and C. The differences (d) were less than 13 mm with maximum standard deviation 9 mm for large males, and the differences were less than 10 mm with maximum standard deviation 6 mm for the small females.

However, at the front of the chair, the thigh postures affected the deformed thigh shape measurement simply because the thigh might not fully

contact the seat surface. So at the last sections of the contour curves, some deviation could be seen. In Table 10 and 11, some of the coefficients of correlation were below 0.9.

CHAPTER 6 CONCLUSIONS

Both seating postures and seat contours are very important to seat design and seating comfort. The focus of this study was to determine (relative to a skeletal linkage) the contours between people and seats that are deformed by contact for a useful range of human subject sizes and postures. For this study, three representative human subject groups were chosen: 5^{th} percentile small adult female, 50^{th} percentile average adult male, and 95^{th} percentile large adult male. Ten subjects from each anthropometric group were measured. To determine the seated contours, the subject's posterior contours, including back, buttocks, and thighs, were acquired in a specially designed contour chair simultaneously with supporting force data from several load cells and posture data from a video system.

The contour data from average size males were analyzed by sectioning splined surfaces into two-dimensional curves based on axes systems in major anatomical segments, thorax, lumbar, pelvis, and thigh. Even though human beings are not exactly symmetrical, the measured postures and contours were interpreted to provide symmetrical contours for development of the ASPECT manikin and RAMSIS computer models. These contours were compared to contours of the J826 SAE manikin.

The thigh and buttocks surface contour of the ASPECT manikin was defined by selecting one subject's contour, which was consistently near the middle of the nine subjects' contours at each of several cross-sections of the thigh and

buttocks region; this was done to provide a contour that was realistic because the variation between subjects was small.

Because of the greater number of mobile segments in the torso compared to the thigh and buttocks region, there are greater postural and contour variability in the back area. After the data were transformed, and scaled to the average distance between lower neck joint and mid-HJC, the back data and postures were averaged in the X direction (generally posterior to anterior direction) in each local segmental coordinate system to better represent the range of the variation.

For the aesthetics in the development in the back contours for the RAMSIS model, the ASPECT back contours were adjusted a few millimeters, less than measurement variability. To develop the RAMSIS contour, the postural linkages of the contours by Frost and ASPECT contours were aligned and the differences between these contours were averaged to generate the RAMSIS contour. Both ASPECT and RAMSIS contours could be used for the applications of the seat design and all purposes of dummy design.

Representations of mid-size males have been extensively used as the basis and starting point for design and evaluation of seating. Thus, it is very useful to explore the relationships between mid-size males and other commonly used human sizes, which are small females and large males. The present study is the first to scale mid-male contours to the anthropometric dimensions of small females and large males and to validate these scaled contours with the measurement data from small females and large males. A system was established in this study to scale the contours of mid-size males to represent

contours for small females and large males. In the scaling process, the body regions of mid-male's thorax, lumbar, pelvis, and thigh were separately scaled to the anthropometric dimension of each individual subject in the small female or large male subgroups, and then rotated to align with the body postural linkage of the subject.

Verified by the analysis of correlation, the scaling results were in very close agreement with the measurement data and most of the coefficients of correlation were within 0.95-0.99. The corridors were created to illustrate the possible range of contour shapes at the interesting sections. First, the average of the measurement contour curve was found at each section, and then the standard deviations of the measured data were computed, and were used to calculate the corridors. For most of the scaled contour curves, they were within the corridors of the measured average with $\pm\sigma$. In a few extreme cases, the maximum average difference between the scaled and measured contour curves was within 15 mm, and maximum standard deviations were 9 mm.

Because of the closeness of the scaled contours to measured contours for this broad range of human sizes, the contours developed in this work for average size males can be used with confidence in computer models for scaling to represent people of different sizes such as small females and large males based on anthropometric dimension. This is a very useful result of a very simple scaling process to represent various human back contours. The sample sizes in the present study are limited, and future work could add confidence to representing and scaling human back contours. However, the contours and scaling provided

in this study can be easily and usefully implemented in computer models such a RAMSIS.

The contours provided by this study represent the interface between two deformable objects: seats and people. The back shape of the torso is highly dependant on posture, and these can be represented by the contours and skeletal linkage of this study.

Consideration should be given to regional deformability. For a particular posture, the back of the torso (where the skeletal structures are close to the contact surface) is not highly deformable relative to regions beneath the buttocks and thighs (where pelvis and femurs are prominent only in the central regions). Also, the deformability of seats varies from place to place. So, the contours of this study should be used and interpreted with consideration of seat and body deformability. Future work could add useful represent of the deformability of the human soft tissues and seats.

APPENDICES

APPENDIX A

Scaling Factors Used for Scaling Procedures

Table 12 Body Dimensions for Large Male Scaling

Body Dimensions	ASPECT Mid-Male (mm)	Subject 1 (MD) (mm)	Subject 2 (TH) (mm)	Subject 3 (EL) (mm)	Subject 4 (HR) (mm)	Subject 5 (JA) (mm)	Subject 6 (JS) (mm)	Subject 7 (JH) (mm)
Chest Length	292	332	333	328	326	332	329	314
Chest Breadth	325	335	356	296	366	337	306	354
Chest Depth	246	275	270	248	264	237	243	273
Waist Length	149	191	176	165	174	171	158	151
Waist Breadth	306	314	324	299	350	335	293	322
Waist Depth	241	225	238	220	256	220	198	262
Buttock Length	97	99	137	107	109	114	102	118
Buttock Breadth	386	388	400	358	374	373	388	372
Buttock Depth	260	266	270	242	252	253	246	269

Table 13 Body Dimensions for Small Female Scaling

Body Dimensions	ASPECT Mid-Male (mm)	Subject 1 (AC) (mm)	Subject 2 (CC) (mm)	Subject 3 (CH) (mm)	Subject 4 (CL) (mm)	Subject 5 (ED) (mm)	Subject 6 (JT) (mm)	Subject 7 (LC) (mm)	Subject 8 (LH) (mm)	Subject 9 (NK) (mm)
Chest Length	292	283	283	295	281	270	293	286	295	294
Chest Breadth	325	259	271	290	275	252	271	264	253	260
Chest Depth	246	218	213	240	258	215	197	210	215	200
Waist Length	149	134	112	121	115	113	109	160	113	129
Waist Breadth	306	256	286	286	273	254	266	260	240	256
Waist Depth	241	166	194	195	193	164	184	166	148	163
Buttock Length	97	90	80	94	90	94	90	75	84	98
Buttock Breadth	386	392	348	362	387	340	341	331	341	353
Buttock Depth	260	205	266	228	238	210	212	233	197	196

APPENDIX B

Scaled and Measured Small Females Results

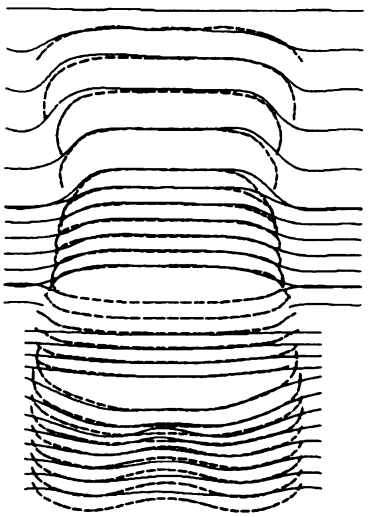

Figure 56 Female Subject 2 Rear View

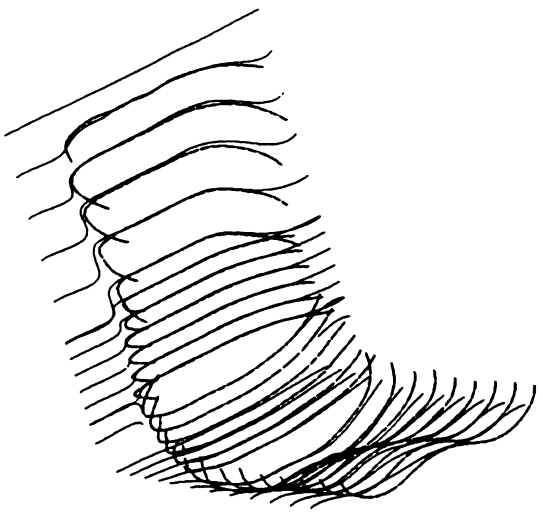

Figure 57 Small Female Subject 2 Iso View

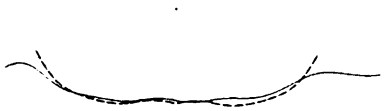

SF2 Thorax 2nd

SF2 Thorax 6th

SF2 Thorax 3rd

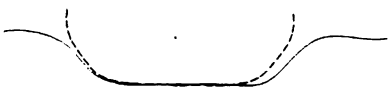

SF2 Lumbar 1st

SF2 Thorax 4th

SF2 Lumbar 2nd

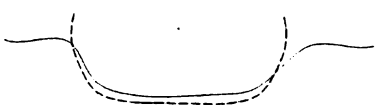

SF2 Thorax 5th

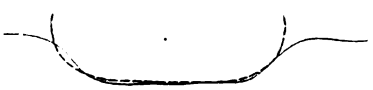

SF2 Lumbar 3rd

Figure 58 Scaled and Measured Curves of Small Female Subject 2

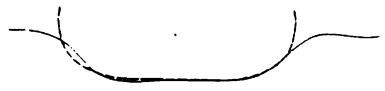

SF2 Lumbar 4th

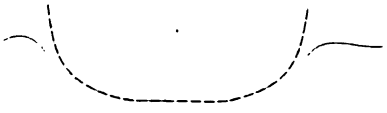

SF2 Pelvic 2nd

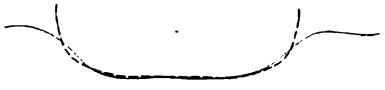

SF2 Lumbar 5th

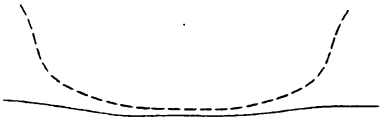

SF2 Pelvic 3rd

SF2 Lumbar 6th

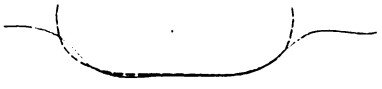

SF2 Pelvic 4th

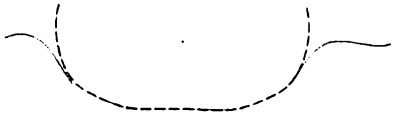

SF2 Pelvic 1st

SF2 Pelvic 5th

Figure 58 Continued

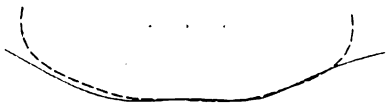

SF2 Thigh 1st

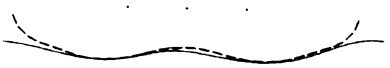

SF2 Thigh 5th

SF2 Thigh 2nd

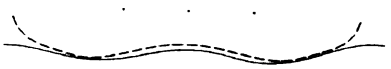

SF2 Thigh 6th

SF2 Thigh 3rd

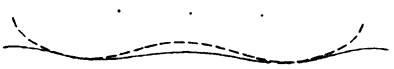

SF2 Thigh 7th

SF1 Thigh 4th

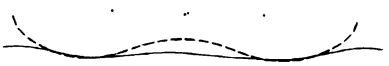

SF2 Thigh 8th

Figure 58 Continued

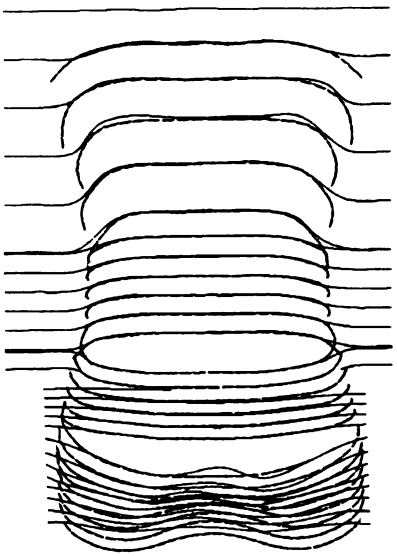

Figure 59 Small Female Subject 3 Rear View

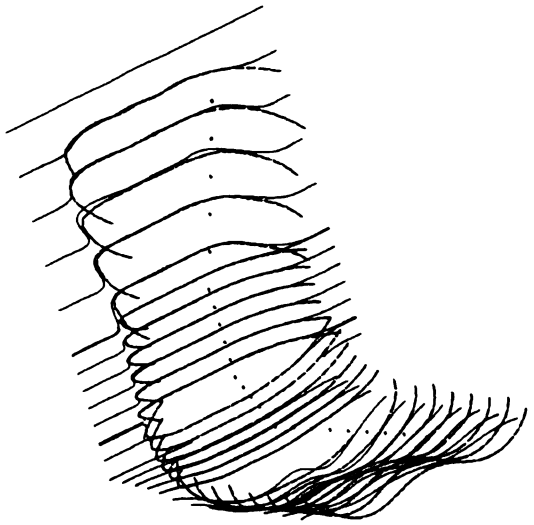

Figure 60 Small Female Subject 3 Iso View

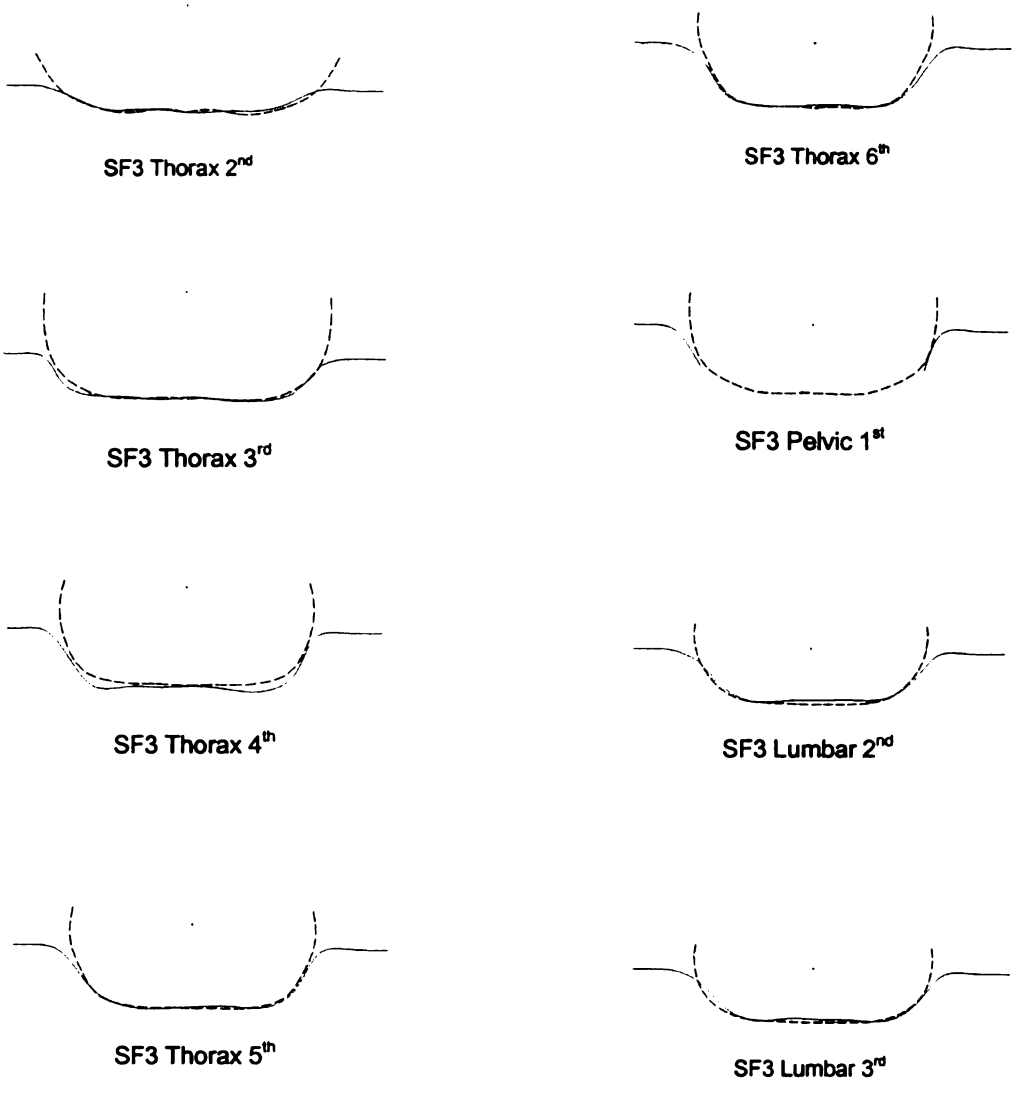

Figure 61 Scaled and Measured Curves of Small Female Subject 3

SF3 Lumbar 4th

SF3 Pelvic 3rd

SF3 Lumbar 5th

SF3 Pelvic 4th

SF3 Lumbar 6th

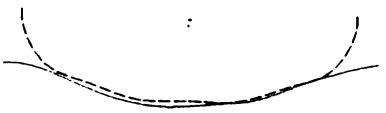

SF3 Pelvic 5th

SF3 Pelvic 1st

SF3 Pelvic 6th

SF3 Pelvic 2nd

SF3 Thigh 1st

Figure 61 Continued

SF3 Thigh 2nd

SF3 Thigh 6th

SF3 Thigh 3rd

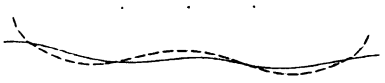

SF3 Thigh 7th

SF3 Thigh 4th

SF3 Thigh 8th

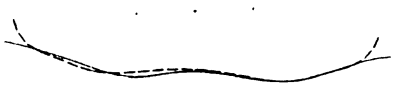

SF3 Thigh 5th

Figure 61 Continue

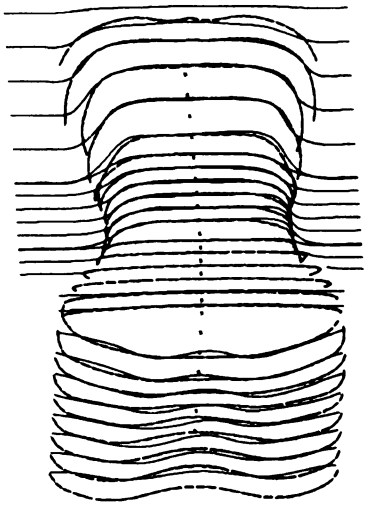

Figure 62 Small Female Subject 4 Rear View

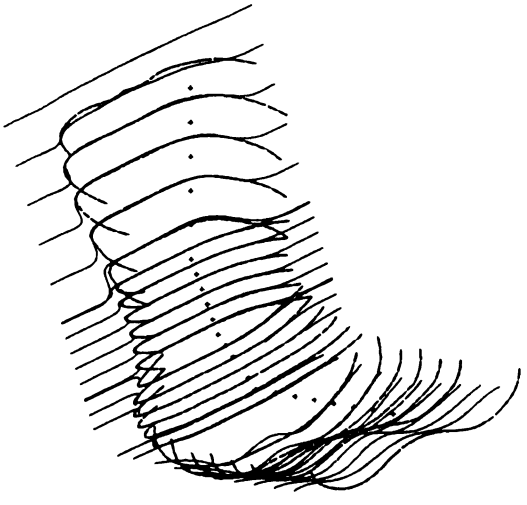

Figure 63 Small Female Subject 4 Iso View

SF4 Thorax 1st

SF4 Lumbar 1st

SF4 Thorax 2nd

SF4 Lumbar 2nd

SF4 Thorax 3rd

SF4 Lumbar 3rd

SF4 Thorax 4th

SF4 Lumbar 4th

SF4 Thorax 5th

SF4 Lumbar 5th

Figure 64 Scaled and Measured Curves of Small Female 4

SF4 Lumbar 6th

SF4 Pelvic 6th

SF4 Pelvic 1st

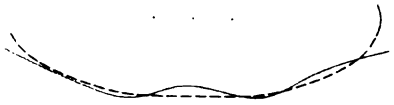

SF4 Thigh 1st

SF4 Pelvic 2nd

SF4 Thigh 2nd

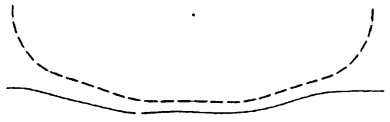

SF4 Pelvic 5th

SF4 Thigh 3rd

SF4 Pelvic 3rd

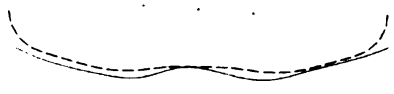

SF4 Thigh 4th

Figure 64 Continued

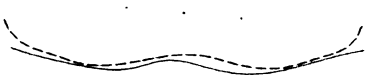

SF4 Thigh 5th

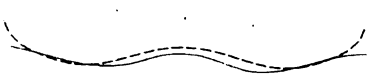

SF4 Thigh 7th

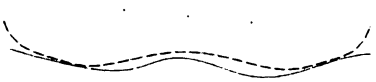

SF4 Thigh 6th

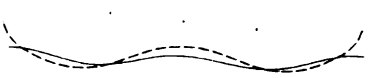

SF4 Thigh 8th

Figure 64 Continued

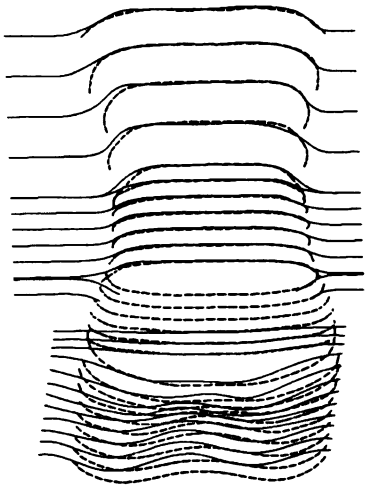

Figure 65 SmalFemale Subject 5 Rear View

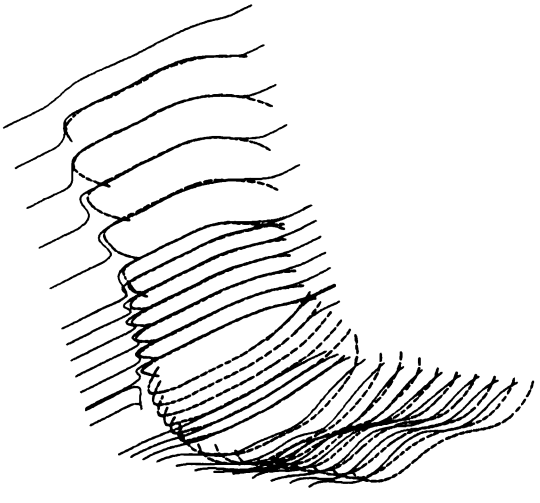

Figure 66 Small Female Subject 5 Iso View

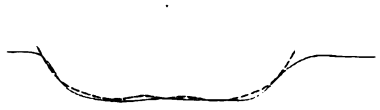

SF5 Thorax 1st

SF5 Lumbar 1st

SF5 Thorax 2nd

SF5 Lumbar 2nd

SF5 Thorax 3rd

SF5 Lumbar 3rd

SF5 Thorax 5th

SF5 Lumbar 4th

SF5 Thorax 4th

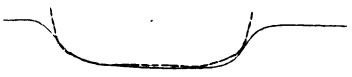

SF5 Lumbar 5th

Figure 67 Scaled and Measured Curves of Small Female Subject 5

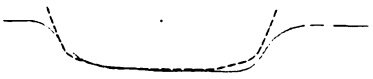

SF5 Lumbar 6th

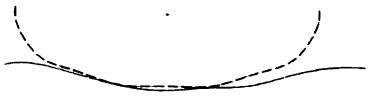

SF5 Pelvic 5th

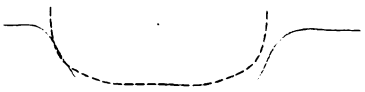

SF5 Pelvic 1st

SF5 Pelvic 6th

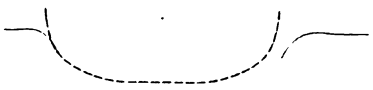

SF5 Pelvic 2nd

SF5 Thigh 1st

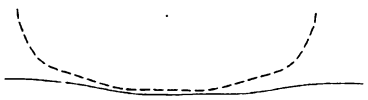

SF5 Pelvic 4th

SF5 Thigh 2nd

Figure 67 Continued

SF5 Thigh 3rd

SF5 Thigh 6th

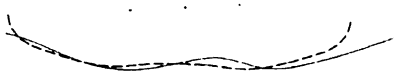

SF5 Thigh 4th

SF5 Thigh 7th

SF5 Thigh 5th

SF5 Thigh 8th

Figure 67 Continued

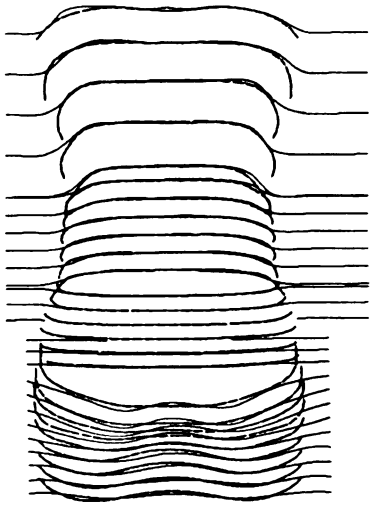

Figure 68 Small Female Subject 6 Rear View

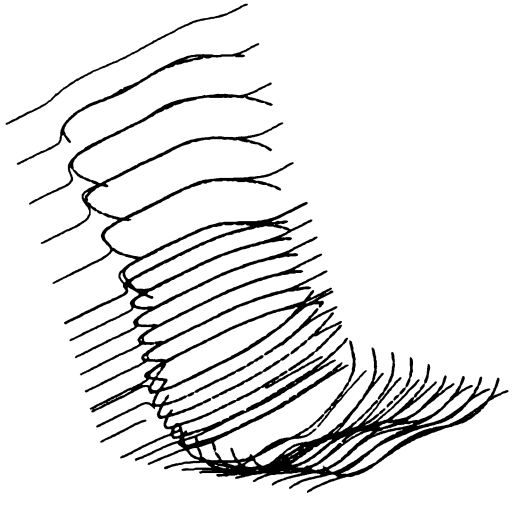

Figure 69 Small Female Subject 6 Iso View

SF6 Thorax 1st

SF6 Lumbar 1st

SF6 Thorax 2nd

SF6 Lumbar 2nd

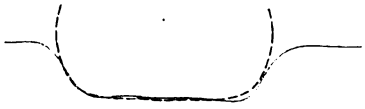

SF6 Thorax 3rd

SF6 Lumbar 3rd

SF6 Thorax 4th

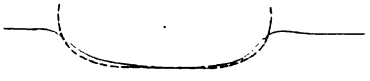

SF6 Lumbar 4th

SF6 Thorax 5th

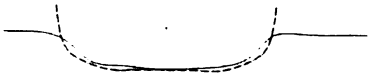

SF6 Lumbar 5th

Figure 70 Scaled and Measured Curves of Small Female Subject 6

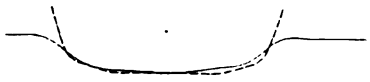

SF6 Lumbar 6th

SF6 Pelvic 5th

SF6 Pelvic 1st

SF6 Pelvic 6th

SF6 Pelvic 2nd

SF6 Thigh 1st

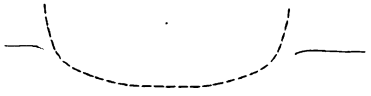

SF6 Pelvic 3rd

SF6 Thigh 2nd

SF5 Pelvic 4th

SF6 Thigh 3rd

Figure 70 Continued

SF6 Thigh 4th

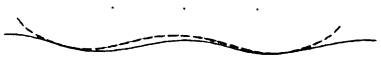

SF6 Thigh 7th

SF6 Thigh 5th

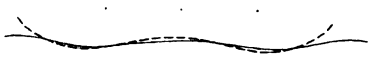

SF6 Thigh 8th

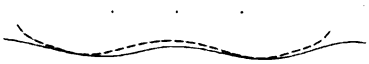

SF6 Thigh 6th

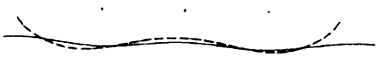

SF6 Thigh 9th

Figure 70 Continued

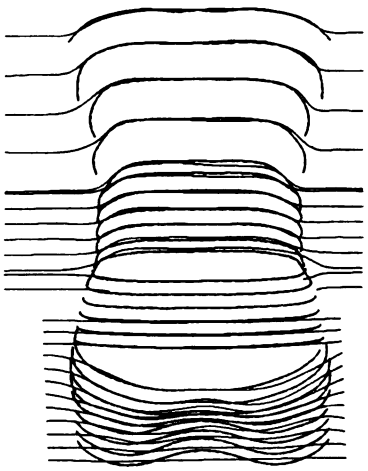

Figure 71 Small Female Subject 7 Rear View

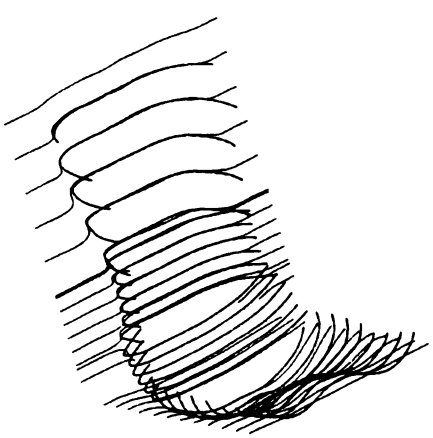

Figure 72 Small Female Subject 7 Iso View

SF7 Thorax 1st

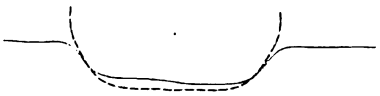

SF7 Lumbar 1st

SF7 Thorax 2nd

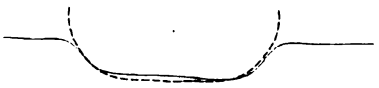

SF7 Lumbar 2nd

SF7 Thorax 3rd

SF7 Lumbar 3rd

SF7 Thorax 4th

SF7 Lumbar 4th

SF7 Thorax 5th

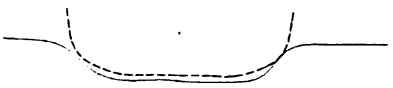

SF7 Lumbar 5th

Figure 73 Scaled and Measured Curves of Small Female Subject 7

SF7 Lumbar 6th

SF7 Pelvic 5th

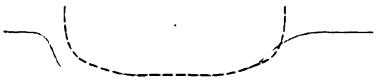

SF7 Pelvic 1st

SF7 Pelvic 6th

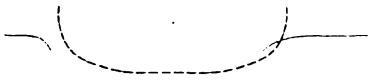

SF7 Pelvic 2nd

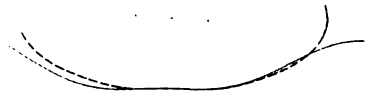

SF7 Thigh 1st

SF7 Pelvic 4th

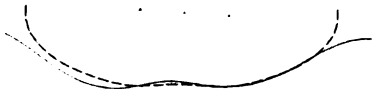

SF7 Thigh 2nd

Figure 73 Continued

SF7 Thigh 3rd

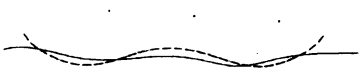

SF7 Thigh 7th

SF7 Thigh 4th

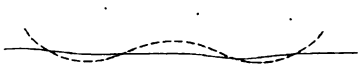

SF7 Thigh 8th

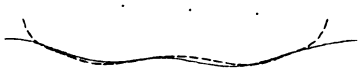

SF7 Thigh 5th

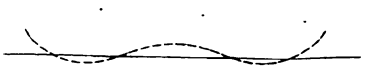

SF7 Thigh 9th

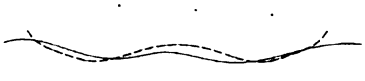

SF7 Thigh 6th

Figure 73 Continued

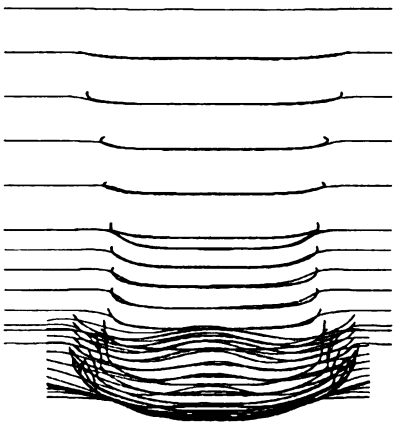

Figure 74 Small Female Subject 8 Rear View

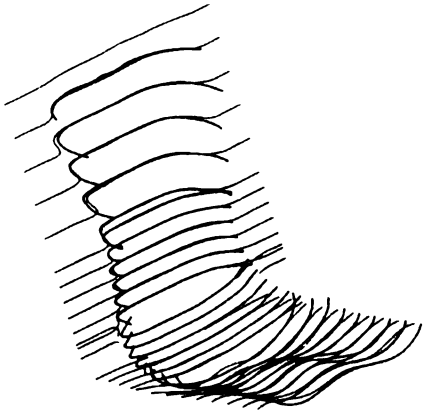

Figure 75 Small Female Subject 8 Iso View

SF7 Thorax 1st

SF7 Lumbar 1st

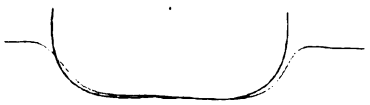

SF7 Thorax 2nd

SF7 Lumbar 2nd

SF7 Thorax 3rd

SF7 Lumbar 3rd

SF7 Thorax 4th

SF7 Lumbar 4th

SF7 Thorax 5th

SF7 Lumbar 5th

Figure 76 Scaled and Measured Curves of Small Female Subject 8

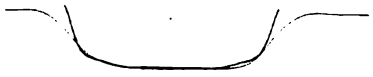

SF7 Lumbar 6th

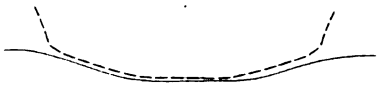

SF7 Pelvic 4th

SF7 Pelvic 1st

SF8 Pelvic 5th

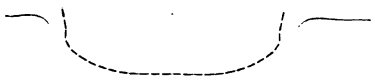

SF7 Pelvic 2nd

SF8 Pelvic 6th

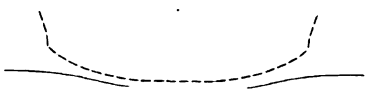

SF7 Pelvic 3th

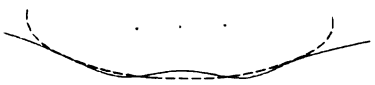

SF8 Thigh 1st

Figure 76 Continued

SF8 Thigh 2nd

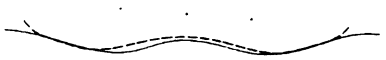

SF8 Thigh 6th

SF8 Thigh 3rd

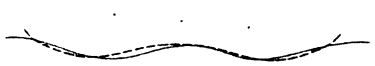

SF8 Thigh 7th

SF8 Thigh 4th

SF8 Thigh 8th

SF8 Thigh 5th

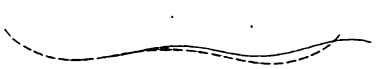

SF8 Thigh 9th

Figure 76 Continued

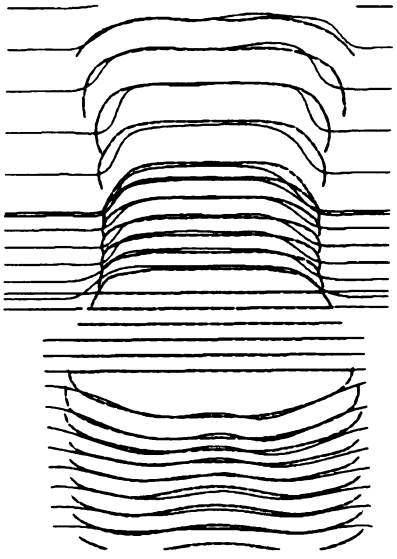

Figure 77 Small Female Subject 9 Rear View

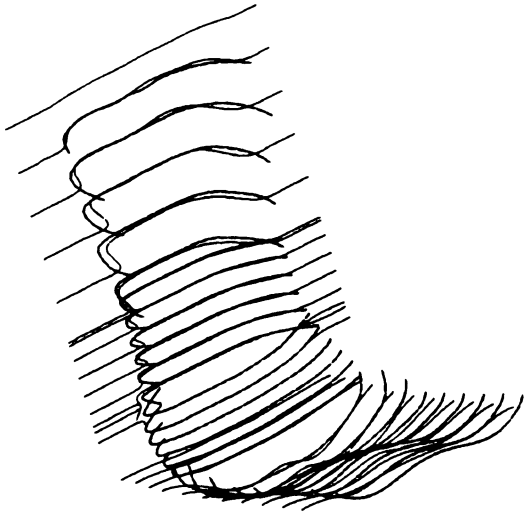

Figure 78 Small Female Subject 9 Iso View

SF9 Thorax 1st

SF9 Lumbar 1st

SF9 Thorax 2nd

SF9 Lumbar 2nd

SF9 Thorax 3rd

SF9 Lumbar 3rd

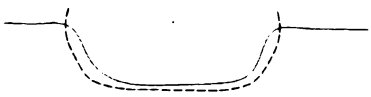

SF9 Thorax 4th

SF9 Lumbar 4th

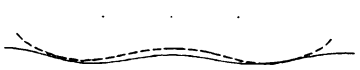

SF9 Thigh 7th

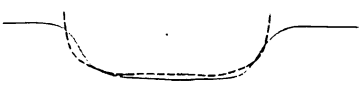

SF9 Lumbar 5th

Figure 79 Scaled and Measured Curves of Small Female Subject 9

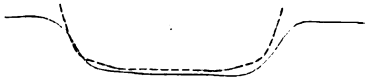

SF9 Lumbar 6th

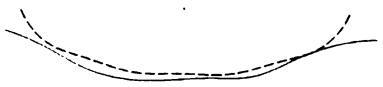

SF9 Pelvic 6th

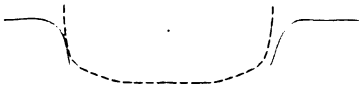

SF9 Pelvic 1st

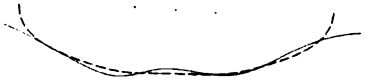

SF9 Thigh 1st

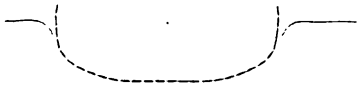

SF9 Pelvic 2nd

SF9 Thigh 2nd

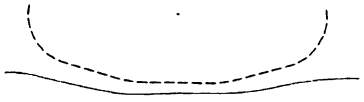

SF9 Pelvic 4th

SF9 Thigh 3rd

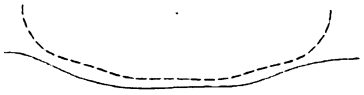

SF9 Pelvic 5th

SF9 Thigh 4th

Figure 79 Continued

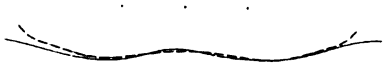

SF9 Thigh 5th

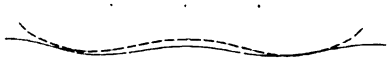

SF9 Thigh 7th

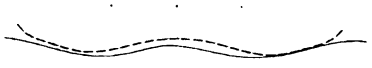

SF9 Thigh 6th

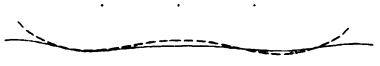

SF9 Thigh 8th

Figure 79 Continued

APPENDIX C

Scaled and Measured Large Males Results

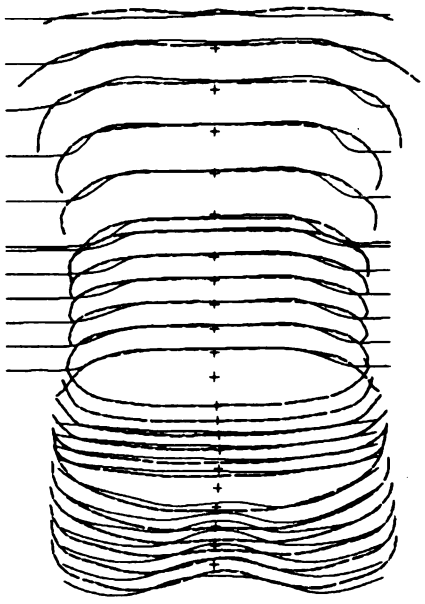

Figure 80 Large Male Subject 2 Rear View

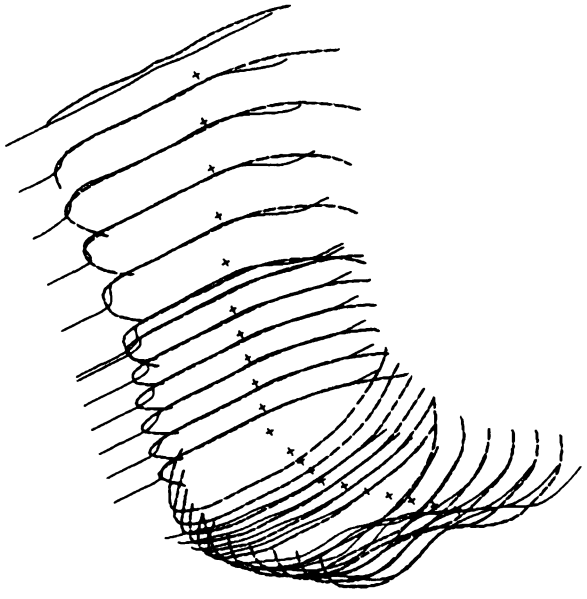

Figure 81 Large Male Subject 2 Iso View

LM2 Thorax 1st

LM2 Thorax 6th

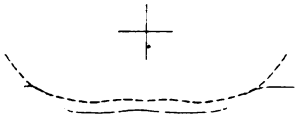

LM2 Thorax 2nd

LM2 Lumbar 1st

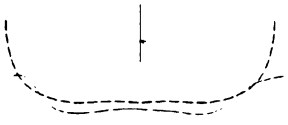

LM2 Thorax 3rd

LM2 Lumbar 2nd

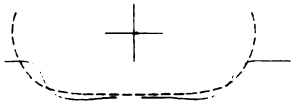

LM2 Thorax 4th

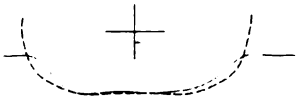

LM2 Lumbar 5th

LM2 Thorax 5th

Figure 82 Scaled and Measured Curves of Large Male Subject 2

LM2 Lumbar 4th

LM2 Pelvis 3rd

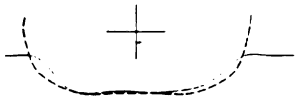

LM2 Lumbar 5th

LM2 Pelvis 4th

LM2 Lumbar 6th

LM2 Pelvis 5th

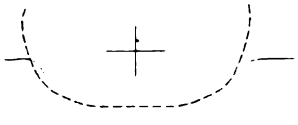

LM2 Pelvis 1st

LM2 Pelvis 6th

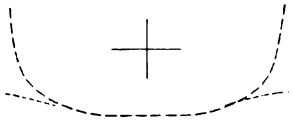

LM2 Pelvis 2nd

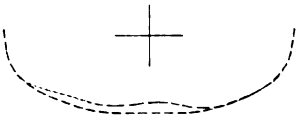

LM2 Thigh 1st

Figure 82 Continued

LM2 Thigh 2nd

LM2 Thigh 5th

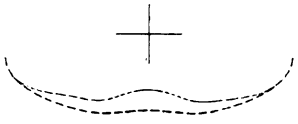

LM2 Thigh 3rd

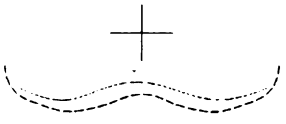

LM2 Thigh 6th

LM2 Thigh 4th

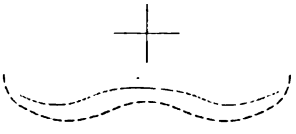

LM2 Thigh 7th

Figure 82 Continued

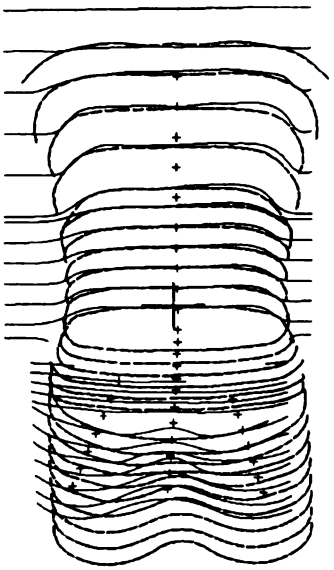

Figure 83 Large Male Subject 3 Rear View

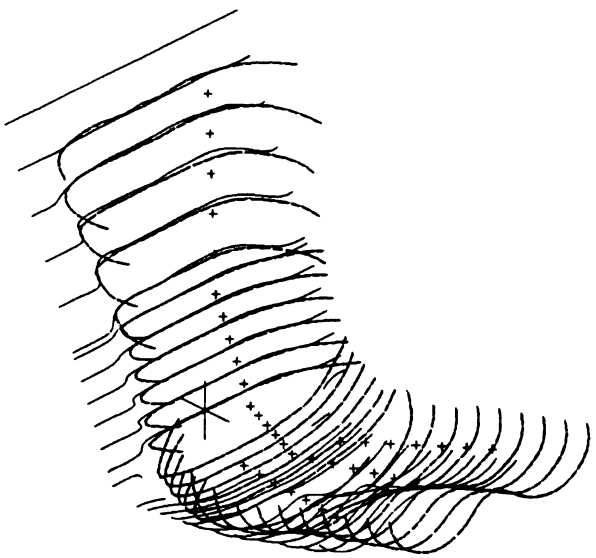

Figure 84 Large Male Subject 3 Iso View

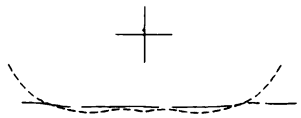

LM3 Thorax 2nd

LM3 Thorax 6th

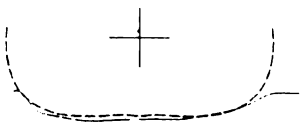

LM3 Thorax 3rd

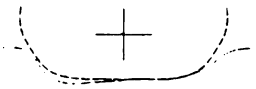

LM3 Lumbar 1st

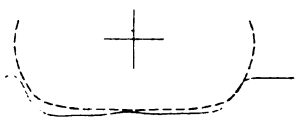

LM3 Thorax 4th

LM3 Lumbar 2nd

LM3 Thorax 5th

LM3 Lumbar 3rd

Figure 85 Scaled and Measured Curves of Large Male Subject 3

LM3 Lumbar 5th

LM3 Thigh 4th

LM3 Lumbar 6th

LM3 Thigh 5th

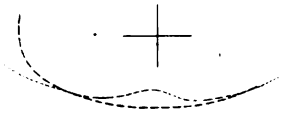

LM3 Thigh 1st

LM3 Thigh 6th

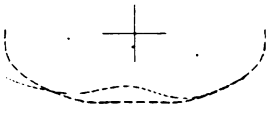

LM3 Thigh 2nd

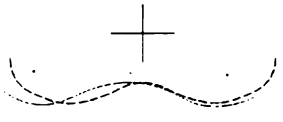

LM3 Thigh 7th

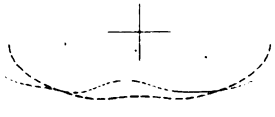

LM3 Thigh 3rd

Figure 85 Continued

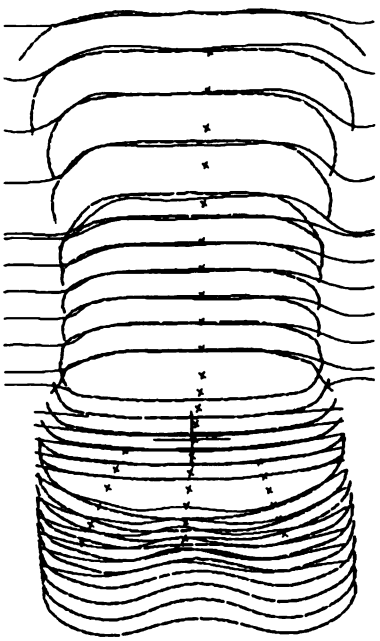

Figure 86 Large Male Subject 4 Rear View

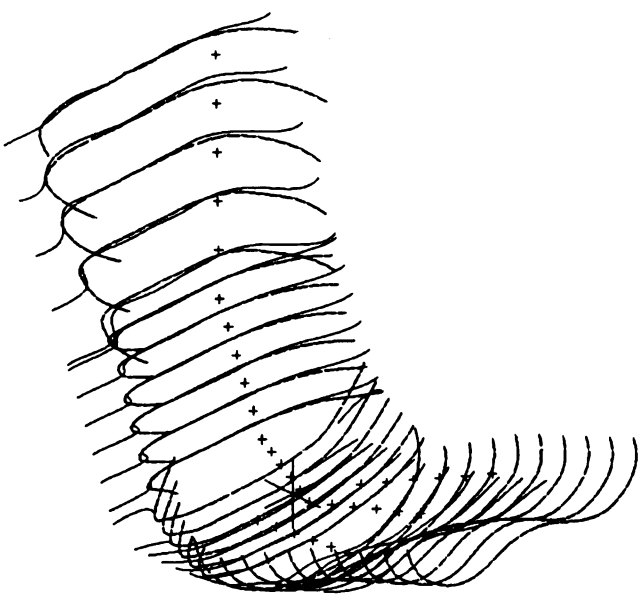

Figure 87 Large Male Subject 4 Iso View

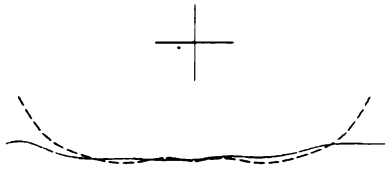

LM4 Thorax 2nd

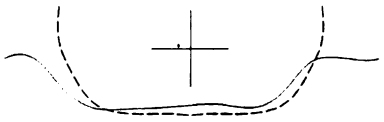

LM4 Thorax 6th

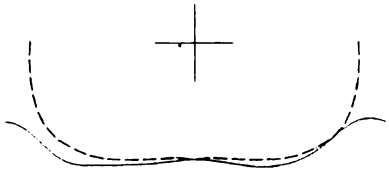

LM4 Thorax 3rd

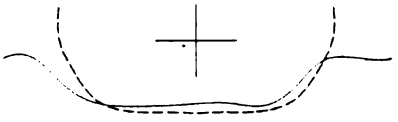

LM4 Lumbar 1st

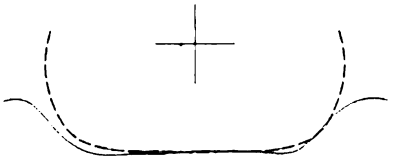

LM4 Thorax 4th

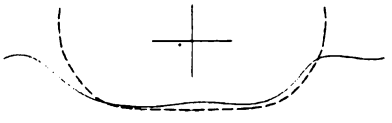

LM4 Lumbar 2nd

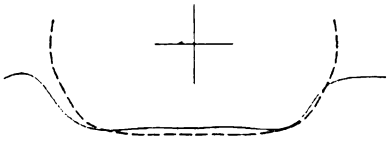

LM4 Thorax 5

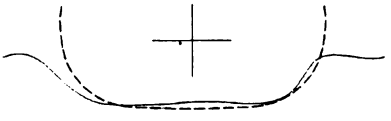

LM4 Lumbar 3

Figure 88 Scaled and Measured Curves of Large Male Subject 4

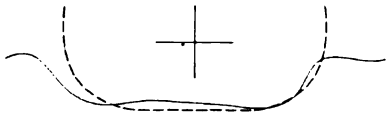

LM4 Lumbar 4th

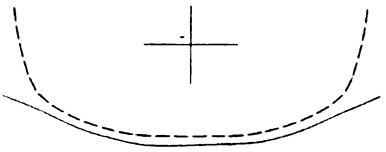

LM4 Pelvic 3rd

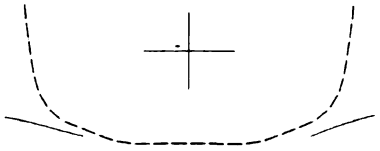

LM4 Pelvic 2nd

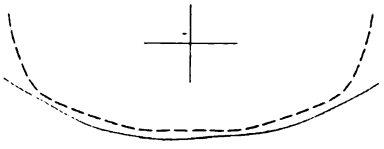

LM4 Pelvic 4th

LM4 Lumbar 5th

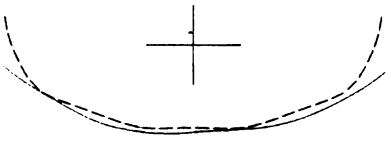

LM4 Pelvic 5th

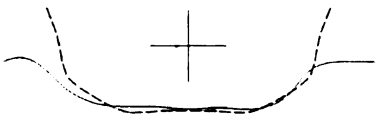

LM4 Lumbar 6th

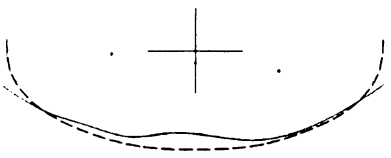

LM4 Thigh 1st

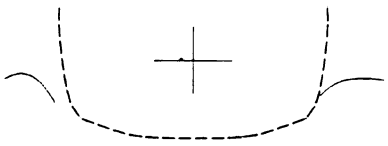

LM Pelvic 1st

LM4 Pelvic 6th

Figure 88 Continue

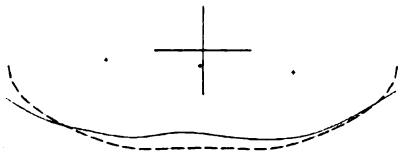

LM4 Thigh 2nd

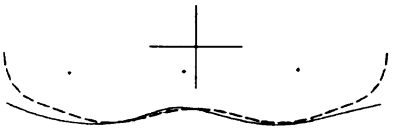

LM4 Thigh 5th

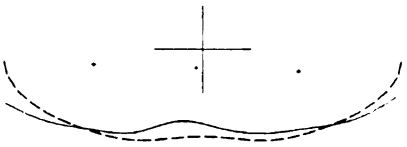

LM4 Thigh 3rd

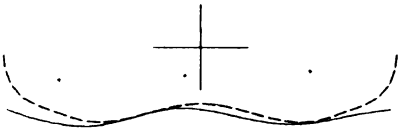

LM4 Thigh 6th

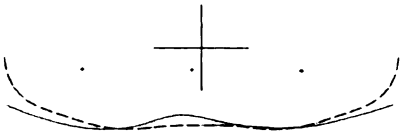

LM4 Thigh 4th

Figure 88 Continued

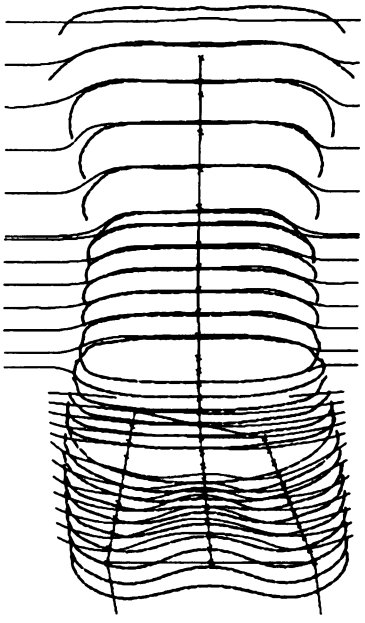

Figure 89 Large Male Subject 5 Rear View

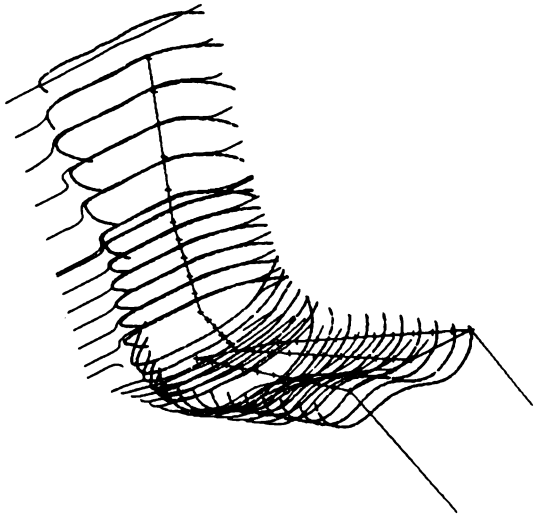

Figure 90 Large Male Subject 5 Iso View

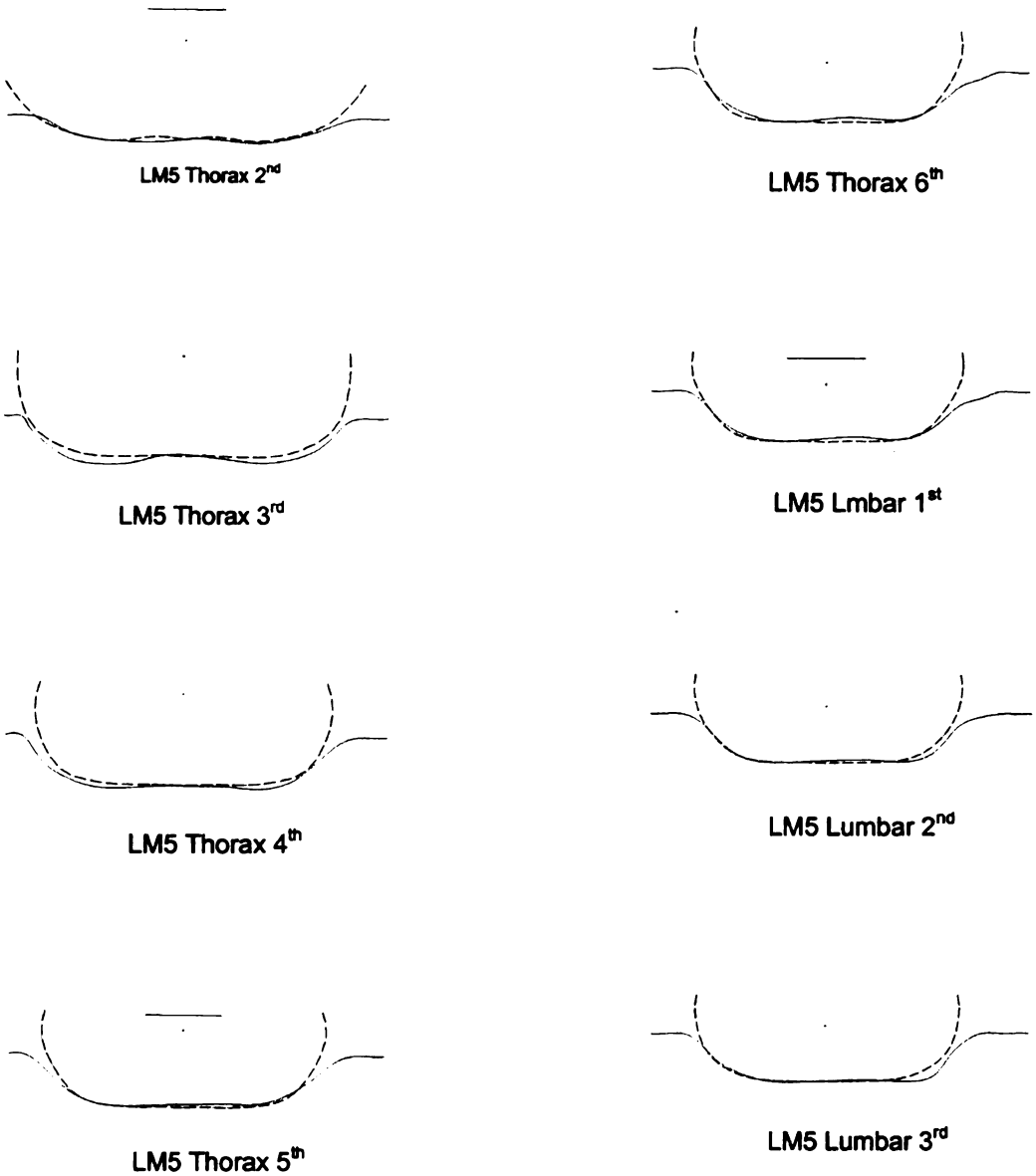

Figure 91 Scaled and Measured Curves of Large Male Subject 5

LM4 Lumbar 4th

LM5 Pelvic 2nd

LM5 Lumbar 5th

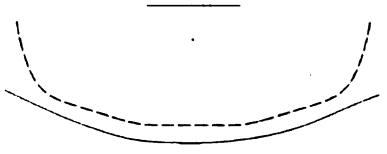

LM5 Pelvic 3rd

LM5 Lumbar 6th

LM5 Pelvic 4th

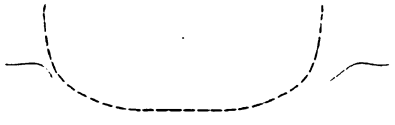

LM5 Pelvic 1st

LM5 Pelvic 5th

Figure 91 Continue

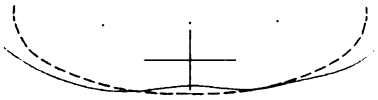

LM5 Thigh 1st

LM5 Thigh 5th

LM5 Thigh 2nd

LM5 Thigh 6th

LM5 Thigh 3rd

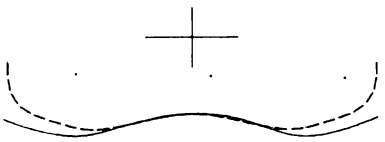

LM5 Thigh 7th

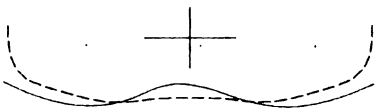

LM5 Thigh 4th

Figure 91 Continued

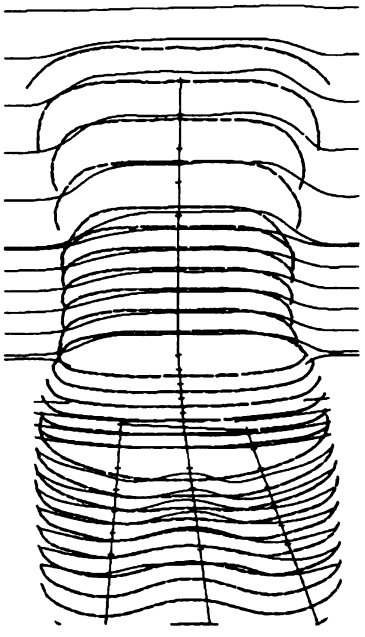

Figure 92 Large Male Subject 6 Rear View

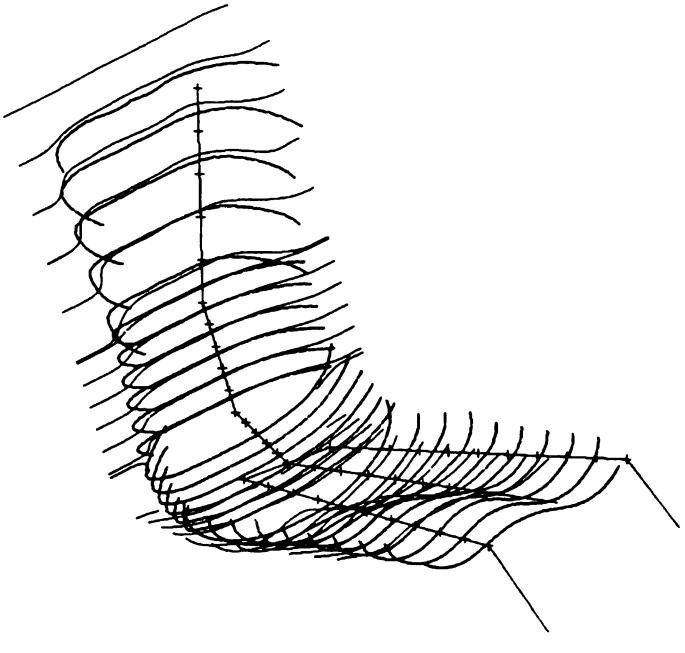

Figure 93 Large Male Subject 6 Iso View

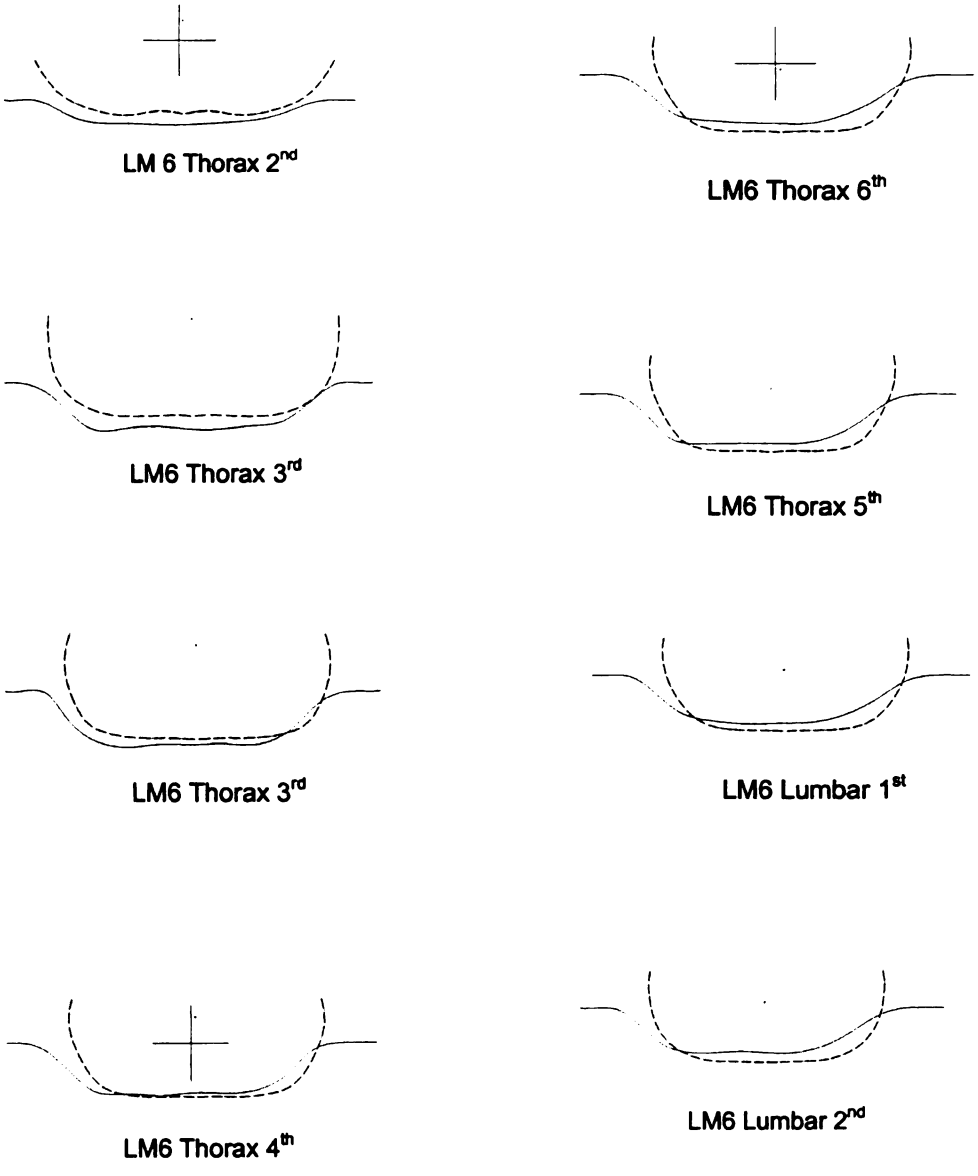

Figure 94 Scaled and Measured Curves of Large Male Subject 6

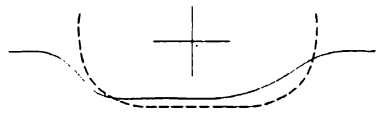

LM6 Lumbar 3rd

LM6 Pelvic 2nd

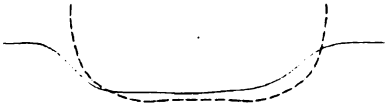

LM6 Lumbar 4th

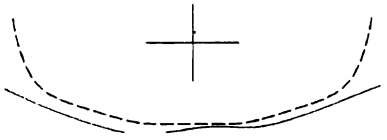

LM6 Pelvic 3rd

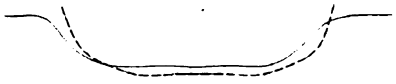

LM6 Lumbar 5th

LM6 Pelvic 4th

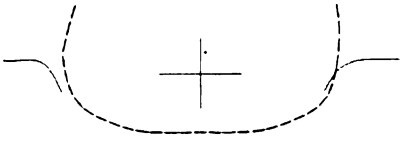

LM6 Lumbar 6th

LM6 Pelvic 5th

Figure 94 Continued

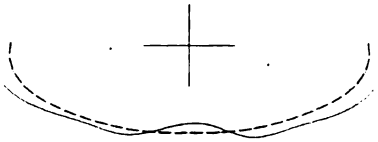

LM6 Pelvic 6th

LM6 Thigh 4th

LM6 Thigh 1st

LM6 Thigh 5th

LM6 Thigh 2nd

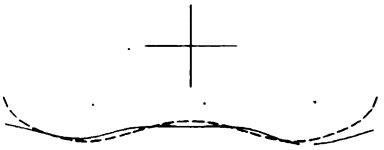

LM6 Thigh 6th

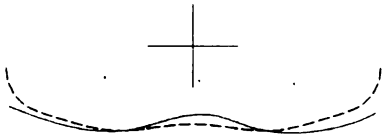

LM6 Thigh 3rd

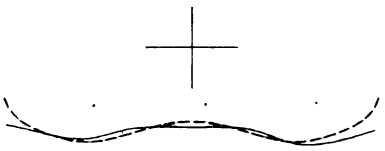

LM6 Thigh 7th

Figure 94 Continued

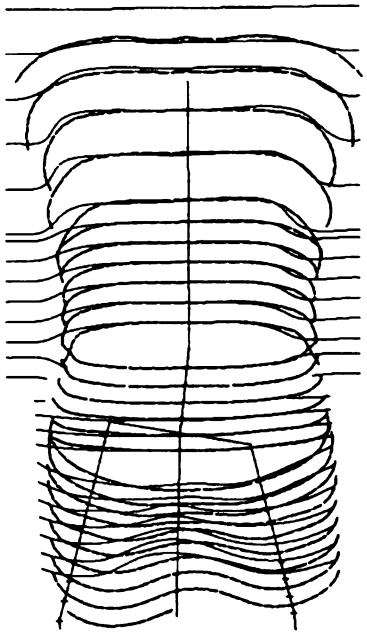

Figure 95 Large Male Subject 7 Rear View

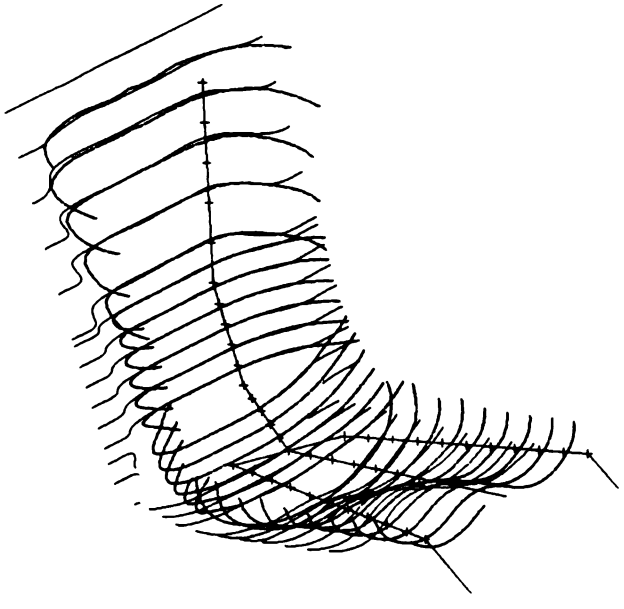

Figure 96 Large Male Subject 7 Iso View

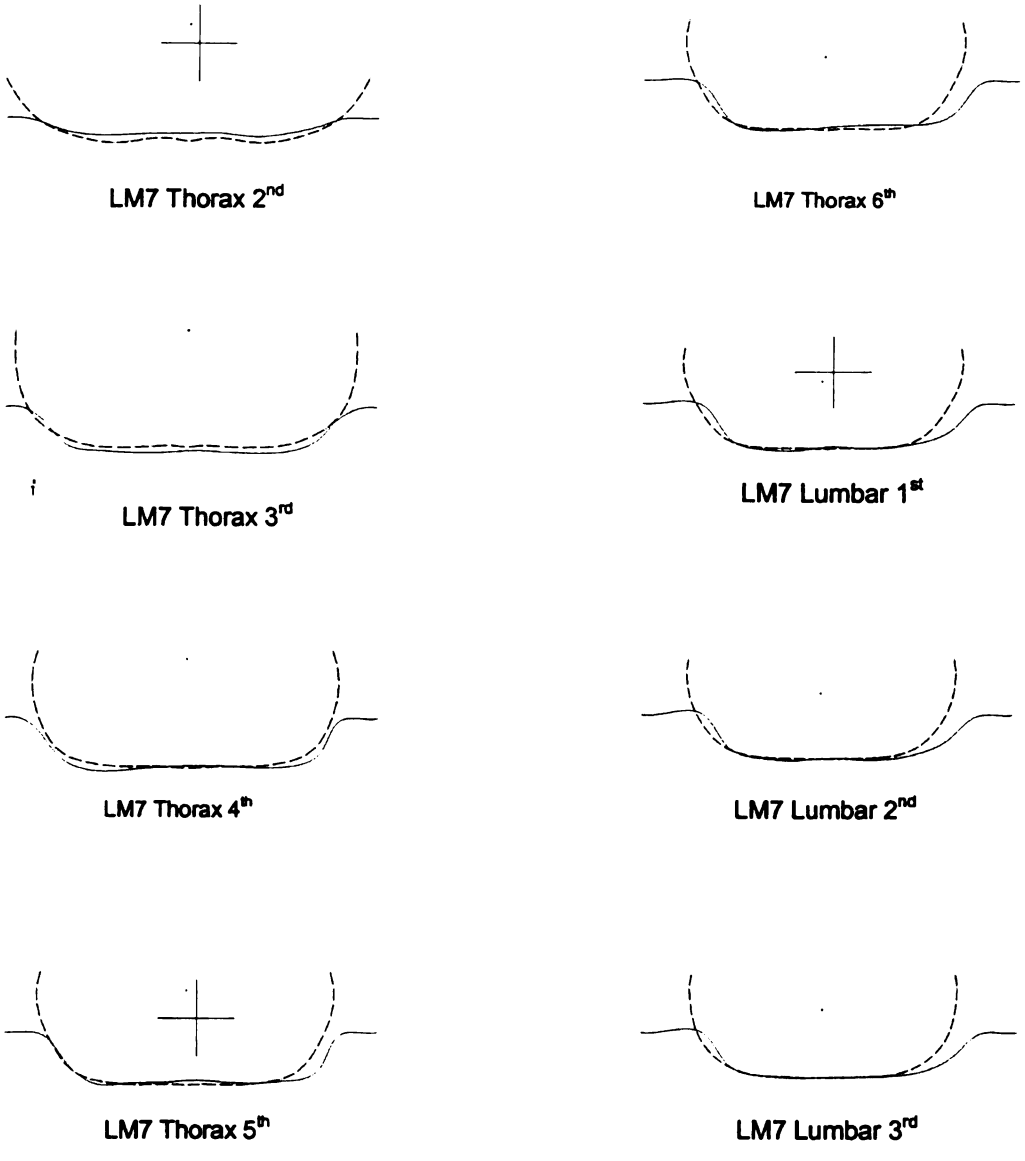

Figure 97 Scaled and Measured Curves of Large Male Subject 7

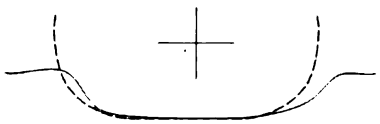

LM7 Lumbar 4th

LM7 Pelvic 2nd

LM7 Lumbar 5th

LM7 Pelvic 3rd

LM7 Lumbar 6th

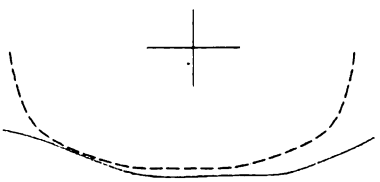

LM7 Pelvic 4th

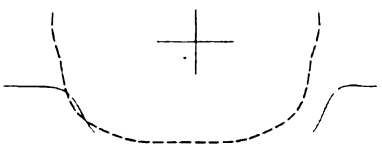

LM7 Pelvic 1st

LM7 Pelvic 5th

Figure 97 Continued

LM7 Pelvic 6th

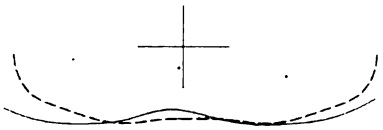

LM7 Thigh 4th

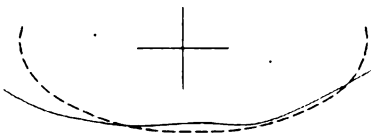

LM7 Thigh 1st

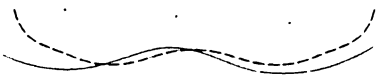

LM7 Thigh 5th

LM7 Thigh 3rd

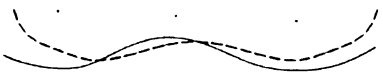

LM7 Thigh 6th

LM7 Thigh 2nd

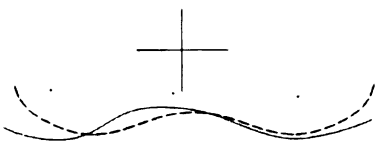

LM7 Thigh 7th

Figure 97 Continued

LIST OF REFERENCES

1 S.A.E. Handbook 1980 - Part 2, Society of Automotive Engineers, Warrendale, PA.

2 Hubbard, R. P., M. P. Reed, etc., "ASPECT Task 1: Foundational Activities, Interim Report", February 1997.

3 Hubbard, R. P., W. A. Haas, R. L. Boughner, R. A. Canole and N. J. Bush, "New Biomechanical Models for Automobile Seat Design", paper no. 930110, International Congress, Society of Automotive Engineers, 1992.

4 Haas, W. A., "Geometric Model and Spinal Motions of the Average Male in Seated Postures," Master Thesis, Michigan State University, 1989.

5 Robbins, D. H., "Anthropometric Specifications for the Mid-Sized Male Dummy, Volume 2", UMTRI-83-53-3, U.S. Department of Transportation, National Highway Traffic Safety Administration, Washington, D.C., 1983.

6 Seidl, A., "RAMSIS - A New CAD-Tool for Ergonomic Analysis of Vehicles Developed by Order of the German Automotive Industry," TecMath GmbH, January 1994.

7 Boughner, R. L., "A Model of Average Adult Male Human Skeletal and Leg Muscle Geometry and Hamstring Length for Automotive Seat Designers," Master Thesis, Michigan State University, 1991.

8 Bush, N. J., "two-dimensional Drafting Template and Three-Dimensional Computer Model Representing the Average Adult Male in Automotive Seated Postures", Master Thesis, Michigan State University, 1992.

9 Koritké, J.C., and H. Sick, "Atlas of Sectional Human Anatomy", Urban & Schwarzenberg, Baltimore, Md. 1983.

10 Frost, B. L. III, "A Three-Dimensional Computer Model of Human Back Contours for Automotive Seat Design", Master Thesis, Michigan State University, 1999.

11 Schakle, B., K. D. Chidsey, and P. Shipley, "The Assessment of Chair Comfort," in E.Grandjean, Ed., Sitting Posture, Taylor, London, 1969.

12 Bush, TR, "Posture and Force Measures of Mid-Sized Men in Seated Positions", Ph. D. Dissertation, Michigan State University, 2000.

13 Chaffin D., Andersson G. "Occupational Biomechanics: Second Edition. John Wiley and Sons, New York. 1991.

14 Claire C. Gordon, etc.,"1988 Anthropometric Survey of U. S. Army Personnel: Summary Statistics Interim Report", March 1989.

15 Abraham, S., Johnson, C. L., and Najjar, F., "Weight and Height of adults 18-74 Years of Age, United States, 1971-74 Vital and Health Statistics, Series 11". DHEW Publications Number 79-1656.

16 Setyabudhy, R., A. Ali, R. Hubbard, C. Beckett, and R. Averil, "Measurement and Modeling of Human Soft Tissue and Seat Interaction," paper 970593, SAE, 1997.

17 Qualisys Mac Reflex Software and Instruction Manual, Qualisys, 148 Eastern Blvd. Ste. 110, Glastonbury CT 06033.

18 3M Product Literature on 7610 High Gain Tape for Motion Systems. Screen Products, Industrial Optics Project/3M St. Paul, MN 55144. Ph. 612-733-4403 and Industrial Tape Division, 3M P. O. Box 358 Southfield, MI 48037, Ph. 1-800-241-0184.

19 Melissa Sloan Gedraitis, "Experimental Determination of a Spinal Linkage Model for the Seated Human Torso", Master Thesis, Michigan State University, 1998.

20 SDRC I-DEAS VI, "Solid Modeling Package", Structural Dynamics Research Corporation, Milford, Ohio, 1991.

21 Mase GE, Mase GT, "Continuum Mechanics for Engineers", CRC Press, Inc., 1992.

22 Seidel, GK, Marchinda, DM, Dijkers, M, and Soutas-Little, RW, 1995, "Hip Joint Center Location from Palpable Bony Landmarks – A Cadaver Study". J. Biomechanics, 28(8): 995-998.

23 Reynolds, HM, Snow, CC, and Young, JW, (1981), "Spatial Geometry of the Human Pelvis (Memorandum Report AAC-119-81-5)". Oklahoma City, OK: federal Aviation Administration, Civil Aeromedical Institute.

24 R.H. Setyabudhy, Z. Liu, R.P. Hubbard, "Measurement and Analysis of Human Thigh and Buttocks Contours for ASPECT Manikin Development", SAE paper no. 1999-01-0964, 1999.

25 Ayyub, BM, McCuen, RH, "Probability, Statistics, & Reliability for Engineers", CRC Press Inc., 1997.

26 Xu, L, Agaram, V, etc., "Repeatability Evaluation of the Pre-Prototype NHTSA Advanced Dummy Compared to the Hybrid III", SAE paper no. 200-01-0165, 2000.

27 Nusholtz, GS, Xu, L, etc., "Comparison of the Pre-Prototype NHTSA Advanced Dummy to the Hybrid III", SAE paper no. 971141, 1997.

28 MatLab Manual: "The Language of Technical Computing". Version 5; The MathWorks, Inc. 2004